Instituto Nacional de Matemática Pura e Aplicada

Modeling of Biophysical Phenomena:
Multiscale Analysis, Parameter Estimation, and Point Pattern Analysis

Nara Bobko
Advisor: Dr. Jorge P. Zubelli

Rio de Janeiro
March, 2015

To my family.

Acknowledgments

I would like to express my gratitude to my advisor, Jorge P. Zubelli, for encouraging and guiding my research. I would also like to thank the committee members, professor Alexei Mailybaev, professor Chiara Mocenni, professor Max Oliveira de Souza, professor Roberto Imbuzeiro Oliveira, and professor Yuan Jin Yun. Thanks for the valuable suggestions, and interest in my work.

My deepest gratitude to my family, specially to my parents, for their encouragement and constant support. Special thanks to my sweet daughter Cecília, whose hugs and smiles motivated me in difficult days. I reserve also a sincere thanks to my husband, friend and co-worker, Francisco Ganacim, for incessantly encouraging me to achieve my goal. My parents, Rosângela M. Bobko and Jaime Bobko, receive my deepest gratitude for their dedication and the many years of support. I also thank all my colleagues and friends. In special Elaís Malheiro, Roberto Ribeiro, Roberto Teodoro, Gisele Teixeira, Alessandro Gaio, Lilian Brambila, and Ricardo Paleari.

Thanks to Chiara Mocenni, Dani Gamerman, Dayse Pastore, Jony A. Pinto Jr., Leonardo de Medeiros Maier, Max Oliveira de Souza, and Yuan Jin Yun for the discussions and suggestions that were of great value to the development of this thesis.

Thank to the Department of STD, AIDS and Viral Hepatitis of the Ministry of Health and the Cascavel Police Department, for providing the data used in this work. In particular, Dr. Fábio Mesquita, Cel. Celso Luiz Borges, Ten. Márcia Bobko, and SD. Daniel de Arruda Gerhardt.

This work was supported by the Conselho Nacional de Desenvolvimento Científico e Tecnológico (CNPq) and by the National Petrol Agency (ANP).

Abstract

This PhD thesis consists of two parts, both of them related to the modeling of biophysical phenomena.

In the first part we study a differential equation system designed to model the dynamics of the human immunodeficiency virus (HIV) within the host organism. This model generalizes a number of other models that have been extensively used to describe the HIV dynamics, including antigenic variation and antiretroviral therapy. Based on global stability properties of this model, we analyze the influence of the antiretroviral therapy in the long term dynamics. We characterize the outcome steady-state as a function of the antiretroviral efficacy. Additionally, we performed a multiscale analysis using Tikhonov's theorem, in order to deal with the two intrinsic time scales of the model. This analysis leads to a way of approximating the solutions of the system by a lower dimensional nonlinear model. This reduced system is faster to evaluate numerically, and is globally asymptotically stable, as we have shown by using Lyapunov's stability theory. We also introduce a method to estimate parameters of the HIV dynamics by comparing clinical data in the chronic stage with predicted equilibrium points of a well accepted mathematical model. We apply this method to estimate two parameters, using clinical data.

In the second part, our focus is the study of the dynamics of residential burglaries. Aiming to explain the presence of agglomerations (hotspots) in this dynamics, many theories have been raised. In order to investigate such theories, we analyze real data of residential burglaries of a Brazilian city with respect to the point pattern. Specifically, we analyze the data regarding the spatial, temporal, and spatio-temporal agglomerations. The main tool used in the analysis was the measure of homogeneity given by the Ripley's K function. The analysis shows that, on a small scale, the dynamics of residential burglaries looks like a homogeneous Poisson process. On the other hand, on a larger scale, such dynamics cannot be explain as a homogeneous Poisson process, since the intensity of burglaries varies significantly along the regions of the city.

Keywords: HIV Dynamics, Multiscale Analysis, Parameter Estimation, Dynamics of Residential Burglaries, Point Pattern Analysis.

Contents

Introduction

The subject of this PhD thesis is the study of biophysical phenomena using mathematical methods. Mathematical tools are of great importance in the natural sciences by enabling to improve the understanding of complex systems, study the effects of different components, perform simulations, test hypotheses, and so forth. In this work we study two distinct phenomena. The first one, addressed in Part I, is the HIV dynamics within the host organism. The second one concerns the dynamics of residential burglaries. It is addressed in Part II. Hereafter we clarify which problems have been addressed and what results have been obtained.

In Part I, *HIV-1 Dynamics*, we study a system of ordinary differential equations designed to model the dynamics of HIV-1[1] within host organism. This model, originally proposed by Nowak and Bangham [NB96], addresses the disease dynamics describing the interaction between the HIV-1 particles and the host immune system. Additionally, it includes the antigenic variation, which significantly increases the complexity of the system. In fact, we consider a slightly generalized form of this system, since we also consider the antiretroviral therapy (ART). We start by rewriting the system in a dimensionless form. The change of variables that we made allowed us to simplify the units involved and emphasize system properties. Based on global stability properties of this model made by Souza and Zubelli [SZ11], we analyze the influence of the ART in the long term dynamics. Strictly speaking, we compare the steady-state of the system that considers ART with the steady-state of the system that does not consider it. From this, we obtain Theorem 3.1, which provides what will be the steady-state to the system with ART, from the expected steady-state before the treatment, and from the value of the efficiency of the antiretrovirals. From biological view point, this result allows evaluating the minimum efficacy required for a successful treatment. This is very relevant, since the treatment may be associated with unwanted side effects not directly related to the HIV-1 infection, such as cardiovascular disease, liver abnormalities, bone loss, as well as cancers and loss of neurocognitive functions [dep13]. Another aspect of this system concerns the presence of two time scales. While

[1] HIV type 1, the most common and pathogenic type of HIV [DRK09, C+08].

$CD4^+T$ cells have a half-life of the order of days, virions[2] have a half-life of about a few hours. This leads to a singularly perturbed system with numerical as well as biological implications. In order to deal with this problem, we perform a multiscale analysis, using Tikhonov's theorem. Thus, we obtain Theorems 4.5 and 4.6 that provide a way of approximating the solutions of the perturbed system by solutions of a reduced system. The interest in such a reduction lies on the fact that the complexity of the problem is considerably reduced. Furthermore, for certain parameters, the original system becomes very stiff, while the reduced system offers a robust approximation. These results were published in the article *A Singularly Perturbed HIV Model with Treatment and Antigenic Variation*, written by the author in collaboration with Jorge P. Zubelli. Finally, we introduce a method to estimate parameters of the HIV-1 dynamics by comparing clinical data in the chronic stage with predicted equilibrium points of a mathematical model. This system is a particular case of the model mentioned above, and is considered to appropriately describe the dynamics of HIV-1 in the acute infection phase. To show the efficiency of our approach, we analyzed the errors obtained from synthetic data generated by the mathematical model, added multiplicative noise to our simulations. Applying the proposed method, we estimate the basic reproductive ratio in the presence of the immune response and the infection rate of 31 patients. Furthermore, we estimate a lower bound to the basic reproductive ratio in the absence of the immune response of those patients.

In Part II, *Dynamics of Residential Burglaries*, our focus is the study of the agglomerations (hotspots) of residential burglaries. A better understanding of such dynamics is very relevant, with major implications for the development of strategies for effective prevention of it. An important aspect in crime dynamics are the hotspots, i.e. regions with a high crime intensity. These hotspots maybe occur not only in the spatial domain, but also in temporal and spatio-temporal domains. Aiming to explain the hotspots, many theories have been presented. Among them are the repeat (or near-repeat) effects, the broken windows effects, the structure of the urban environment, and seasonal conditions. In order to investigate these theories, we analyze real data from a Brazilian city. This data refers to the residential burglaries that have been reported to police over three years. We analyze the data with respect to the presence of statistically significant agglomerations in the spatial, temporal, and spatio-temporal domains. According to the temporal analysis, at the end of the first year there is a spike in the number of residential burglaries that cannot be explained by simply randomness. However, this spike seems to be an outlier, and not a pattern of the dynamics of residential burglaries. For the spatial and spatio-temporal analysis, the main tool used was the measure of homogeneity given by the Ripley's K function. The spatial analysis shows that, on a small scale, the dynamic of residential burglaries looks like a homogeneous Poisson process. This is also the outcome of the spatio-temporal analysis. However, the intensity of burglaries varies significantly along the residential regions of the city. This indicates that, on a larger scale, the residential burglaries cannot be explain as a simple homogeneous Poisson process.

[2]Viral particles outside the host cell.

Outline of the Thesis. This work is organized in two parts that can be read independently.

Part I (Chapters 1 to 5), deals with the HIV-1 dynamics within the host organism. In Chapter 1 we introduce an extended version of HIV-1 model proposed by Nowak and Bangham [NB96, NM00], providing the necessary biological background. This model is described by a system of ordinary differential equations. In Chapter 2, we propose a dimensionless form of this system. Then, we review some of its properties that will be used in the other chapters. In Chapter 3, we analyze the changes in the system steady-state due to the antiretroviral therapy. Our analysis allows us to determine the necessary efficiency of the antiretroviral to ensure a successful treatment. In Chapter 4, we perform a multiscale analysis of the HIV system, using Tikhonov's theorem. This chapter is a transcription of the published paper *A Singularly Perturbed HIV Model with Treatment and Antigenic Variation*, written by the author in collaboration with Jorge P. Zubelli. In Chapter 5, we introduce a novel method to estimate parameter of the HIV system by comparing clinical data with predicted equilibrium points.

Part II (Chapter 6), concerns the study of residential burglaries. In this chapter, we present an analysis about the spatial, temporal, and spatio-temporal agglomerations for residential burglary data of a Brazilian city.

Part I
HIV-1 Dynamics

CHAPTER 1

Mathematical Modeling of the HIV-1 dynamics

In this chapter we will introduce the HIV model studied along of this work. Motivated by the epidemic of the acquired immunodeficiency syndrome (AIDS), that started in the early 1980s, several models have been proposed in order to describe the HIV in-vivo [NB96, PKDB93, PN99, FM94, Kir96, NP02, NM00, Kor04, SZ11, Pas05, Bob10, BMSN97, SDL03, WS07, PH$^+$00, BZ15, Coo86, PH$^+$95, PH$^+$96, GKCM13]. Among them, is the as well accepted model proposed by Nowak and Bangham [NB96]. This model addresses the disease dynamics within an infected individual, describing the interaction between the HIV and the cells of the host. In this thesis, we consider a slightly generalized form of this model, as we describe in Section 1.2. Before explaining this model in details, we provide a brief biological background in Section 1.1.

1.1 Biological Background

The HIV is a retrovirus that causes AIDS, one of the most devastating infectious diseases to have emerged in recent history [DRK09, SH11, C$^+$08, MK06, LF85, oH12]. As with all viruses, HIV replicates only inside the living cells of other organisms. However, the main target cells of HIV are vital cells of the human immune system, the CD4$^+$T cells. Therefore, the HIV infection causes the depletion and dysregulation of the immune system and leads to life-threatening tumors and opportunistic infections [DRK09, C$^+$08, MK06].

The replication cycle of the HIV begins with fusion of the viral envelope with the host cell membrane. After the HIV has bound to the target cell, the HIV RNA and various enzymes are injected into the cell. Then, an enzyme called reverse transcriptase liberates the single-stranded RNA genome from the attached viral proteins and copies it into a complementary DNA molecule. This process is extremely error-prone, generating a high genetic variability of HIV which may allow the virus to evade the body's immune response. After that occurs, the integration of the

viral DNA into the host cell's genome is carried out by another viral enzyme called the integrase. Mediated by the viral protease, the final step of the viral cycle is the assembly of the new HIV virions. Finally, the viral protease mediates the assembly of the new HIV virions, and then these new virions are released.

The entry of viral genetic material into host cells triggers the adaptive immune system. The adaptive immune system, or acquired immune, is part of a sophisticated network of biological processes within the body. These processes result in the activation of $CD8^+$T lymphocytes that will bind to infected cells and induce apoptosis.

Despite the induction of the immune response, this is late and insufficient in magnitude to eradicate the HIV infection [SdMB$^+$13]. Then, to avoid the progressive failure of the immune system, medical treatments are required.

The treatments consist of antiretrovirals drugs that aim at suppressing the virus and stop the progression of the HIV disease. There are several classes of drugs to treat the HIV infection and the use of these drugs in combination is termed antiretroviral therapy (ART). The antiretrovirals are classified by the phase of the replication cycle that the drug inhibits

Entry inhibitors (or fusion inhibitors) interfere with binding, fusion and entry of HIV into the host cell;

Reverse transcriptase inhibitors inhibit the transcription of the viral RNA to DNA;

Integrase inhibitors inhibit the enzyme integrase, which is responsible for integration of viral DNA into the DNA of the infected cell;

Protease inhibitors inhibit enzyme protease necessary to produce mature virions, then the new copies of HIV will not be able to infect new cells.

One difficulty of the HIV treatment is its high genetic variability, especially for HIV type 1 [SdMB$^+$13, GC04, MK06, RHS95, RPCH04]. Despite the difference between the mechanisms of the two types of HIV is not clearly defined, it is known that HIV-1 is more virulent, more pathogenic and is the cause of the majority of the HIV infections [DRK09, C$^+$08].

In the first stage of the HIV-1 infection, the acute phase, the virus enters the body and it begins to infect $CD4^+$T lymphocytes. The virus uses $CD4^+$T cells to replicate and destroys them in the process. Since large amounts of virus are being produced, the $CD4^+$T count decreases rapidly. On the other hand, the dissemination of the virus induces the immune response, causing the increase of $CD8^+$T cells, which in turn will begin to bring the level of virus back down to a level called a viral set point, which is a relatively stable level of the viral load [SdMB$^+$13, RP$^+$10]. This set point is a strong predictor for the HIV-1 disease chronicity [SdMB$^+$13, SH03]. After the acute stage of the HIV-1 infection, the disease moves into a stage called chronic stage or clinical latency stage. In this stage, $CD8^+$T cells exert partial control of the infection, but not enough to prevent, in the absence of therapy, the slow and progressive depletion of $CD4^+$T cells. This will lead eventually to AIDS[1]. Figure 1.1 depicts the progression of the HIV-1 infection.

[1]When the number of $CD4^+$T cells falls below 200 cells per cubic millimeter of blood.

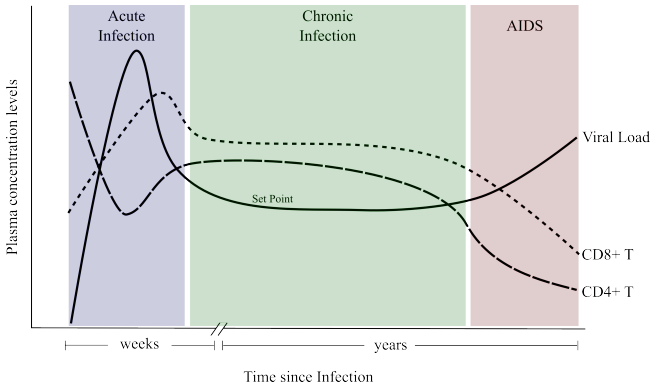

Figure 1.1: **Typical HIV-1 infection course.** The graph shows the typical course of the HIV-1 in an untreated individual. After an individual becomes infected, the viral load rises rapidly to a very high peak level, and then drops sharply to a set point level that remains more or less stable for several years (chronic infection). Eventually, $CD4^+T$ cells fall below a critical level (200 $CD4^+T$ cells per cubic millimeter of blood), which defines the onset of AIDS.

1.2 The Mathematical Model

The model proposed by Nowak and Bangham [NB96] has four variables: uninfected $CD4^+T$ cells (X), infected $CD4^+T$ cells (Y), virions (V) and $CD8^+T$ cells (Z). These quantities denote the abundance of the corresponding quantities in a given volume of blood or tissue. The model considers that uninfected $CD4^+T$ cells are produced at a constant rate λ and die at a rate dX. Virions attack uninfected cells at a rate proportional to the product of their concentrations, βXV. The infection rate β describes the efficacy of this process, including the rate at which viral particles find uninfected cells, the rate of virus entry, and the probability of successful infection. Infected cells produce virions at a rate proportional to their abundance, kY, die at a rate aY and are killed by $CD8^+T$ cells at a rate pYZ. Free viral particles die at a rate uV. $CD8^+T$ cells have a proliferation rate given by cYZ and, in absence of stimulation, decay at a rate bZ. Figure 1.2 depicts the dynamics described above.

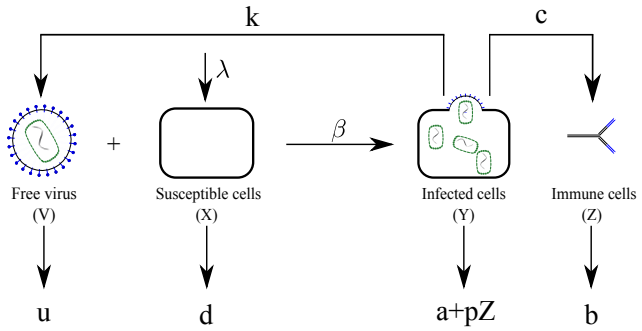

Figure 1.2: **Schematic illustration of the dynamics of the HIV-1 infection.** The virions infect $CD4^+T$ cells with an infection rate, β and then these infected cells will produce virions at a rate k. Uninfected $CD4^+T$ cells, $CD8^+T$ cells and virions die at a rate d, b and u, respectively. Infected $CD4^+T$ cells die at a rate a and are eliminated by $CD8^+T$ response at the rate pZ. Uninfected $CD4^+T$ cells are replenished at a rate λ. The rate of the $CD8^+T$ cells proliferation is given by cYZ.

This dynamics leads to the following four-by-four system of ordinary differential equations

$$\begin{aligned} \dot{X} &= \lambda - dX - \beta XV \\ \dot{Y} &= \beta XV - aY - pYZ \\ \dot{V} &= kY - uV \\ \dot{Z} &= cYZ - bZ \end{aligned} \tag{1.1}$$

with initial conditions $X(0) = X_0$, $Y(0) = Y_0$, $V(0) = V_0$ and $Z(0) = Z_0$.

Furthermore, taking into account the ART, we will have another variable in the model: the defective virions (H), whose dynamic is analogous to the dynamics of the active virions. Additionally, the efficacy of the inhibitors affects the process of cell infection and virion production.

To describe the high genetic variability of HIV-1 and its interaction with the immune response, Nowak and Bangham [NB96] consider n strains of virus, and the corresponding infected cells and CD8$^+$T cells. Following Souza and Zubelli [SZ11], we consider a generalized form of this model, since we consider that the parameters a, p, u, c and b can depend on the strain. Thus we obtain the following first-order system of ordinary differential equations

$$\begin{aligned} \dot{X} =& \lambda - dX - (1 - E_E)X \sum_{i \in \mathcal{N}} \beta_i V_i \\ \dot{Y}_i =& (1 - E_E)X\beta_i V_i - a_i Y_i - p_i Y_i Z_i \\ \dot{V}_i =& (1 - E_T)(1 - E_P)(1 - E_I)k_i Y_i - u_i V_i \\ \dot{H}_i =& E_P k_i Y_i - u_i H_i \\ \dot{Z}_i =& c_i Y_i Z_i - b_i Z_i \end{aligned} \tag{1.2}$$

for $i \in \mathcal{N} = \{1, \ldots, n\}$. Table 1.1 summarizes the biological meaning of the parameters.

Parameter	Meaning
λ	CD4$^+$T cells supply rate
β_i	infection rate for the i-th strain
k_i	free virus production rate
c_i	CD8$^+$T cells production rate
p_i	elimination rate of infected CD4$^+$T due to CD8$^+$T cells
E_T	efficacy of the reverse transcriptase inhibitor
E_E	efficacy of the entry inhibitor
E_P	efficacy of the protease inhibitor
E_I	efficacy of the integrase inhibitor
$1/d$	mean lifetime of uninfected CD4$^+$T cells
$1/a_i$	mean lifetime of infected CD4$^+$T cells
$1/u_i$	mean lifetime of free virus
$1/b_i$	mean lifetime of cytotoxic T cells

Table 1.1: **Parameters description.** Meaning of the parameters involved in the compartmental Model (1.3). The parameters E_T, E_E, E_P and E_I are in $[0, 1)$. The other parameters are positive. For the parameters with subscript i, the meaning described corresponds to the i-th strain.

Note that the equation describing the evolution of H_i is uncoupled from the other ones in Equation (1.2). Therefore, we will consider the system without these equations

$$\begin{aligned}
\dot{X} =& \lambda - dX - (1 - E_E)X \sum_{i \in \mathcal{N}} \beta_i V_i \\
\dot{Y}_i =& (1 - E_E)X\beta_i V_i - a_i Y_i - p_i Y_i Z_i \\
\dot{V}_i =& (1 - E_T)(1 - E_P)(1 - E_I)k_i Y_i - u_i V_i \\
\dot{Z}_i =& c_i Y_i Z_i - b_i Z_i.
\end{aligned} \tag{1.3}$$

Discussion

Although the model described in this chapter adequately describes several aspects of the HIV-1 dynamics, it has some limitations. This model does not consider the latent infected cells, neither the other cells susceptible to the HIV-1 infection, such as macrophages and dendritic cells [WDP98]. However, the latent cells are only a minor source [PH$^+$97] and the other cells susceptible to HIV-1 are responsible for the generation of only 1% of virions [BMSN97, NM00].

The main limitation of this model concerns the efficacy of the ART. The model assumes that the efficacy of each inhibitor is constant over time, ignoring the saturation of these drugs. The model also assumes that the inhibitors are homogeneously distributed in the body. However, not all drugs penetrate the blood–brain barrier effectively, and thus drug concentrations in the brain and central nervous system tend to be lower than in the circulation [PN99]. Also, the immune-system cells have limited access to the central nervous system, and hence this site may act as sanctuary for the virus [P$^+$97]. Considering these aspects open up a variety of new directions for modeling and studying the HIV-1 dynamics.

Another aspect omitted in this model is the intracellular delays. A possible future work would be to consider models that take into account this aspect, as those proposed by Nelson et al. [NP02].

Finally, many authors include drug-resistant viruses in order to describe the lack of success of therapy for many patients [KW97, BMSN97, NM00, VRM$^+$10, GKCM13, WDP98]. Although the model described in this chapter does not consider such viruses, we can still interpret this phenomenon due to the basic reproductive ratios. Indeed, as we will show in Chapter 5, the infection rate (β) will depend on the patient. Consequently, the basic reproductive ratios also depend on the individual. Then, the minimum efficacy of ART necessary to ensure the eradication of the infection will also vary according to the patient, as we will show in Chapter 3. This explains why the HIV-1 treatment is more effective for some than for other patients.

Note that if we consider that the effectiveness of each of the inhibitors varies from one strain to another, then we cover the case where the drug-resistant virus are included. However the descending order regarding the basic reproductive numbers post-treatment $\overline{R_0^i}$ would be lost, affecting the results of Chapter 3, since it is necessary to ensure that system with ART meets the conditions of the Theorem 2.2.

CHAPTER 2

Model Properties

In this chapter we briefly review some properties of System (1.3), which are used in the results of the following chapters. These properties, shown in Section 2.2, concern the equilibrium points and the global stability and have been proven by Souza and Zubelli [SZ11] for an equivalent model (without antiretroviral therapy). Bobko [Bob10] details the proof of these properties and extends them to a model that considers the latent period of the infected cells and the antiretroviral therapy.

In order to simplify the units involved and to emphasize system properties, we will show these properties considering the system in a dimensionless form, which we describe in Section 2.1.

2.1 The Dimensionless System

Note that we can reduce some parameters by renaming $(1 - E_T)(1 - E_P)(1 - E_I)k_i$ by k_i and $(1 - E_E)\beta_i$ by β_i, for $i \in \mathcal{N}$.

Before perform the adimensionalization of System (1.3), we should take into account that are already known some dimensionless parameters which are important in determining the asymptotic equilibrium, see [NB96, NM00, Kor04, Pas05, SZ11]. These constants are the *basic reproductive ratio in the absence of the immune response*

$$R_0^i = \frac{\beta_i \lambda k_i}{d a_i u_i},$$

and the *basic reproductive ratio in the presence of the immune response*

$$R_I^i = 1 + \frac{R_0^i}{I_0^i},$$

where $I_0^i = \frac{c_i \lambda}{a_i b_i}$, for $i \in \mathcal{N}$.

Letting $t = d \cdot T$, $x = \frac{d}{\lambda} X$, $y_i = \frac{a_i}{\lambda} Y_i$, $v_i = \frac{\beta_i}{d} V_i$, $z_i = \frac{p_i}{a_i} Z_i$ and taking the derivatives w.r.t. t, we obtain the following system

$$\begin{aligned} \dot{x} =& 1 - x - x \sum_{i \in \mathcal{N}} v_i \\ \dot{y}_i =& \gamma_i \left(x v_i - y_i - y_i z_i \right) \\ \dot{v}_i =& \eta_i \left(R_0^i y_i - v_i \right) \\ \dot{z}_i =& \sigma_i \left(I_0^i y_i z_i - z_i \right) \end{aligned} \tag{2.1}$$

for $i \in \mathcal{N}$, where $\gamma_i = \frac{a_i}{d}$, $\eta_i = \frac{u_i}{d}$ and $\sigma_i = \frac{b_i}{d}$.

2.2 Equilibrium Points and Global Stability

Before describing the equilibrium points, we shall introduce some notation in order to deal with the variety of equilibria that arises in System (2.1). Following [SZ11] and without loss of generality, we assume that the strains are indexed in a non increasing order of the constants R_0^i.

Given a set of indices $\mathcal{I} \subseteq \mathcal{N}$, we denote $R_I^{\mathcal{I}} = 1 + \sum_{i \in \mathcal{I}} \frac{R_0^i}{I_0^i}$. Additionally, for a more concise notation, y denotes the vector $(y_1, y_2, ..., y_n)$ (similarly for v and z), and $W_{j\mathcal{J}} = (x_{j\mathcal{J}}, y_{j\mathcal{J}}, v_{j\mathcal{J}}, z_{j\mathcal{J}})$ where $\mathcal{J}$ is a subset of $\mathcal{N}$ and $j \in \{\mathcal{N} - \mathcal{J}\}$. From the biological viewpoint, $\mathcal{J}$ is the set of indices of the strains that remain in the organism and are fought by the immune system while j is the strain index that remains in the organism without being fought by the immune system.

Using this notation, we have

Theorem 2.1. [SZ11] *If the basic reproductive ratios of the virus strains are distinct, then Equation* (2.1) *has* $2^{n-1}(2+n)$ *equilibrium points* $W_{j\mathcal{J}}$ *where*

1. *For* $\mathcal{J} = \emptyset$ *and* $j = 0$, *we have* $x_{0\emptyset} = 1$ *and* $y_{0\emptyset}^i = v_{0\emptyset}^i = z_{0\emptyset}^i = 0$, $\forall i \in \mathcal{N}$.
2. *For* $\mathcal{J} = \emptyset$ *and* $j \in \mathcal{N}$, *we have* $x_{j\emptyset} = 1/R_0^j$, $y_{j\emptyset}^j = 1 - \frac{1}{R_0^j}$, $v_{j\emptyset}^j = R_0^j - 1$, $z_{j\emptyset}^j = 0$, *and* $y_{j\emptyset}^i = v_{j\emptyset}^i = z_{j\emptyset}^i = 0$, $\forall i \neq j$.
3. *For* $\mathcal{J} \neq \emptyset$ *and* $j = 0$, *we have* $x_{0\mathcal{J}} = 1/R_I^{\mathcal{J}}$, $y_{0\mathcal{J}}^i = \frac{1}{I_0^i}$, $v_{0\mathcal{J}}^i = \frac{R_0^i}{I_0^i}$, $z_{0\mathcal{J}}^i = \frac{R_0^i}{R_I^{\mathcal{J}}} - 1$, $\forall i \in \mathcal{J}$, *and* $y_{0\emptyset}^i = v_{0\emptyset}^i = z_{0\emptyset}^i = 0$, $\forall i \notin \mathcal{J}$.
4. *For* $\mathcal{J} \neq \emptyset$ *and* $j \in \mathcal{N} - \mathcal{J}$, *we have* $x_{j\mathcal{J}} = 1/R_I^{\mathcal{J}}$, $y_{j\mathcal{J}}^j = 1 - \frac{R_I^{\mathcal{J}}}{R_0^j}$, $v_{j\mathcal{J}}^j = R_0^j - R_I^{\mathcal{J}}$, $z_{j\mathcal{J}}^j = 0$. *Furthermore if* $i \in \mathcal{J}$, *we have* $y_{j\mathcal{J}}^i = \frac{1}{I_0^i}$, $v_{j\mathcal{J}}^i = \frac{R_0^i}{I_0^i}$, $z_{j\mathcal{J}}^i = \frac{R_0^i}{R_I^{\mathcal{J}}} - 1$, *and* $y_{j\mathcal{J}}^i = v_{j\mathcal{J}}^i = z_{j\mathcal{J}}^i = 0$ *otherwise.*

Although there is a large number of equilibria, Theorem 2.2 guarantees that only four of them can be globally stable. Before presenting this theorem we shall introduce some definitions.

Definition 2.1. *We define the set of the strong responders as*

$$\mathcal{S} = \{i \in \mathcal{N}; R_0^i > R_I^i\}.$$

Definition 2.2. *We shall say that the set S of strong responders is consistent if $j \in \mathcal{S}$ implies $i \in \mathcal{S}$ for all $i \in \mathcal{N}$ such that $i < j$.*

Definition 2.3. *We shall say that $\mathcal{I} \subseteq \mathcal{S}$ is an antigenic set if $R_0^i \geqslant R_I^{\mathcal{I}}$ for all $i \in \mathcal{I}$. In addition, if $R_0^i \leqslant R_I^{\mathcal{I}}$ for all $i \notin \mathcal{I}$ also holds, we shall say that I is a purely antigenic set.*

Definition 2.4. *Let l be the largest integer such that $\mathcal{I} = \{1, 2, ..., l\}$ is an antigenic set. If $\mathcal{I} \neq \emptyset$, then we shall say that $\mathcal{I}$ is the maximal antigenic set.*

We are now ready to present the result about the global stability

Theorem 2.2. [SZ11] *Assume that $R_0^i > R_0^{i+1}$ for $i = 1, ..., n-1$ and that the set of strong responders is consistent. Then, System (2.1), defined on $\mathbb{R}^{3n+1}_{\geqslant 0}$, with initial condition in its interior, has a globally asymptotically stable equilibrium given as follows*

1. *$W_{0\emptyset}$ if $R_0^1 \leqslant 1$;*
2. *$W_{1\emptyset}$ if $R_0^1 > 1$ and $R_0^1 \leqslant R_I^1$;*
3. *If $R_0^1 > R_I^1$, let $\mathcal{J}$ be the antigenic maximal set.*
   a. *$W_{0\mathcal{J}}$ if $\mathcal{J}$ is a purely antigenic set;*
   b. *$W_{j\mathcal{J}}$ otherwise, where j is the smallest integer outside $\mathcal{J}$.*

The proof of Theorems 2.1 and 2.2 can be found in [SZ11]. See also [Bob10].

CHAPTER 3

Influence of the Antiretroviral Therapy

A number of viral dynamics models including antiretroviral therapy (ART) have been proposed and studied to understand better the influence of these drugs in the HIV-1 dynamics [SDL03, KW97, BMSN97, PN99, NP02, VRM$^+$10, PH$^+$97, GKCM13, WDP98]. In order to predict whether the ART can eradicate HIV-1 or maintain viral loads at low levels, Perelson et al. [PN99] and Wein et al. [WDP98] analyze the steady-state behavior of a mathematical model that incorporates two types of antiretroviral (reverse transcriptase and protease inhibitors). We perform this analysis considering further CD8$^+$T cells, antigenic variation and the inhibitors of entry and integrase.

Specifically, we compare the steady-state of the system considering ART with the steady-state of the system without considering it. Both are given by Equation (1.3). Note that, for the system without ART, the inhibitor efficacy vanishes ($E_T = E_E = E_P = E_I = 0$). Although these two systems can be written in the dimensionless form of System (2.1), the change of variables needed for this results in different values for the basic reproductive rates R_0^i and R_I^i. Consequently, the steady-state provided by Theorem 2.2 will also change, as we will show in Theorem 3.1.

Before the main result, Theorem 3.1, shown in Section 3.2, we introduce some notation and prove some lemmas, which will be useful in the proof of the main theorem (Section 3.1).

3.1 Preliminaries Results

Let us fix the parameters β_i, λ, k_i, d, a_i, u_i, b_i, c_i and p_i of Equation (1.3), which will fix the parameters γ_i, η_i and σ_i in System (2.1).

In order to simplify the notation, we define the *efficacy of the ART* as

$$\psi = 1 - (1 - E_P)(1 - E_E)(1 - E_T)(1 - E_I).$$

Then, we consider two cases of System (1.3): *without* ART and *with* ART. That is, the first system considers $\psi = 0$, while the second one considers a given $\psi \in (0,1)$. Note that we do not consider the case that $\psi = 1$ because this implies in inhibitors 100% effective, which is not realistic.

For the system without ART we denote the basic reproductive ratio in the absence of the immune response by R_0^i, while for the system with ART by $\overline{R_0^i}$. Analogous notation will be used for the basic reproductive ratio in presence of the immune response, the set of strong responders, the maximal antigenic set and the equilibrium points.

As our intention is to apply Theorem 2.2 to both systems, the following assumption will be considered.

Assumption 3.1. *Assume that $R_0^i > R_0^{i+1}$ for $i = 1, .., n-1$ and that the set of strong responders $\mathcal{S} = \{i \in \mathcal{N}; R_0^i > R_I^i\}$ and $\overline{\mathcal{S}} = \{i \in \mathcal{N}; \overline{R_0^i} > \overline{R_I^i}\}$ are consistent.*

Note that

$$\overline{R_0^i} = R_0^i(1-\psi) < R_0^i. \tag{3.1}$$

Thus, $R_0^i > R_0^{i+1}$ for $i = 1, .., n-1$ implies that $\overline{R_0^i} > \overline{R_0^{i+1}}$ for $i = 1, .., n-1$, and then Assumption 3.1 ensures that both systems will satisfy the hypotheses of Theorem 2.2.

Before enunciating the main theorem of this chapter, we will prove some results.

Lemma 3.1. *Let Assumption 3.1 be satisfied and suppose that the maximal antigenic set is equal for both systems ($\mathcal{J} = \overline{\mathcal{J}}$). If $\mathcal{J}$ is purely antigenic, then so is $\overline{\mathcal{J}}$.*

Proof. Suppose $\mathcal{J}$ is purely antigenic and $\overline{\mathcal{J}}$ is not. As $\overline{\mathcal{J}}$ is the maximal antigenic set and is not purely antigenic, we have that $\overline{\mathcal{J}} \neq \mathcal{N}$. Then, let $j \in \mathcal{N}$ be the smallest integer outside $\overline{\mathcal{J}}$. Note that this index will satisfy

$$\overline{R_0^j} > 1 + \sum_{l \in \overline{\mathcal{J}}} \frac{\overline{R_0^l}}{I_0^l} \tag{3.2}$$

otherwise $\overline{\mathcal{J}}$ would be purely antigenic since, for all $i > j$,

$$\overline{R_0^i} < \overline{R_0^j} \leqslant 1 + \sum_{l \in \overline{\mathcal{J}}} \frac{\overline{R_0^l}}{I_0^l}.$$

On the other hand $j \notin \mathcal{J}$, since $\overline{\mathcal{J}} = \mathcal{J}$ and $j \notin \mathcal{J}$. As $\mathcal{J}$ is purely antigenic, it follows that $R_0^j \leqslant 1 + \sum_{l \in \mathcal{J}} \frac{R_0^l}{I_0^l}$. From this and using that $\psi \in (0,1)$, he have

$$\overline{R_0^j} = R_0^j(1-\psi) \leqslant \left(1 + \sum_{l \in \mathcal{J}} \frac{R_0^l}{I_0^l}\right)(1-\psi) \leqslant 1 + \sum_{l \in \mathcal{J}} \frac{R_0^l}{I_0^l}(1-\psi) = 1 + \sum_{l \in \mathcal{J}} \frac{\overline{R_0^l}}{I_0^l},$$

since $\psi \in (0,1)$. This contradicts the inequality (3.2), since $\overline{\mathcal{J}} = \mathcal{J}$. □

Lemma 3.2. *Let Assumption 3.1 be satisfied and $R_0^i > R_I^i$. Then, $\overline{R_0^i} \leqslant \overline{R_I^i}$ if, and only if, $\psi \geqslant \frac{R_0^i - R_I^i}{R_0^i - R_I^i + 1}$. Additionally, $\overline{R_0^i} > \overline{R_I^i}$ if, and only if, $\psi < \frac{R_0^i - R_I^i}{R_0^i - R_I^i + 1}$.*

Proof. Note that

$$\begin{aligned} \overline{R_0^i} \leqslant \overline{R_I^i} \quad &\Leftrightarrow \quad R_0^i(1-\psi) \leqslant 1 + \frac{R_0^i}{I_0^i}(1-\psi) = R_I^i(1-\psi) + \psi \\ &\Leftrightarrow \quad R_0^i - R_I^i \leqslant (R_0^i - R_I^i + 1)\psi. \end{aligned}$$

As $R_0^i > R_I^i$, we have that $R_0^i - R_I^i + 1 > 0$ and the above inequality is equivalent to

$$\psi \geqslant \frac{R_0^i - R_I^i}{R_0^i - R_I^i + 1}.$$

Similarly we prove the other case. □

Lemma 3.3. *Let Assumption 3.1 be satisfied. Then, the sets of strong responders satisfy $\overline{\mathcal{S}} \subseteq \mathcal{S}$. Additionally, let i be an element of $\mathcal{S}$. Then $i \notin \overline{\mathcal{S}}$ if, and only if, $\psi \geqslant \frac{R_0^i - R_I^i}{R_0^i - R_I^i + 1}$.*

Proof. If $i \notin \mathcal{S}$, then $R_0^i \leqslant R_I^i$ and

$$\overline{R_0^i} = R_0^i(1-\psi) \quad \leqslant \quad R_I^i(1-\psi) = 1 + \frac{R_0^i}{I_0^i}(1-\psi) - \psi = \overline{R_I^i} - \psi < \overline{R_I^i}.$$

Then, $i \notin \overline{\mathcal{S}}$ and thus $\overline{\mathcal{S}} \subseteq \mathcal{S}$. On the other hand if $i \in \mathcal{S}$, then $i \notin \overline{\mathcal{S}}$ if, and only if, $\overline{R_0^i} \leqslant \overline{R_I^i}$. By Lemma 3.2 this is equivalent to

$$\psi \geqslant \frac{R_0^i - R_I^i}{R_0^i - R_I^i + 1}.$$

□

Lemma 3.4. *Let Assumption 3.1 be satisfied. Then, the maximal antigenic sets satisfy $\overline{\mathcal{J}} \subseteq \mathcal{J}$.*

Proof. Suppose that the lemma is false. As $\mathcal{J} = \{1, ..., j-1\}$ and $\overline{\mathcal{J}} = \{1, ..., \overline{j} - 1\}$, for some j and $\overline{j}$, we must have that $j < \overline{j}$. Then $j \in \overline{\mathcal{J}} \subseteq \overline{\mathcal{S}} \subseteq \mathcal{S}$ where the last inclusion is due to Lemma 3.3. It follows that $R_0^j < 1 + \sum_{l \in \mathcal{J}} \frac{R_0^l}{I_0^l} + \frac{R_0^j}{I_0^j}$, otherwise $\mathcal{J}$ is not the maximal antigenic set once $\mathcal{J} \cup \{j\} \in \mathcal{S}$ would also be antigenic. As $\mathcal{J} \cup \{j\} \in \overline{\mathcal{J}}$, then

$$\begin{aligned} R_0^j(1-\psi) \quad &< \quad 1 - \psi + \sum_{l \in \mathcal{J}} \frac{R_0^l}{I_0^l}(1-\psi) + \frac{R_0^j}{I_0^j}(1-\psi) \\ &< \quad 1 + \sum_{l \in \mathcal{J}} \frac{R_0^l}{I_0^l}(1-\psi) + \frac{R_0^j}{I_0^j}(1-\psi) \leqslant 1 + \sum_{l \in \overline{\mathcal{J}}} \frac{R_0^l}{I_0^l}(1-\psi). \end{aligned}$$

But this contradicts $j \in \overline{\mathcal{J}}$. □

Lemma 3.5. *Let Assumption 3.1 be satisfied and let $\overline{j}$ be the smallest integer outside $\mathcal{J}$. If $W_{0\emptyset}$ is the asymptotic equilibrium of the system without ART, then the system with ART cannot has $\overline{W_{1\emptyset}}$, $\overline{W_{0\overline{\mathcal{J}}}}$, and $\overline{W_{\overline{j}\overline{\mathcal{J}}}}$ as asymptotic equilibriums. Furthermore, if $W_{1\emptyset}$ is the asymptotic equilibrium of the system without ART, then the system with ART cannot has $\overline{W_{0\overline{\mathcal{J}}}}$ and $\overline{W_{\overline{j}\overline{\mathcal{J}}}}$ as asymptotic equilibriums.*

Proof. Let $W_{0\emptyset}$ be the asymptotic equilibrium of the system without ART. By Theorem 2.2 we have that $R_0^1 \leqslant 1$. From this and using Equation (3.1), it follows that $\overline{R_0^1} \leqslant 1$. This ensures that $\overline{W_{1\emptyset}}$, $\overline{W_{0\overline{\mathcal{J}}}}$, and $\overline{W_{\overline{j}\overline{\mathcal{J}}}}$ cannot be the asymptotic equilibrium point.

Consider now that $W_{1\emptyset}$ is the asymptotic equilibrium point of the system without ART. Using Theorem 2.2 we have that $R_0^1 \leqslant R_I^1$. Multiplying this inequality by $(1-\psi)$ we get $\overline{R_0^1} \leqslant \overline{R_I^1} - \psi < \overline{R_I^1}$. This ensures that $\overline{W_{0\overline{\mathcal{J}}}}$ and $\overline{W_{\overline{j}\overline{\mathcal{J}}}}$ cannot be the asymptotic equilibrium point. □

Lemma 3.6. *Let Assumption 3.1 be satisfied and let $W_{j\mathcal{J}}$ and $\overline{W_{\overline{j}\overline{\mathcal{J}}}}$ be the asymptotic equilibrium points of the systems without and with ART, respectively. Then $\overline{\mathcal{J}} \cup \{\overline{j}\} \subseteq \mathcal{J} \cup \{j\} \cup \{0\}$.*

Proof. Lemma 3.4 ensures that $\overline{\mathcal{J}} \subseteq \mathcal{J}$. Then, if $\mathcal{J}$ is an empty set, so is $\overline{\mathcal{J}}$. In this case, the possible values for j and $\overline{j}$ are 0 and 1. Thus, the only case that would contradict the result is $j = 0$ and $\overline{j} = 1$. However, Lemma 3.5 ensures that this is not possible.

Consider now the case where $\mathcal{J} \neq \emptyset$. As $\overline{W_{\overline{j}\overline{\mathcal{J}}}}$ is the asymptotic equilibrium point of the system without ART, we have the following possibilities:

1. $\overline{\mathcal{J}} = \emptyset$ and $\overline{j} = 0$: then $\overline{\mathcal{J}} \cup \{\overline{j}\} = \{0\}$.
2. $\overline{\mathcal{J}} = \emptyset$ and $\overline{j} = 1$: then $\overline{\mathcal{J}} \cup \{\overline{j}\} = \{1\} \subseteq \mathcal{J}$, since $\mathcal{J}$ is an antigenic maximal set.
3. $\overline{\mathcal{J}} \neq \emptyset$ and $\overline{j} = 0$: then $\overline{\mathcal{J}} \cup \{\overline{j}\} = \overline{\mathcal{J}} \cup \{0\} \subseteq \mathcal{J} \cup \{0\}$, since $\overline{\mathcal{J}} \subseteq \mathcal{J}$ by Lemma 3.4.
4. $\overline{\mathcal{J}} \neq \emptyset$ and $\overline{j}$ the smallest integer outside $\overline{\mathcal{J}}$:
   - if $j = 0$, then $\mathcal{J}$ is a purely antigenic set but $\overline{\mathcal{J}}$ is not. In this case we have $\overline{\mathcal{J}} \subsetneq \mathcal{J}$, by Lemmas 3.1 and 3.4. From this we get $\overline{\mathcal{J}} \cup \{\overline{j}\} \subseteq \mathcal{J}$.
   - if $j \neq 0$, then j is the smallest integer outside $\mathcal{J}$. As $\overline{\mathcal{J}} \subset \mathcal{J}$ by Lemmas 3.4, it follows that $\overline{j} = j$ or $\overline{j} \in \mathcal{J}$. Thus $\overline{\mathcal{J}} \cup \{\overline{j}\} \subseteq \mathcal{J} \cup \{j\}$.

□

3.2 Changes in the Steady-state

In this section we will state the main theorem of this chapter. This result will indicate which changes in the steady-state of the system are due to the inclusion of ART. Surprisingly, this theorem shows that ART may change the equilibrium $W_{0\mathcal{J}}$ to $\overline{W_{\overline{j}\overline{\mathcal{J}}}}$ with $\overline{j} \neq 0$. In biological terms, this means that the immune system will tend to stop combating the $\overline{j}$ strain. Nevertheless, the theorem also ensures that, in all cases, the viral load equilibrium of each strain will not increase.

Theorem 3.1. *Let Assumption 3.1 be satisfied. For each possible asymptotic equilibrium point of the system without ART, the efficacy of the ART, ψ, determines which point will be the asymptotic equilibrium point of the system with ART, according to table bellow. Furthermore, the components of the asymptotic equilibrium points will satisfy $x \leqslant \overline{x}$ and $v_i \geqslant \overline{v_i}$ for all $i \in \mathcal{N}$, with strict inequality for the viral loads in the case $v_i \neq 0$.*

	$\psi \in \left(0, \frac{R_0^1 - R_I^1}{R_0^1 - R_I^1 + 1}\right)$	$\psi \in \left[\frac{R_0^1 - R_I^1}{R_0^1 - R_I^1 + 1}, 1 - \frac{1}{R_0^1}\right)$	$\psi \in \left[1 - \frac{1}{R_0^1}, 1\right)$
$W_{0\emptyset}$	$\overline{W_{0\emptyset}}$	$\overline{W_{0\emptyset}}$	$\overline{W_{0\emptyset}}$
$W_{1\emptyset}$	$\overline{W_{1\emptyset}}$	$\overline{W_{1\emptyset}}$	$\overline{W_{0\emptyset}}$
$W_{0\mathcal{J}}$	$\overline{W_{0\overline{\mathcal{J}}}}$ if $\overline{\mathcal{J}}$ purely antigenic $\overline{W_{j\overline{\mathcal{J}}}}$ otherwise	$\overline{W_{1\emptyset}}$	$\overline{W_{0\emptyset}}$
$W_{j\mathcal{J}}$	$\overline{W_{0\overline{\mathcal{J}}}}$ if $\overline{\mathcal{J}}$ purely antigenic $\overline{W_{j\overline{\mathcal{J}}}}$ otherwise	$\overline{W_{1\emptyset}}$	$\overline{W_{0\emptyset}}$

Proof. We analyze every possible combination of steady-states, i.e. the combinations that are not addressed in Lemma 3.5. In each case, we find out the values of ϕ that allow the occurrence of it. In addition, we compare the equilibrium components corresponding to viral load and CD4$^+$T cells concentration, according to Theorem 2.1.

1. $W_{0\emptyset}$ and $\overline{W_{0\emptyset}}$
   If $\psi \in (0,1)$, then $\overline{R_0^1} = (1-\psi)R_0^1 < 1$, since $R_0^1 \leqslant 1$. This ensures that $\overline{W_{0\emptyset}}$ will be the asymptotic equilibrium point of the system with ART. Furthermore,

$$\begin{aligned} x_{0\emptyset} - \overline{x_{0\emptyset}} &= 1 - 1 = 0 \leqslant 0 \quad \text{and} \\ v_{0\emptyset}^i - \overline{v_{0\emptyset}^i} &= 0 - 0 = 0 \geqslant 0 \ \ \forall i \in \mathcal{N}. \end{aligned}$$

2. $W_{1\emptyset}$ and $\overline{W_{0\emptyset}}$
   As $R_0^1 > 1$, it is possible to take $\psi \in \left[1 - \frac{1}{R_0^1}, 1\right) \subseteq (0,1)$, and then $\overline{R_0^1} = (1-\psi)R_0^1 \leqslant 1$. This ensures that $\overline{W_{0\emptyset}}$ will be the asymptotic equilibrium point of the system with ART. Furthermore,

$$\begin{aligned} x_{1\emptyset} - \overline{x_{0\emptyset}} &= \frac{1}{R_0^1} - 1 < 0, \\ v_{1\emptyset}^1 - \overline{v_{0\emptyset}^1} &= (R_0^1 - 1) - 0 > 0, \quad \text{and} \\ v_{1\emptyset}^i - \overline{v_{0\emptyset}^i} &= 0 - 0 = 0 \geqslant 0 \ \ \forall i \neq 1. \end{aligned}$$

3. $W_{1\emptyset}$ and $\overline{W_{1\emptyset}}$
   As $R_0^1 > 1$, it is possible to take $\psi \in \left(0, 1 - \frac{1}{R_0^1}\right) \subseteq (0,1)$, and then $\overline{R_0^1} = (1-\psi)R_0^1 > 1$. This ensures that $\overline{W_{1\emptyset}}$ will be the asymptotic equilibrium point of the system with ART.

Furthermore,

$$\begin{aligned} x_{1\emptyset} - \overline{x_{1\emptyset}} &= \frac{1}{R_0^1} - \frac{1}{(1-\psi)R_0^1} = -\frac{1}{R_0^1}\frac{\psi}{1-\psi} < 0, \\ v_{1\emptyset}^1 - \overline{v_{1\emptyset}^1} &= [R_0^1 - 1] - [R_0^1(1-\psi) - 1] = R_0^1\psi > 0, \quad \text{and} \\ v_{1\emptyset}^i - \overline{v_{1\emptyset}^i} &= 0 - 0 = 0 \geqslant 0 \ \ \forall i \neq 1. \end{aligned}$$

4. $W_{0\mathcal{J}}$ and $\overline{W_{0\emptyset}}$

   As $R_0^1 > 1$, it is possible to take $\psi \in \left[1 - \frac{1}{R_0^1}, 1\right) \subseteq (0,1)$, and then $\overline{R_0^1} = (1-\psi)R_0^1 \leqslant 1$. This ensures that $\overline{W_{0\emptyset}}$ will be the asymptotic equilibrium point of the system with ART. Furthermore,

$$\begin{aligned} x_{0\mathcal{J}} - \overline{x_{0\emptyset}} &= \frac{1}{R_I^{\mathcal{J}}} - 1 = -\frac{\sum_{i\in\mathcal{J}} \frac{R_0^i}{I_0^i}}{R_I^{\mathcal{J}}} < 0, \\ v_{0\mathcal{J}}^i - \overline{v_{0\emptyset}^i} &= (R_I^i - 1) - 0 > 0 \ \ \forall i \in \mathcal{J}, \quad \text{and} \\ v_{0\mathcal{J}}^i - \overline{v_{0\emptyset}^i} &= 0 - 0 = 0 \ \ \forall i \notin \mathcal{J}. \end{aligned}$$

   Note that the first inequality is strict because $1 \in \mathcal{J}$, and thus $\sum_{i\in\mathcal{J}} \frac{R_0^i}{I_0^i} > 0$.

5. $W_{0\mathcal{J}}$ and $\overline{W_{1\emptyset}}$

   As $R_0^1 > R_I^1$, Lemma 3.2 ensures that $\overline{R_0^1} \leqslant \overline{R_I^1}$ if, and only if, $\psi \geqslant \frac{R_0^1 - R_I^1}{R_0^1 - R_I^1 + 1}$. On the other hand $\overline{R_0^1} > 1$ if, and only if, $\psi < 1 - \frac{1}{R_0^1}$. Note that this interval is not empty because

$$\left[1 - \frac{1}{R_0^1}\right] - \left[\frac{R_0^1 - R_I^1}{R_0^1 - R_I^1 + 1}\right] = \frac{1}{R_0^1(I_0^1 - 1)} > 0.$$

   Then, $\overline{W_{1\emptyset}}$ will be the asymptotic equilibrium point of the system with ART if, and only if, $\psi \in \left[\frac{R_0^1 - R_I^1}{R_0^1 - R_I^1 + 1}, 1 - \frac{1}{R_0^1}\right) \subset (0,1)$. Furthermore, as $1 \in \mathcal{J}$ we have $\overline{R_0^1} \leqslant \overline{R_I^1} < R_I^1 \leqslant R_I^{\mathcal{J}}$. Whence,

$$\begin{aligned} x_{0\mathcal{J}} - \overline{x_{1\emptyset}} &= \frac{1}{R_I^{\mathcal{J}}} - \frac{1}{\overline{R_0^1}} < 0, \\ v_{0\mathcal{J}}^1 - \overline{v_{1\emptyset}^1} &= \left[R_I^1 - 1\right] - \left[\overline{R_0^1} - 1\right] > 0, \\ v_{0\mathcal{J}}^i - \overline{v_{1\emptyset}^i} &= (R_I^i - 1) - 0 > 0 \ \ \forall i \in \mathcal{J} \setminus \{1\}, \quad \text{and} \\ v_{0\mathcal{J}}^i - \overline{v_{1\emptyset}^i} &= 0 - 0 = 0 \ \ \forall i \notin \mathcal{J}. \end{aligned}$$

6. $W_{0\mathcal{J}}$ and $\overline{W_{0\overline{\mathcal{J}}}}$

   It follows from Lemma 3.2 that $\overline{W_{0\overline{\mathcal{J}}}}$ will be the asymptotic equilibrium point of the system with ART if, and only if, $\psi \in \left(0, \frac{R_0^1 - R_I^1}{R_0^1 - R_I^1 + 1}\right) \subset (0,1)$ and $\overline{\mathcal{J}}$ is purely antigenic.

Furthermore, as $\psi \in (0,1)$ and $\overline{\mathcal{J}} \subseteq \mathcal{J}$ (Lemma 3.4), we have $R_i^{\mathcal{J}} > \overline{R_I^{\overline{\mathcal{J}}}}$, whence

$$x_{0\mathcal{J}} - \overline{x_{0\overline{\mathcal{J}}}} = \frac{1}{R_I^{\mathcal{J}}} - \frac{1}{\overline{\overline{R_I^{\overline{\mathcal{J}}}}}} < 0.$$

From $R_I^i > \overline{R_I^i}$ for all i such that $R_0^i \neq 0$ (particularly for all $i \in \mathcal{J}$), it follows that

$$\begin{aligned} v_{0\mathcal{J}}^i - \overline{v_{0\overline{\mathcal{J}}}^i} &= \left[R_I^i - 1\right] - \left[\overline{R_I^i} - 1\right] > 0 \ \ \forall i \in \mathcal{J} \cap \overline{\mathcal{J}}, \\ v_{0\mathcal{J}}^i - \overline{v_{0\overline{\mathcal{J}}}^i} &= \left[R_I^i - 1\right] - 0 > 0 \ \ \forall i \in \mathcal{J} \setminus \overline{\mathcal{J}}, \quad \text{and} \\ v_{0\mathcal{J}}^i - \overline{v_{0\overline{\mathcal{J}}}^i} &= 0 - 0 = 0 \ \ \forall i \notin \mathcal{J}. \end{aligned}$$

7. $W_{0\mathcal{J}}$ and $\overline{W_{\overline{j}\overline{\mathcal{J}}}}$

It follows from Lemma 3.2 that $\overline{W_{0\overline{\mathcal{J}}}}$ will be the asymptotic equilibrium point of the system with ART if, and only if, $\psi \in \left(0, \frac{R_0^1 - R_I^1}{R_0^1 - R_I^1 + 1}\right) \subset (0,1)$ and $\overline{\mathcal{J}}$ is not purely antigenic. Similarly to the Case 6 we have

$$x_{0\mathcal{J}} - \overline{x_{\overline{j}\overline{\mathcal{J}}}} = \frac{1}{R_I^{\mathcal{J}}} - \frac{1}{\overline{\overline{R_I^{\overline{\mathcal{J}}}}}} < 0.$$

We know that the maximal sets have the form $\mathcal{J} = \{1, ..., j-1\}$ and $\overline{\mathcal{J}} = \{1, ..., \overline{j} - 1\}$, with $j \geqslant \overline{j}$ is due to Lemma 3.4. Furthermore, as $\mathcal{J}$ is purely antigenic and $\overline{\mathcal{J}}$ is not, Lemma 3.1 ensures that $j \neq \overline{j}$. Consider then the following cases to analyze the values of the viral load components.

(a) $i < \overline{j}$

In this case $i \in \mathcal{J} \cap \overline{\mathcal{J}}$. Then

$$v_{0\mathcal{J}}^i - \overline{v_{\overline{j}\overline{\mathcal{J}}}^i} = \left[\frac{R_0^i}{I_0^i}\right] - \left[\frac{\overline{R_0^i}}{I_0^i}\right] = \psi \frac{R_0^i}{I_0^i} > 0.$$

(b) $i = \overline{j}$

In this case $i \in \mathcal{J}$. Then

$$v_{0\mathcal{J}}^i - \overline{v_{\overline{j}\overline{\mathcal{J}}}^i} = \left[\frac{R_0^{\overline{j}}}{I_0^{\overline{j}}}\right] - \left[\overline{R_0^{\overline{j}}} - \overline{R_I^{\overline{\mathcal{J}}}}\right] = \frac{R_0^{\overline{j}}}{I_0^{\overline{j}}} - \overline{R_0^{\overline{j}}} + 1 + \sum_{l \in \overline{\mathcal{J}}} \frac{\overline{R_0^l}}{I_0^l}. \tag{3.3}$$

If $\overline{j} \in \overline{\mathcal{S}}$ then $\overline{R_0^{\overline{j}}} < 1 + \sum_{l \in \overline{\mathcal{J}}} \frac{\overline{R_0^l}}{I_0^l} + \frac{\overline{R_0^{\overline{j}}}}{I_0^{\overline{j}}}$, otherwise $\overline{\mathcal{J}}$ is not the maximal antigenic set. Returning to Equation (3.3)

$$v_{0\mathcal{J}}^i - \overline{v_{\overline{j}\overline{\mathcal{J}}}^i} > \frac{R_0^{\overline{j}}}{I_0^{\overline{j}}} - \left[1 + \sum_{l \in \overline{\mathcal{J}}} \frac{\overline{R_0^l}}{I_0^l} + \frac{\overline{R_0^{\overline{j}}}}{I_0^{\overline{j}}}\right] + 1 + \sum_{l \in \overline{\mathcal{J}}} \frac{\overline{R_0^l}}{I_0^l} = \frac{R_0^{\overline{j}}}{I_0^{\overline{j}}} - \frac{\overline{R_0^{\overline{j}}}}{I_0^{\overline{j}}} = \frac{R_0^{\overline{j}}}{I_0^{\overline{j}}} \psi > 0.$$

If $\overline{j} \notin \overline{\mathcal{S}}$ then $\overline{R_0^{\overline{j}}} \leqslant 1 + \frac{\overline{R_0^{\overline{j}}}}{I_0^{\overline{j}}}$. Returning to Equation (3.3)

$$v_{0\mathcal{J}}^i - \overline{v_{\overline{j}\mathcal{J}}^i} \;>\; \frac{R_0^{\overline{j}}}{I_0^{\overline{j}}} - \left[1 + \frac{\overline{R_0^{\overline{j}}}}{I_0^{\overline{j}}}\right] + 1 + \sum_{l \in \overline{\mathcal{J}}} \frac{\overline{R_0^l}}{I_0^l} = \frac{R_0^{\overline{j}}}{I_0^{\overline{j}}}\psi + \sum_{l \in \overline{\mathcal{J}}} \frac{\overline{R_0^l}}{I_0^l} > 0.$$

(c) $i > \overline{j}$ and $i < j$

In this case $i \in \mathcal{J}$ and $i \notin \overline{\mathcal{J}} \cup \{\overline{j}\}$. Then,

$$v_{0\mathcal{J}}^i - \overline{v_{\overline{j}\mathcal{J}}^i} \;=\; \left[R_I^i - 1\right] - 0 > 0.$$

(d) $i \geqslant j$

In this case $i \notin \mathcal{J}$ and $i \notin \overline{\mathcal{J}} \cup \{\overline{j}\}$. Then,

$$v_{0\mathcal{J}}^i - \overline{v_{\overline{j}\mathcal{J}}^i} \;=\; 0 - 0 = 0.$$

8. $W_{j\mathcal{J}}$ and $\overline{W_{0\emptyset}}$

Similarly to the Item 4, we have that $x_{j\mathcal{J}} - \overline{x_{0\emptyset}} < 0$ and that $\overline{W_{0\emptyset}}$ will be the asymptotic equilibrium point of the system with ART if, and only if, $\psi \in \left[1 - \frac{1}{R_0^1}, 1\right)$. Furthermore

$$\begin{aligned}
v_{j\mathcal{J}}^i - \overline{v_{0\emptyset}^i} &= \frac{R_0^i}{I_0^i} - 0 > 0 \;\; \forall i \in \mathcal{J}, \\
v_{j\mathcal{J}}^j - \overline{v_{0\emptyset}^j} &= (R_0^j - R_I^j) - 0 > 0, \text{ and} \\
v_{j\mathcal{J}}^i - \overline{v_{0\emptyset}^i} &= 0 - 0 = 0 \;\; \forall i \notin \mathcal{J} \cup \{j\}.
\end{aligned}$$

9. $W_{j\mathcal{J}}$ and $\overline{W_{1\emptyset}}$

Similarly to the Item 5, we have that $x_{j\mathcal{J}} - \overline{x_{1\emptyset}} < 0$ and that $\overline{W_{1\emptyset}}$ will be the asymptotic equilibrium point of the system with ART if, and only if, $\psi \in \left[\frac{R_0^1 - R_I^1}{R_0^1 - R_I^1 + 1}, 1 - \frac{1}{R_0^1}\right)$.

Furthermore, as $1 \in \mathcal{J}$ and $\overline{R_I^1} \geqslant \overline{R_0^1}$, we have

$$\begin{aligned}
v_{j\mathcal{J}}^1 - \overline{v_{1\emptyset}^1} &= \frac{R_0^1}{I_0^1} - (\overline{R_0^1} - 1) = \overline{R_I^1} - \overline{R_0^1} + \psi\frac{R_0^1}{I_0^1} \geqslant \psi\frac{R_0^1}{I_0^1} > 0 \;\; \forall i \in \mathcal{J}, \\
v_{j\mathcal{J}}^i - \overline{v_{1\emptyset}^i} &= \frac{R_0^i}{I_0^i} - 0 > 0 \;\; \forall i \in \mathcal{J} \setminus \{1\}, \\
v_{j\mathcal{J}}^j - \overline{v_{1\emptyset}^j} &= (R_0^j - R_I^j) - 0 > 0, \text{ and} \\
v_{j\mathcal{J}}^i - \overline{v_{1\emptyset}^i} &= 0 - 0 = 0 \;\; \forall i \notin \mathcal{J} \cup \{j\}.
\end{aligned}$$

10. $W_{j\mathcal{J}}$ and $\overline{W_{0\overline{\mathcal{J}}}}$

Similarly to the Item 6, we have that $x_{j\mathcal{J}} - \overline{x_{0\overline{\mathcal{J}}}} < 0$ and that $\overline{W_{0\overline{\mathcal{J}}}}$ will be the asymptotic equilibrium point of the system with ART if, and only if, $\psi \in \left(0, \frac{R_0^1 - R_I^1}{R_0^1 - R_I^1 + 1}\right)$ and $\overline{\mathcal{J}}$ is purely antigenic.

Furthermore

$$\begin{aligned}
v^i_{j\mathcal{J}} - \overline{v^i_{0\overline{\mathcal{J}}}} &= \frac{R^i_0}{I^i_0} - \left[\overline{R^i_I} - 1\right] = \psi\frac{R^i_0}{I^i_0} > 0 \ \ \forall i \in \mathcal{J} \cap \overline{\mathcal{J}} \\
v^i_{j\mathcal{J}} - \overline{v^i_{0\overline{\mathcal{J}}}} &= \frac{R^i_0}{I^i_0} - 0 > 0 \ \ \forall i \in \mathcal{J} \setminus \overline{\mathcal{J}}, \\
v^j_{j\mathcal{J}} - \overline{v^j_{0\overline{\mathcal{J}}}} &= \left[R^j_0 - R^j_I\right] - 0 > 0, \quad \text{and} \\
v^i_{j\mathcal{J}} - \overline{v^i_{0\overline{\mathcal{J}}}} &= 0 - 0 = 0 \ \ \forall i \notin \mathcal{J} \cup \{j\}.
\end{aligned}$$

11. $W_{j\mathcal{J}}$ and $\overline{W_{\overline{j}\overline{\mathcal{J}}}}$
Similarly to the Item 7, we have that $x_{j\mathcal{J}} - \overline{x_{\overline{j}\overline{\mathcal{J}}}} < 0$ and that $\overline{W_{\overline{j}\overline{\mathcal{J}}}}$ will be the asymptotic equilibrium point of the system with ART if, and only if, $\psi \in \left(0, \frac{R^1_0 - R^1_I}{R^1_0 - R^1_I + 1}\right)$ and $\overline{\mathcal{J}}$ is not purely antigenic. Furthermore,

$$\begin{aligned}
v^i_{j\mathcal{J}} - \overline{v^i_{\overline{j}\overline{\mathcal{J}}}} &= \frac{R^i_0}{I^i_0} - \frac{\overline{R^i_0}}{I^i_0} = \psi\frac{R^i_0}{I^i_0} > 0 \ \ \forall i < \overline{j}, \\
v^i_{j\mathcal{J}} - \overline{v^i_{\overline{j}\overline{\mathcal{J}}}} &= \frac{R^i_0}{I^i_0} - 0 > 0 \ \ \forall i > \overline{j} \text{ and } i < j, \\
v^j_{j\mathcal{J}} - \overline{v^j_{\overline{j}\overline{\mathcal{J}}}} &= \left[R^j_0 - R^{\mathcal{J}}_I\right] - 0 > 0, \text{ and} \\
v^i_{j\mathcal{J}} - \overline{v^i_{\overline{j}\overline{\mathcal{J}}}} &= 0 - 0 = 0 \ \ \forall i > j.
\end{aligned}$$

Finally, for $i = \overline{j}$ the proof is similar to the Item 7(b).

□

Remark 1. Theorem 3.1 is also true to original System (1.3). The first part of this theorem follows from the fact that the conditions that determine the asymptotically stable equilibrium point depend on the dimensionless parameters R^i_0 and R^i_I. These parameters do not change in the dimensionless system. Denote by X and V_i the components of the stable equilibrium point of original System (1.3) without ART corresponding to the concentration of $CD4^+T$ and the viral load, respectively. Analogously to the original system with ART, $\overline{X}$ and $\overline{V_i}$. Note that

$$V_i - \overline{V_i} = \frac{\beta_i}{d}\left(v_i - \overline{v_i}\right) \ \text{ and } \ X - \overline{X} = \frac{\lambda}{d}\left(x - \overline{x}\right).$$

Since λ/d and β_i/d are positive parameters, the second part of Theorem 3.1 also holds.

3.3 Numerical Example

According to Theorem 3.1, it is possible that the ART changes the equilibrium point $W_{0\mathcal{J}}$ to $\overline{W_{\overline{j}\overline{\mathcal{J}}}}$, with $\overline{j}$ not null. This means that the introduction of the treatment induces the immune system to stop fighting the $\overline{j}$-th strain, in the long term. However, Theorem 3.1 also ensures that the viral load equilibrium of the $\overline{j}$-th strain will be reduced, even in this case.

In this section, we illustrate this case with an example. Consider System (2.1) with one virus strain and with basic reproductive ratios given by $R_0^1 = 15$ and $R_I^1 = 6$. By Theorem 2.2, the globally asymptotic stable equilibrium is $W_{0\{1\}}$.

From the biological viewpoint, the infection tends to remain in the host organism, while being fought by the immune system.

Now, consider the case with ART and suppose that the treatment efficacy is $\psi = 0.92$. Then, $\overline{R_0^1} = 1.2$ and $\overline{R_I^1} = 1.4$. As $\psi \in [0.9, 0.9\overline{3}) = \left[\frac{R_0^1 - R_I^1}{R_0^1 - R_I^1 + 1}, 1 - \frac{1}{R_0^1}\right)$, Theorem 3.1 ensures that the globally asymptotic stable equilibrium is $\overline{W}_{1\emptyset}$.

In this case, the virions tend to remain in the host organism without being fought by the immune system. Figure. 3.1(c) illustrates this change in behavior of the immune system ($CD8^+T$ cells). In red we can see the $CD8^+T$ cells converging to a non-null value. This solutions corresponds to the system without ART. The blue line depicts the $CD8^+T$ cells for the system with ART. In this case, it vanishes.

Despite the immune system having stopped fighting the infection, note that the viral load equilibrium shows a significant reduction (Figures. 3.1(b)). Furthermore, the concentration of healthy $CD4^+T$ cells is larger for the case with ART (Figures. 3.1(a)).

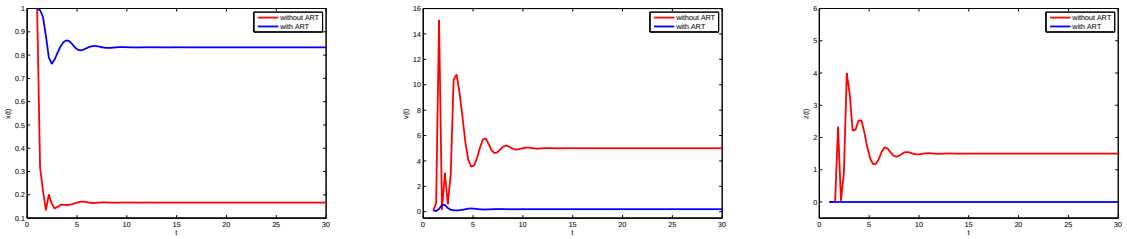

(a) healthy $CD4^+T$ cells (b) virions (c) $CD8^+T$ cells

Figure 3.1: **Numerical Example of the ART influence.** Numerical solutions of the system without ART (in red) and with ART (in blue). The parameters considered are $R_0^1 = 15$, $R_I^1 = 6$, and $\psi = 0.92$. Figures (a), (b), and (c) depict the concentrations of the health $CD4^+T$ cells, the virions, and the $CD8^+T$, respectively

3.4 Conclusion

Since the HIV-1 treatment consists of antiretroviral drugs that affect the virus replication cycle, it is natural to expected that the treatment will reduce the basic reproductive ratios (R_0^i and R_I^i) of each viral strain. Indeed, we saw in Section 2.1 that the entry inhibitor affects the infection rate (β_i), while the other inhibitors affect the virions production rate (k_i). This causes a reduction in the basic reproductive ratio in the absence of the immune response of all strains. More than this, we have that the reduction will be proportional to $(1-\psi)$, according to Equation (3.1). This mean that, the higher the efficiency of ART, the greater is the reduction in the basic reproductive ratios. The same occurs with the basic reproductive ratios in the presence of the immune response (R_I^i). For a model without the immune response or antigenic variation and just for two of these inhibitors, similar results were obtained by Perelson et al. [PN99] and also reported by Bonhoeffer et al. [BMSN97], for other HIV-1 models.

Another important aspect concerns the combination therapy. Since the efficacy of ART is given by $\psi = 1-(1-E_P)(1-E_E)(1-E_T)(1-E_I)$, our analysis shows that combined inhibitors provide a better treatment than using them alone (consider fixed the efficacies of the inhibitors). This is in accordance with [PR08, WDP98, PN99, KW97, NM00] and with the current medical recommendation [dep13].

Moreover, our analysis allows much more than just ensuring that the treatment has a positive effect. Firstly, Lemma 3.6 ensures that the strains that tend to vanish, in the long term, will continue with this property after ART. This is quite consistent from the biological view point. Additionally, Lemma 3.5 ensures that, depending on the expected equilibrium before ART, some asymptotic steady state cannot be obtained regardless of the ART efficacy ψ. The first case of the lemma is to be expected to happen since an individual capable of eradicating the infection, in the long term, without ART, should still be able to do it with ART. The second case is not so obvious. Along with Lemma 3.4, it ensures that the introduction of ART, regardless of ψ, cannot increase the number of strains which are combated by the body. The other combinations of steady-states of the systems with and without ART may be obtained depending on the ART efficacy ψ. The detailed description of the intervals at which the efficiency must belong, in each case, is given by Theorem 3.1.

Theorem 3.1 allows us to choose, strictly speaking, an ART with efficacy, ψ, that leads to a more beneficial steady-state for the patient. In fact, by this theorem, if we take ART with efficacy greater than $1-1/R_0^1$, then the new expected equilibrium will be the equilibrium free of the infection. This value gives us the necessary minimum efficacy for a successful treatment. Note that this minimum efficacy depends only on the basic reproductive number of the most virulent strain (R_0^1). As this infection rate is a parameter whose value depends on the patient, this minimum efficacy also depends on the patient. This corroborates to the recommendation of specific treatments for each patient. Furthermore, we emphasize that it is very relevant to know this minimal efficacy, especially taking into account that the treatment may be associated with unwanted side effects not directly related to the HIV-1 infection, such as cardiovascular disease,

liver abnormalities, bone loss, as well as cancers and loss of neurocognitive functions [dep13].

From the biological viewpoint, maybe it is not possible to obtain this necessary minimum efficacy for a successful treatment. Nevertheless, $\overline{W_{1\emptyset}}$, $\overline{W_{0\overline{\mathcal{J}}}}$, and $\overline{W_{\overline{j}\overline{\mathcal{J}}}}$ can mean an appropriate treatment if the viral load equilibriums are small enough. In fact, the aim of ART is to maintain low viral loads and to increase the concentration of $CD4^+T$ cells, preventing opportunistic infections [dep13]. So it is also important to assess the change of the equilibrium components, even in the case where there is no change in the equilibrium type. Note that, according to Theorem 3.1, ART always results in a decrease of the viral load equilibrium (unless it is null), and increase (or at least stay the same) the equilibrium of $CD4^+T$ cells concentrations. This is in accordance with publications [PH^+97,W^+99,Xia07,WDP98,NP02,BMSN97,NM00,PN99,VRM^+10]. Furthermore, as the viral load equilibrium directly depends on the basic reproductive ratio, R_0^i, the reduction in the viral load will be proportional to the efficacy of the ART. This generalizes the result obtained by Equation [PN99] for a model without antigenic variation, $CD8^+T$ cells, integrase and entry inhibitors.

Theorem 3.1 further shows that ART may induce, in the long term, the body to stop fighting a strain, i.e. it changes the equilibrium $W_{0\mathcal{J}}$ to $\overline{W_{\overline{j}\overline{\mathcal{J}}}}$, with $\overline{j}$ not null. Although this seems unexpected from the biological view point, note again that the non-null viral load equilibrium will decrease, even in this case. As mentioned above, the key point for a successful treatment is to keep the viral load low.

Note that our study concerns the changes in the asymptotic equilibrium points. This represents the behavior of the system in the long term. Therefore, even in the case that the new equilibrium point will be the equilibrium free of the infection, there is no way to ensure the eradication of the infection in finite time. What we know is that the viral load will be close to zero for large enough time. Thus, in finite time, we still have all the components positive (even if very small). Hence, if the treatment is interrupted, the asymptotic equilibrium point return to be the same as before the treatment, that is, the infection may return. This shows the importance of not interrupting the HIV-1 treatment.

CHAPTER 4

Multiscale Analysis of HIV Dynamics

This chapter is a transcription of the published paper *A Singularly Perturbed HIV Model with Treatment and Antigenic Variation*, written by the author in collaboration with Jorge P. Zubelli.

The dynamics of the virions of HIV-1 is much faster than the dynamics of the cells that host the viruses [GKCM13, Llo01, Kir96, PH$^+$95, SR88, Qui96, M$^+$00, Imm13]. While CD4$^+$T cells have a half-life of the order of days, virions have a half-life of about a few hours [SR88, Qui96, M$^+$00]. These two intrinsic time scales of the HIV-1 dynamics leads to a singularly perturbed system. In order to deal with perturbed problems, multiscale analysis techniques have been used in many areas [OB78, Was02, KC96, VB90], including biological modeling of infectious diseases in [BPL13, Sou11, Sie12].

In this chapter we perform a multiscale analysis of System (2.1), using Tikhonov's theorem. This result leads to a way of approximating the solutions of the perturbed system by solutions of a reduced system. The interest in such a reduction lies on the fact that, in many cases, the complexity of the problem is considerably reduced. Indeed, for certain parameters, System (2.1) becomes very stiff and the respective reduced system offers a robust approximation, as we shall see here.

We start the chapter providing the necessary background on Tikhonov's theorem. After that, we analyze the properties of the reduced system with respect to steady-state and global stability. We prove the global stability of such system by exhibiting an appropriate Lyapunov's function. This function is inspired by the one used by Souza and Zubelli [SZ11]. Then we present the main result, which consists of applying Tikhonov's theorem to System (2.1). We conclude with some numerical examples and a brief analysis of the performance of the systems involved in our result, thus substantiating the applicability of our results.

4.1 Preliminaries: Tikhonov's Theorem

The singularly perturbed system that we are interested on has the form

$$\begin{aligned} \dot{x} &= f(t,x,y), \quad x(0) = x_0, \\ \varepsilon\dot{y} &= g(t,x,y), \quad y(0) = y_0, \end{aligned} \tag{4.1}$$

where $\varepsilon \ll 1$ and x and y can be vectors. Thus, this system has two time scales of order 1 and ε. The degenerate system associated with System (4.1) is obtained by considering $\varepsilon = 0$

$$\begin{aligned} \dot{x} &= f(t,x,y), \quad x(0) = x_0 \\ 0 &= g(t,x,y). \end{aligned} \tag{4.2}$$

To apply Tikhonov's theorem we need several assumptions, described below.

Assumption 4.1. *Assume that the functions f and g*

$$\begin{aligned} f &: [0,T] \times \bar{\mathcal{U}} \times \mathcal{V} \mapsto \mathbb{R}^{m_1}, \\ g &: [0,T] \times \bar{\mathcal{U}} \times \mathcal{V} \mapsto \mathbb{R}^{m_2}, \end{aligned}$$

are continuous and satisfy the Lipschitz condition w.r.t. the variables x and y in $[0,T] \times \bar{\mathcal{U}} \times \mathcal{V}$, where $\bar{\mathcal{U}}$ is a compact set in $\mathbb{R}^{m_1}$, $\mathcal{V}$ is a bounded open set in $\mathbb{R}^{m_2}$, and $T > 0$.

Assumption 4.2. *Assume that there exists a function $\phi(t,x)$ continuous in $[0,T] \times \bar{\mathcal{U}}$ such that $\phi(t,x) \in \mathcal{V}$ and*

$$g(t,x,\phi(t,x)) \equiv 0.$$

This function will be referred to as a root of the equation $g(t,x,y) = 0$. Furthermore, assume that the root ϕ is isolated in $[0,T] \times \bar{\mathcal{U}}$, i.e. there exists $\delta > 0$, independently of x, such that

$$0 < ||y - \phi(t,x)|| < \delta$$

implies $g(t,x,y) \neq 0$ in $[0,T] \times \bar{\mathcal{U}}$.

Definition 4.1. *The system of differential equations*

$$\frac{d\tilde{y}}{d\tau} = g(t,x,\tilde{y}) \tag{4.3}$$

for which t and x are treated as parameters, is called the boundary layer equation associated to System (4.1).

Assumption 4.3. *Let $\tilde{y}$ be the solution of the boundary layer equation associated to System (4.1). Assume that for any $\eta > 0$ there exists $\delta > 0$ such that, for all $(t,x) \in [0,T] \times \bar{\mathcal{U}}$, the inequality $||\tilde{y}(0,t,x) - \phi(t,x)|| < \delta$ implies*

$$||\tilde{y}(\tau,t,x) - \phi(t,x)|| < \eta \quad \text{and} \quad \lim_{\tau \to \infty} \tilde{y}(\tau,t,x) = \phi(t,x),$$

for all $\tau > 0$, where the above convergence is uniform for $(t,x) \in [0,T] \times \bar{\mathcal{U}}$.

In other words, Assumption 4.3 requires that the singular point $\phi(t,x)$ of the boundary layer is an asymptotically stable equilibrium, uniformly w.r.t. $(t,x) \in [0,T] \times \bar{\mathcal{U}}$.

Definition 4.2. *The reduced system associated to System* (4.1) *is*

$$\begin{aligned} \dot{\bar{x}} &= f(t, \bar{x}, \phi(t, \bar{x})), \\ \bar{x}(0) &= x_0, \end{aligned} \tag{4.4}$$

where $\phi(t,x)$ is a root of the equation $g(t,x,y,) = 0$.

Note that the reduced system is the first equation of degenerate System (4.2), replacing a root $\phi(t,x)$.

Assumption 4.4. *Assume that the function $(t,x) \mapsto f(t,x,\phi(t,x))$ satisfies the Lipschitz condition w.r.t. x in $[0,T] \times \bar{\mathcal{U}}$. Additionally, assume that the unique solution of reduced System* (4.4) *on $[0,T]$ satisfies $\bar{x}(t) \in \operatorname{int}(\bar{\mathcal{U}})$ for all $t \in (0,T)$.*

Assumption 4.5. *Assume that y_0 belongs to the basin of attraction of the solution $y = \phi(0,x_0)$ of equation $g(0,x_0,y) = 0$. That is, the solution $\hat{y} = \hat{y}(\tau)$ of the simplified initial layer equation*

$$\frac{d\hat{y}}{d\tau} = g(0, x_0, \hat{y}), \tag{4.5}$$

with $\hat{y}(0) = y_0$, satisfies $\hat{y}(\tau) \in \mathcal{V}$ for all $\tau \geqslant 0$, and

$$\lim_{\tau \to \infty} \hat{y}(\tau) = \phi(0, x_0).$$

Theorem 4.1 (Tikhonov's Theorem)**.** *Under Assumptions 4.1-4.5, there exists $\varepsilon_0 > 0$ such that for any $\varepsilon \in]0, \varepsilon_0]$ there exists a unique solution $(x(t,\varepsilon), y(t,\varepsilon))$ of the singularly perturbed System* (4.1) *on $[0,T]$ satisfying*

$$\lim_{\varepsilon \to 0} x(t,\varepsilon) = \bar{x}(t), \quad t \in [0,T]$$

and

$$\lim_{\varepsilon \to 0} y(t,\varepsilon) = \bar{y}(t), \quad t \in (0,T],$$

where $(\bar{x}(t), \bar{y}(t))$ is the solution of degenerate System (4.2)*.*

Tikhonov's theorem connects the solutions of the singularly perturbed system and the degenerate system. Note that only the first convergence in Tikhonov's theorem is uniform (w.r.t. $t \in [0,T]$). However, in the second limit the convergence is uniform on any interval $[T_0, T]$ with $T_0 > 0$. This is the so-called initial layer effect and one can include the initial layer term to obtain the uniform convergence on $[0,T]$.

Proposition 4.1. *Let Assumptions 4.1-4.5 be satisfied. Then,*

$$\lim_{\varepsilon \to 0} [y(t,\varepsilon) - \bar{y}(t) - \hat{y}(t/\varepsilon) + \phi(0,x_0)] = 0, \quad t \in [0,T],$$

where $\bar{y}(t)$ is the solution of degenerate System (4.2)*, $\hat{y}(t/\varepsilon)$ is the solutions of the simplified initial layer problem given by equation* (4.5)*, and ϕ is the root of Assumption 2.*

We now add one extra assumption, namely

Assumption 4.6. *Suppose that $|\delta_1| < \mu$ and $|\delta_2| < \mu$ where μ is a sufficiently small but fixed number independent of ε. Assume that, for $t \in [0,T]$, $f(t, \bar{x}+\delta_1, \bar{y}+\hat{y}+\delta_2)$ and $g(t, \bar{x}+\delta_1, \bar{y}+\hat{y}+\delta_2)$ are continuous together with their derivatives w.r.t. δ_1 and δ_2 up and including the second order.*

Under this further assumption, one can prove the stronger result

Theorem 4.2. *Let Assumptions 4.1-4.6 be satisfied and suppose that the partial derivative $\frac{\partial g}{\partial y}(t,x,y)\Big|_{y=\phi(t,x)}$ exists, is continuous and is negative for $t \in [0,T]$. Then, we have the following estimates*

$$x(t,\varepsilon) = \bar{x}(t) + \mathcal{O}(\varepsilon),$$

and

$$y(t,\varepsilon) = \bar{y}(t) + \hat{y}\left(t/\varepsilon\right) - \phi(0,x_0) + \mathcal{O}(\varepsilon),$$

uniformly on $[0,T]$.

For the proof of the above results we refer the reader to [TVS84, Was02, BPL13, VB90].

4.2 The Perturbed System

The difference in the time scales of the HIV-1 virions and the lymphocytes leads to a singularly perturbed system. Indeed, the CD8$^+$T cells and the healthy CD4$^+$T cells have a half-life about 80 days, while the virions have a half-life of about 6 hours [H$^+$99, SR88, Qui96, M$^+$00]. This leads to a η_i much bigger than γ_i and σ_i. Therefore, it is natural to consider the dynamics of System (2.1) for $\eta_i = \overline{\eta}_i/\varepsilon$, where ε is a small parameter and $\overline{\eta}_i$ has the same order of magnitude of γ_i and σ_i. Applying the change of variables described above, System (2.1) takes the form

$$\begin{aligned}
\dot{x} =& 1 - x - x\sum_{i\in\mathcal{N}} v_i \\
\dot{y}_i =& \gamma_i\left(x v_i - y_i - y_i z_i\right) \\
\varepsilon\dot{v}_i =& \overline{\eta}_i\left(R_0^i y_i - v_i\right) \\
\dot{z}_i =& \sigma_i\left(I_0^i y_i z_i - z_i\right)
\end{aligned} \tag{4.6}$$

subject to initial conditions x_0, y_0^i, v_0^i and z_0^i. Note that this system has the form of System (4.1). Thus, we can use Tikhonov's theorem to connect its solutions with the solutions of the reduced system associated. In this case, the reduced system is

$$\begin{aligned}
\dot{x} =& 1 - x - x\sum_{i\in\mathcal{N}} R_0^i y_i \\
\dot{y}_i =& \gamma_i\left(x R_0^i y_i - y_i - y_i z_i\right) \\
\dot{z}_i =& \sigma_i\left(I_0^i y_i z_i - z_i\right)
\end{aligned} \tag{4.7}$$

with initial conditions x_0, y_0^i and z_0^i.

Note that this system has the form of a food chain System [HS98], where the uninfected $CD4^+T$ cells act as the environmental resources, the infected $CD4^+T$ cells as prey and the $CD8^+T$ cells as predators.

Reduced System Properties

Before applying Tikhonov's theorem, we shall prove some properties of reduced System (4.7). Note that the non-negative orthant of $\mathbb{R}^{2n+1}$ is invariant by the flow of the system. Moreover, if the initial conditions are in the interior of $\mathbb{R}^{2n+1}_{\geqslant 0}$, then all solutions will remain in this open set for all $t \geqslant 0$. We also have that the solutions are bounded, as stated in the proposition below. The proof follows the ideas of Pastore [Pas05].

Proposition 4.2. *Let $\psi : [0, \infty) \to \mathbb{R}^{2n+1}$ be the solution of System (4.7) with $\psi(t_0) \in \mathbb{R}^{2n+1}_{\geqslant 0}$. Then, $\psi \in L^\infty[t_0, \infty)$.*

Proof. As the system is positively invariant, we have

$$\dot{x}(t) = 1 - x(t) - x(t) \sum_{i \in \mathcal{N}} v_i(t) \leqslant 1 - x(t).$$

This implies that $\frac{d}{dt}(e^t x(t)) \leqslant e^t$. Then, integrating this inequality from t_0 to t, we obtain

$$x(t) \leqslant 1 - e^{t_0 - t} + e^{t_0 - t} x(t_0) \leqslant 1 + x(t_0),$$

which proves the limitation of x. With respect to y_i, note that

$$\dot{y}_i(t) = \gamma_i \left(x R_0^i y_i - y_i - y_i z_i \right) \leqslant \gamma_i \left(x R_0^i - 1 \right) y_i \leqslant \left(\gamma_M x R_0^i - \gamma_m \right) y_i,$$

where $\gamma_M = \max_{i \in \mathcal{N}} \{\gamma_i\}$ and $\gamma_m = \min_{i \in \mathcal{N}} \{\gamma_i\}$. Denoting $\mathcal{Y}(t) = \sum_{i \in \mathcal{N}} y_i(t)$, we have

$$\dot{\mathcal{Y}}(t) + \gamma_m \mathcal{Y}(t) \leqslant \gamma_M x(t) \sum_{i \in \mathcal{N}} R_0^i y_i(t) = \gamma_M (-\dot{x} + 1 - x(t)).$$

Thus, integrating from t_0 to t, we have

$$\mathcal{Y}(t) \leqslant \ \mathcal{Y}(t_0) e^{\gamma_m (t_0 - t)} + \gamma_M e^{-\gamma_m t} \int_{t_0}^{t} \left(1 - \dot{x}(s) - x(s)\right) e^{\gamma_m s} ds. \tag{4.8}$$

Note that

$$\int_{t_0}^{t} x(s) e^{\gamma_m (s-t)} ds \leqslant \frac{1 + x(t_0)}{\gamma_m} e^{-\gamma_m t_0},$$

since $x(t) \leqslant 1 + x(t_0)$. Using this, $e^{\gamma_m (t_0 - t)} \leqslant 1$, and $x(t) \geqslant 0$, we obtain from Equation (4.8) that

$$\mathcal{Y}(t) \leqslant \mathcal{Y}(t_0) + \frac{\gamma_M}{\gamma_m} + \gamma_M x(t_0) + \frac{\gamma_M}{\gamma_m} \left(\gamma_m - 1\right) \left(1 + x(t_0)\right) e^{-\gamma_m t_0}.$$

Therefore, $\mathcal{Y}(t)$ is limited and, as $y_i(t) \geqslant 0$ for all $t \geqslant t_0$, it follows that $y_i(t)$ is limited.

Similarly, we can prove that

$$\mathcal{Z}(t) \leqslant \mathcal{Z}(t_0) + \frac{\sigma_M}{\sigma_m} + \sigma_M x(t_0) + \frac{\sigma_M}{\sigma_m}\left(\sigma_m - 1\right)\left(1 + x(t_0)\right) e^{-\sigma_m t_0},$$

where $\sigma_M = \max_{i\in\mathcal{N}}\{\sigma_i\}$, $\sigma_m = \min_{i\in\mathcal{N}}\{\sigma_i\}$ and $\mathcal{Z}(t) = \sum_{i\in\mathcal{N}} z_i(t)$. This and the positivity of each $z_i(t)$ imply the result. □

Using the same notation for the equilibrium points that was used in Chapter 2, we have the following result

Theorem 4.3. *If the basic reproductive ratios of each virus strain are distinct, then System* (4.7) *admits* $2^{n-1}(2+n)$ *equilibrium points* $W_{j\mathcal{J}}$ *that correspond to the points described in Theorem 2.1 omitting entries of* v_i*.*

The proof of this theorem follows the same idea of the analogous theorem presented in [SZ11]. Finally, we prove the global stability for System (4.7), using Lyapunov's Theory.

Theorem 4.4. *Assume that* $R_0^i > R_0^{i+1}$ *for* $i = 1, ..., n-1$ *and that the set of strong responders is consistent. Then, System* (4.7)*, defined on* $\mathbb{R}^{2n+1}_{\geqslant 0}$*, with initial condition in its interior, has a globally asymptotically stable equilibrium given as follows*

1. $W_{0\emptyset}$ *if* $R_0^1 \leqslant 1$*;*
2. $W_{1\emptyset}$ *if* $R_0^1 > 1$ *and* $R_0^1 \leqslant R_I^1$*;*
3. *If* $R_0^1 > R_I^1$*, let* $\mathcal{J}$ *be the antigenic maximal set.*
   a. $W_{0\mathcal{J}}$ *if* $\mathcal{J}$ *is a purely antigenic set;*
   b. $W_{j\mathcal{J}}$ *otherwise, where* j *is the smallest integer outside* $\mathcal{J}$*.*

Proof. The existence of the j mentioned in the case (3.a) is proved in [SZ11]. For each asymptotically stable equilibrium point $W^* = (x^*, y_1^*, ..., z_n^*)$ consider the following function

$$V = x - x^* \ln\frac{x}{x^*} + \sum_{i\in\mathcal{N}}\left[\frac{1}{\gamma_i}\left(y_i - y_i^* \ln\frac{y_i}{y_i^*}\right) + \frac{1}{\sigma_i I_0^i}\left(z_i - z_i^* \ln\frac{z_i}{z_i^*}\right)\right],$$

where the term with logarithm should be omitted if the corresponding coordinate is zero. Then,

$$\dot{V} \;=\; 1 - x - \frac{x^*}{x} + x^* + \sum_{i\in\mathcal{N}}\left[x^* y_i R_0^i - y_i - R_0^i y_i^* x + y_i^* + z_i y_i^* - z_i^* y_i + \frac{z_i^*}{I_0^i} - \frac{z_i}{I_0^i}\right].$$

For each case, we will replace the respective equilibrium point in the equation above and we will prove that $\dot{V} \leqslant 0$, i.e. V is a Lyapunov's function. In addition, we have that, for each case, the set for which the equality $\dot{V} = 0$ is satisfied contains only one positively invariant subset and this subset is exactly the respective equilibrium point. This proves the theorem.

Case (1)

Since $R_0^i \leqslant R_0^1 \leqslant 1$, we have

$$\dot{V} = 1 - x - \frac{1}{x} + 1 + \sum_{i\in\mathcal{N}} \left[y_i R_0^i - y_i - \frac{z_i}{I_0^i} \right] = -\frac{(1-x)^2}{x} + \sum_{i\in\mathcal{N}} \left[y_i (R_0^i - 1) - \frac{z_i}{I_0^i} \right] \leqslant 0.$$

Case (2)

Since $R_0^1 \leqslant R_I^1$, we have

$$\begin{aligned}\dot{V} =& 1 - x - \frac{1}{R_0^1 x} + \frac{1}{R_0^1} - R_0^1 x + x + 1 - \frac{1}{R_0^1} + z_1 \left(1 - \frac{1}{R_0^1}\right) - \frac{z_1}{I_0^1} - \sum_{i=2}^{n} \frac{z_i}{I_0^i} \\ =& -\frac{1}{R_0^1 x}(R_0^1 x - 1)^2 + z_1 \left(1 - \frac{R_I^1}{R_0^1}\right) - \sum_{i=2}^{n} \frac{z_i}{I_0^i} \leqslant 0.\end{aligned}$$

Case (3.a)

Using that $1 + \sum_{i\in\mathcal{J}} \frac{R_0^i}{I_0^i} = R_I^{\mathcal{J}}$ and that $\mathcal{J}$ is a purely antigenic set, we have

$$\begin{aligned}\dot{V} =& 1 - x - \frac{1}{R_I^{\mathcal{J}} x} + \frac{1}{R_I^{\mathcal{J}}} + \sum_{i\in\mathcal{J}} \left[-\frac{R_0^i}{I_0^i} x + \frac{R_0^i}{R_I^{\mathcal{J}}} \frac{1}{I_0^i} \right] + \sum_{i\notin\mathcal{J}} \left[\left(\frac{R_0^i}{R_I^{\mathcal{J}}} - 1 \right) y_i - \frac{z_i}{I_0^i} \right] \\ =& -\frac{1}{R_I^{\mathcal{J}} x} \left(R_I^{\mathcal{J}} x - 1 \right)^2 + \sum_{i\notin\mathcal{J}} \left[\left(\frac{R_0^i}{R_I^{\mathcal{J}}} - 1 \right) y_i - \frac{z_i}{I_0^i} \right] \leqslant 0.\end{aligned}$$

Case (3.b)

Using that $\sum_{i\in\mathcal{J}} \frac{R_0^i}{I_0^i} = R_I^{\mathcal{J}} - 1$, we have

$$\begin{aligned}\dot{V} =& 1 - x - \frac{1}{x R_0^j} + \frac{1}{R_0^j} + \sum_{i\in\mathcal{J}} \left[-\frac{R_0^i}{I_0^i} x + \frac{R_0^i}{R_0^j I_0^i} \right] + \sum_{i\notin\mathcal{J}\cup\{j\}} \left[\left(\frac{R_0^i}{R_0^j} - 1 \right) y_i - \frac{z_i}{I_0^i} \right] \\ &+ \left[-R_0^j x \left(1 - \frac{R_I^{\mathcal{J}}}{R_0^j}\right) + \left(1 - \frac{R_I^{\mathcal{J}}}{R_0^j}\right) + z_j \left(1 - \frac{R_I^{\mathcal{J}}}{R_0^j}\right) - \frac{z_j}{I_0^j} \right] + \sum_{i\notin\mathcal{J}\cup\{j\}} \left[\left(\frac{R_0^i}{R_0^j} - 1 \right) y_i - \frac{z_i}{I_0^i} \right] \\ =& -\frac{1}{R_0^j x} \left(R_0^j x - 1 \right)^2 + \frac{z_j}{R_0^j} \left(R_0^j - R_I^{\mathcal{J}} - \frac{1}{I_0^j} \right) + \sum_{i\notin\mathcal{J}\cup\{j\}} \left[\left(\frac{R_0^i}{R_0^j} - 1 \right) y_i - \frac{z_i}{I_0^i} \right] \\ \leqslant& \frac{z_j}{R_0^j} \left(R_0^j - R_I^{\mathcal{J}} - \frac{R_0^j}{I_0^j} \right) + \sum_{i\notin\mathcal{J}\cup\{j\}} \left[\left(\frac{R_0^i}{R_0^j} - 1 \right) y_i \right].\end{aligned}$$

Note that, if j belongs to the set of strong responders then $R_0^j - R_I^{\mathcal{J}} - \frac{R_0^j}{I_0^j} \leqslant 0$ (since $\mathcal{J}$ is maximal). Otherwise we have $R_0^i - 1 \leqslant \frac{R_0^j}{I_0^j}$, and then $R_0^j - R_I^{\mathcal{J}} - \frac{R_0^j}{I_0^j} \leqslant -(R_I^{\mathcal{J}} - 1) \leqslant 0$. Furthermore,

$$\sum_{i\notin\mathcal{J}\cup\{j\}} \left[\left(\frac{R_0^i}{R_0^j} - 1 \right) y_i \right] \leqslant 0,$$

since for every $i \notin \mathcal{J} \cup \{j\}$ we have $i > j$ and then, $R_0^i < R_0^j$. Therefore, we have $\dot{V} \leqslant 0$. $\square$

4.3 The Asymptotic Expansion of the Model

We shall now apply Tikhonov's theorem in order to show that as $\varepsilon \to 0$ the solution of System (4.6) approaches the solution of the degenerate system. We know that solutions of this system are bounded (see [Pas05]) and only the bounds on v_i depend on ε. However, for fixed $\varepsilon_0 > 0$, we have that for all $\varepsilon \leqslant \varepsilon_0$ the concentrations of v_i are bounded by constants independently of ε. Since the solution of the degenerate system is also bounded (independently of ε), we can choose a compact set in $\bar{\mathcal{U}} \subset \mathbb{R}^{2n+1}$ and a bounded open set $\mathcal{V} \subset \mathbb{R}^n$ such that the solutions of both systems belong to $\bar{\mathcal{U}} \times \mathcal{V}$ for all $t > 0$. Moreover, for initial conditions in the interior of $\mathbb{R}^{3n+1}_{\geqslant 0}$, we can choose $\bar{\mathcal{U}}$ such that the solutions (x, y, z) will remain in the interior of this compact set for all $t \geqslant 0$.

Theorem 4.5. *Let $\bar{\mathcal{U}}$ and $\mathcal{V}$ be the sets described above. Then, there exists $\varepsilon_0 > 0$ such that for any $\varepsilon \in (0, \varepsilon_0]$ we have a unique solution $(x(t,\varepsilon), y(t,\varepsilon), v(t,\varepsilon), z(t,\varepsilon))$ of Problem (4.1) with initial conditions in the interior of the corresponding sets. Moreover,*

$$\begin{aligned}
&\lim_{\varepsilon \to 0} [x(t,\varepsilon) - \bar{x}(t)] = 0 \\
&\lim_{\varepsilon \to 0} [y_i(t,\varepsilon) - \bar{y}_i(t)] = 0 \\
&\lim_{\varepsilon \to 0} \left[v_i(t,\varepsilon) - R_0^i \bar{y}_i(t) - \left(v_0^i - R_0^i y_0^i\right) e^{-t/\varepsilon}\right] = 0 \\
&\lim_{\varepsilon \to 0} [z_i(t,\varepsilon) - \bar{z}_i(t)] = 0
\end{aligned}$$

where $(\bar{x}, \bar{y}, \bar{z})$ is the solution of reduced System (4.7).

Proof. The result follows from Tikhonov's Theorem 4.1 and Proposition 4.1 since the Assumptions $1 - 5$ are valid, as we show below.

We write System (4.6) as

$$\begin{aligned}
\dot{x} &= f_1(t, x, y, z, v) \\
\dot{y} &= f_2(t, x, y, z, v) \\
\dot{z} &= f_3(t, x, y, z, v) \\
\varepsilon \dot{v} &= g(t, x, y, z, v)
\end{aligned}$$

where f and g are the appropriate entries of the right hand side of System (4.6).
Assumption 2: Let a $\phi : [0, T] \times \bar{\mathcal{U}} \mapsto \mathbb{R}^n$ be defined by $\phi_i(t, x, y, z) = R_0^i y_i(t)$. Then, ϕ is an isolated root of g since given $\delta > 0$ we have, for any $(t, x, y, z) \in [0, T] \times \bar{\mathcal{U}}$

$$\begin{aligned}
0 < ||v - \phi|| < \delta \Leftrightarrow & 0 < |v_i - R_0^i y_i| < \delta \ \forall i \in \mathcal{N} \\
\Leftrightarrow & g_i(t, x, y, z, \phi) \neq 0 \ \forall i \in \mathcal{N}.
\end{aligned}$$

Assumption 3: The boundary layer equation is given by

$$\frac{d\tilde{v}}{d\tau} = g(t, x, y, z, \tilde{v})$$

where t, x, y, and z are treated as parameters. Then,

$$\tilde{v}_i(\tau, t, x, y, z) = R_0^i y_i(t) + c_i e^{-\overline{\eta}_i \tau},$$

with c_i constants. Given $\nu > 0$, choose $\delta = \nu$. Thus, if

$$|\tilde{v}_i(0, t, x, y, z) - \phi_i(t, x, y, z)| < \delta,$$

then $|c_i| < \delta$ and

$$|\tilde{v}_i(\tau, t, x, y, z) - \phi_i(t, x, y, z)| = |c_i e^{-\overline{\eta}_i \tau}| \leqslant \delta e^{-\overline{\eta}_i \tau} \leqslant \delta = \nu,$$

for all $i \in \mathcal{N}$ and $(t, x, y, z) \in [0, T] \times \bar{\mathcal{U}}$.
Furthermore,

$$\lim_{\tau \to \infty} \tilde{v}_i(\tau, t, x, y, z) = R_0^i y_i(t) = \phi_i(t, x, y, z).$$

Assumption 4: As $\bar{\mathcal{U}}$ is bounded, the Lipschitz condition of f follows and the choice of $\bar{\mathcal{U}}$ yields the second part of the assumption.
Assumption 5: Note that the solution $\hat{v}$ of the simplified initial layer equation is

$$\hat{v}_i(\tau) = R_0^i y_0^i + (v_0^i - R_0^i y_0^i) e^{-\overline{\eta}_i \tau}.$$

Thus, $\hat{v}_i(\tau) \in \mathcal{V}$, due to the choice of $\mathcal{V}$, and

$$\lim_{\tau \to \infty} \hat{v}_i(\tau) = R_0^i y_0^i = \phi_i(0, x_0, y_0, z_0).$$

Therefore, v_0 belongs to the basin of attraction of the solution $v = \phi(0, x_0, y_0, z_0)$ of equation $g(0, x_0, y_0, z_0, v) = 0$.

Applying Tikhonov's Theorem, we have the limits for x, y and z. As for the limit of v, just replace

$$\begin{aligned}
\bar{v}_i &= R_0^i \bar{y}_i(t) \\
\hat{v}_i &= R_0^i y_i(t) + \left(v_0^i - R_0^i y_i(t)\right) e^{-t\overline{\eta}_i/\varepsilon} \\
\phi_i(0, x_0, y_0, z_0) &= R_0^i y_0^i
\end{aligned}$$

in the limit of Proposition 4.1. □

Theorem 4.6. *Let $(x(t,\varepsilon), y_i(t,\varepsilon), v_i(t,\varepsilon), z_i(t,\varepsilon))$ be the solution of Problem (4.1) with initial condition in the interior of $\bar{\mathcal{U}} \times \mathcal{V}$ and $(\bar{x}, \bar{y}_i, \bar{z}_i)$ be the solution of reduced System (4.7). Then, we have the following estimates*

$$\begin{aligned} x(t,\varepsilon) =& \bar{x}(t) + \mathcal{O}(\varepsilon) \\ y_i(t,\varepsilon) =& \bar{y}_i(t) + \mathcal{O}(\varepsilon) \\ v_i(t,\varepsilon) =& R_0^i \bar{y}_i(t) + \left(v_0^i - R_0^i y_0^i\right) e^{-t\overline{\eta}_i/\varepsilon} + \mathcal{O}(\varepsilon) \\ z_i(t,\varepsilon) =& \bar{z}_i(t) + \mathcal{O}(\varepsilon) \end{aligned}$$

uniformly on $[0,T]$.

Proof. Take f and g as in the proof of the previous theorem. Since $y_0^i > 0$, we have that

$$\frac{\partial g_i}{\partial v}(t,x,y,z,v)\bigg|_{v=\phi(t,x,y,z)} = -R_0^i y_i(t) < 0 \ .$$

Furthermore, it is continuous for all $t \in [0,T]$. Also, since $\bar{x}, \bar{y}, \bar{z}$ and $\hat{v}$ are continuous, it is easy to see that Assumption 6 is valid. Applying Theorem 4.2 we obtain the above estimates. □

4.4 Numerical Examples

In this section we present some numerical illustrations of the results presented in this chapter. Note that all parameters involved are non-dimensional. It is worth pointing out that the numerical solutions of the original problem have been computed with relative tolerance of 10^{-10} to avoid any numerical instabilities. For simplicity, we consider first the case of one strain $(n = 1)$ without treatment.

Figure 4.1 shows the attractiveness of the quasi-steady state for viral load, i.e. it compares the solution of the quasi-steady state $\bar{v}(t) = R_0\bar{y}(t)$ with the approximation of $v(t,\varepsilon)$, given by Theorem 4.6, for different values of ε. Here $\bar{y}$ is the solution of reduced System (4.7). This illustrates that the initial layer term, given by $(v_0 - R_0 y_0)\, e^{-t/\varepsilon}$, tends to vanish for ε small enough, except for the very small times due to the difference in initial conditions.

Figure 4.2 illustrates the expressions of Theorems 4.5 and 4.6 for the susceptible cells (x), infected cells (y), viral load (v) and defense cells (z), respectively. According to our results, when we decrease ε, the right hand side of the expressions approximate the solutions of Problem (4.6).

Similarly to the previous ones, Figure 4.3 illustrates the expressions of Theorems 4.5 and 4.6 when considering three strains. Note that the parameters were chosen to represent case (3.b) of Theorem 2.2, where the set of strong responders is $\mathcal{S} = \{1,2\}$ and the antigenic maximal set is $\mathcal{J} = \{1\}$ and it is not purely antigenic. Then, the asymptotically stable equilibrium point is $W_{2\{1\}}$, i.e. the virion whose index is 2 (red) remains in the organism without being fought by the immune system, the virion of index 1 (yellow) also remains in the body but being fought by the immune system, while the other virion (green) vanish.

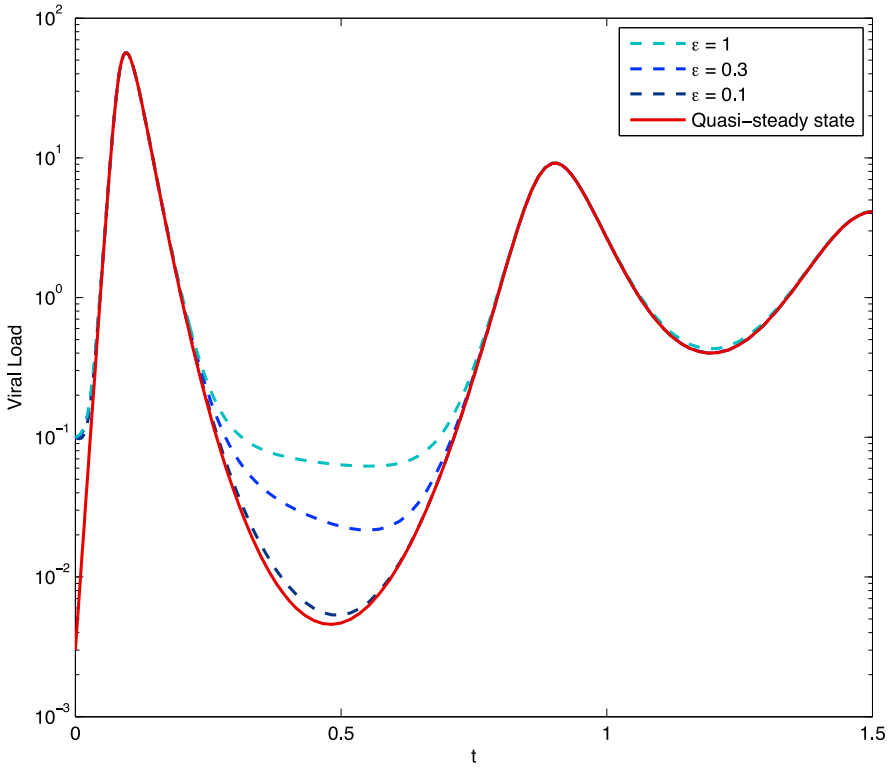

Figure 4.1: **Attractiveness of the quasi-steady state for viral load.** The continuous line is $\bar{v}(t) = R_0\bar{y}(t)$, where $\bar{y}$ is the solution of the reduced system, and the dotted lines is the approximation of $v(t,\varepsilon)$, i.e. $R_0\bar{y}(t) + (v_0 - R_0 y_0)\, e^{-t/\varepsilon}$ for different values of ε. The parameters used are $\gamma = 62$, $\sigma = 5$, $x_0 = 1$, $y_0 = 10^{-3}$, $v_0 = 10^{-1}$, $z_0 = 10^{-6}$, $R_0 = 3$, $I_0 = 2$ and $\varepsilon = 1, 0.3$ and 0.1.

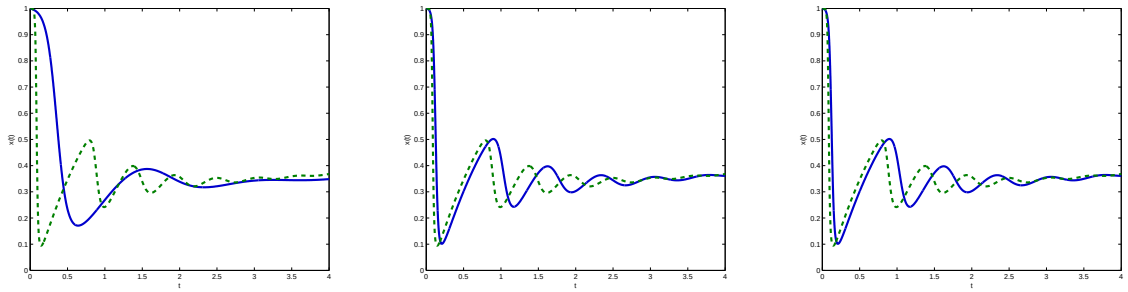

(a) $\varepsilon = 0.1$ (b) $\varepsilon = 0.01$ (c) $\varepsilon = 0.001$

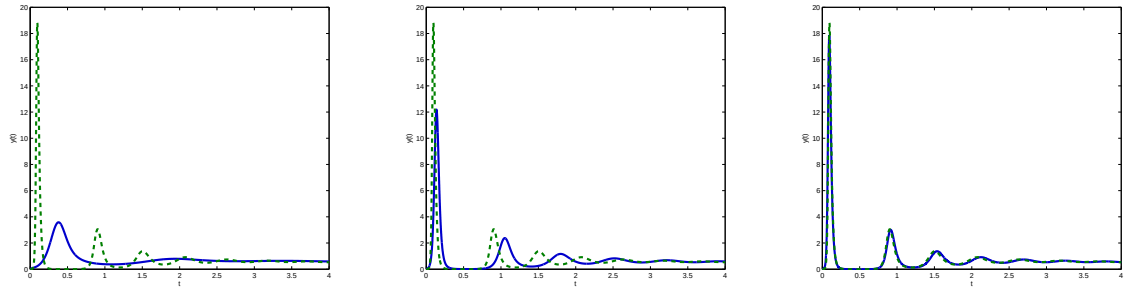

(d) $\varepsilon = 0.1$ (e) $\varepsilon = 0.01$ (f) $\varepsilon = 0.001$

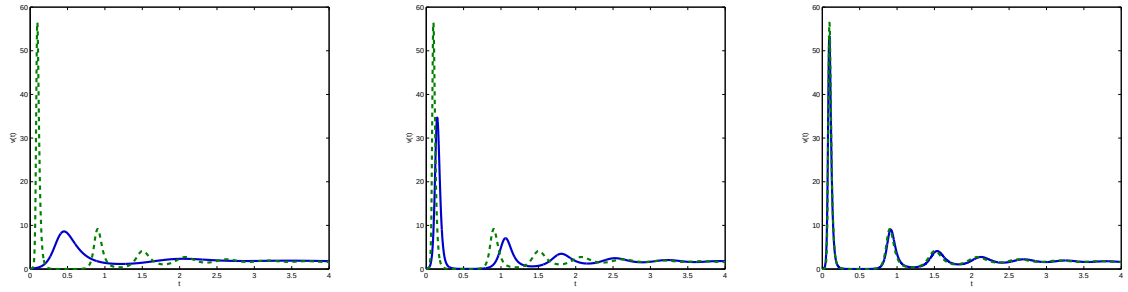

(g) $\varepsilon = 0.1$ (h) $\varepsilon = 0.01$ (i) $\varepsilon = 0.001$

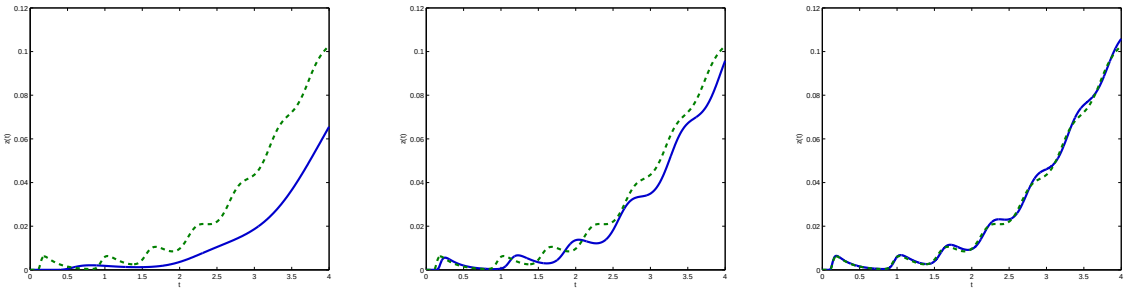

(j) $\varepsilon = 0.1$ (k) $\varepsilon = 0.01$ (l) $\varepsilon = 0.001$

Figure 4.2: **Convergence of the asymptotic solution.** We illustrate the convergence of the asymptotic solution given by Theorems 4.5 and 4.6. The continuous line represents the solution of System (4.6) while the dotted lines are the respective approximations of $x(t,\varepsilon)$, $y(t,\varepsilon)$, $v(t,\varepsilon)$, and $z(t,\varepsilon)$ given by the results of Section 4.3. The parameters used are $\gamma = 62$, $\sigma = 5$, $x_0 = 1$, $y_0 = 10^{-3}$, $v_0 = 10^{-1}$, $z_0 = 10^{-6}$, $R_0 = 3$, $I_0 = 2$, $\bar{\eta} = 1$ and $\varepsilon = 0.1, 0.01$ and 0.001.

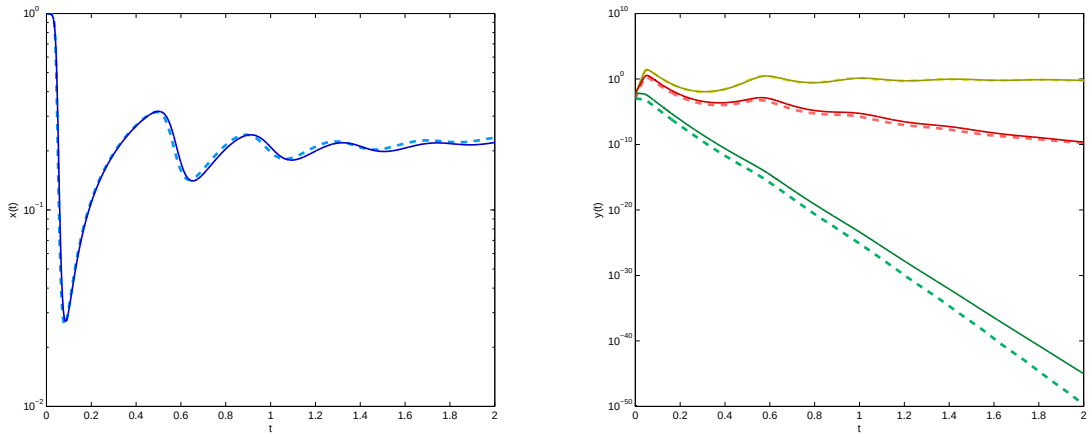

(a) x

(b) y_i

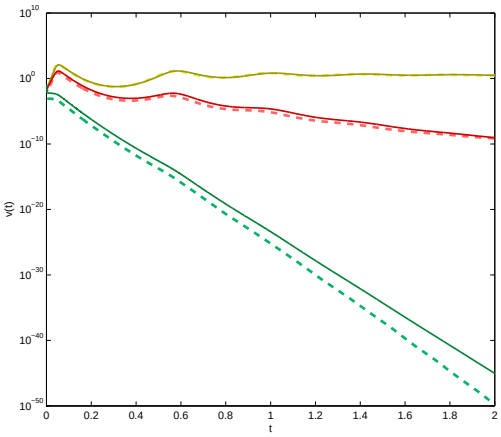

(c) v_i

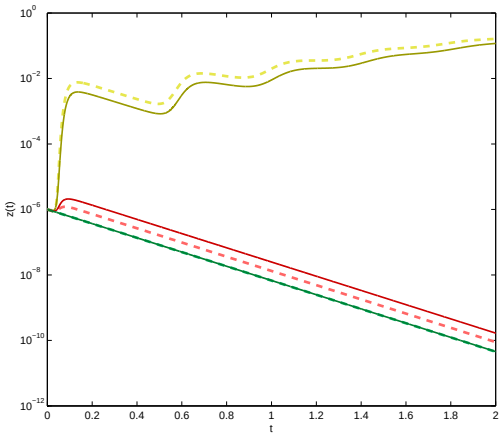

(d) z_i

Figure 4.3: **Convergence of the asymptotic solution for multiple strains.** We illustrate the convergence given by Theorems 4.5 and 4.6 considering three virus strains. The continuous line represents the solution of System (4.6) while the dotted lines are the approximations of the solutions $x(t,\varepsilon)$, $y(t,\varepsilon)$, $v(t,\varepsilon)$ and $z(t,\varepsilon)$ given by the results of Section 4.3. The parameters used are $\gamma_i = 62$, $\sigma_i = 5$, $x(0) = 1$, $y_i(0) = 10^{-3}$, $v_i(0) = 10^{-1}$, $z_i(0) = 10^{-6}$, $I_0^i = 2$, $\bar{\eta}_i = 1$ for $i = 1, 2$ and 3, $\varepsilon = 0.001$, $R_0^1 = 5$, $R_0^2 = 4$ and $R_0^3 = 0.9$. The indices 1, 2 and 3 are represented by the colors yellow, red and green, respectively.

4.5 Computational Performance

In this section we present a brief analysis of the performance of the systems involved in our results. We compare the numerical solution of System (4.6) with the approximate solution of this system provided by our result. For simplicity, in this section we call these systems, respectively, by FS (full system) and RS (once uses the reduced system). For the analysis, we disregard the treatment with inhibitors, since that may be interpreted as a change of variables.

We compare the solutions of the FS and the RS w.r.t. runtime and number of one step of the ordinary differential equation solver. We shall refer to that as one function evaluation.

To analyze each of these aspects we consider different numbers of strains (n), and for each fixed number of strains, we perform 1000 tests with parameters taken randomly according to Table 4.1. The dimensionless time interval considered is $[0, 15]$.

Parameter	Interval
$x(0)$	$1 \pm 20\%$
$y_i(0)$	$6 \times 10^{-9} \pm 20\%$
$v_i(0)$	$6 \times 10^{-9} \pm 20\%$
$z_i(0)$	$4 \times 10^{-6} \pm 20\%$
γ_i	$29 \pm 20\%$
η_i	$350 \pm 20\%$
σ_i	$1 \pm 20\%$
I_0^i	$7 \pm 50\%$
R_0^i	$8 \pm 50\%$

Table 4.1: **Parameters values.** Description of parameters used in the analysis of performance.

Figure 4.4 shows the quartiles of the quotient between the performance of the FS and the RS with regard to runtime and number of evaluations. Note that in all cases, the RS led to a better performance than the FS. In the case of 250 strains, the RS showed a run time approximately 18 times smaller and required about 15 times fewer function evaluations. Although the running time of one system evaluation is relatively small (we obtained 1.89s for the FS and 0.01073s for the RS, both with 250 strains), recall that many methods of parameter estimation require the use of numerical evaluations a large number of times.

Analogously, we studied the performance by varying the size of the time interval (and setting the number of strains to 10). Again, the performance of the RS was much better than that of the FS, as shown in Figure 4.5.

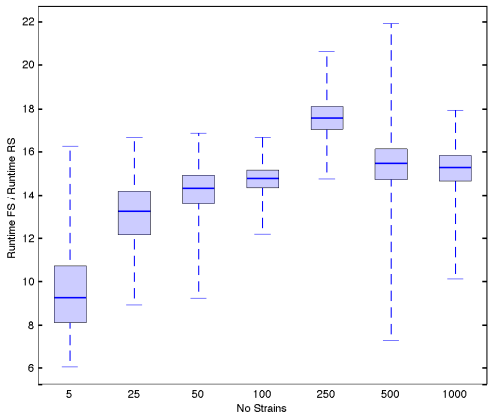

(a) Runtime

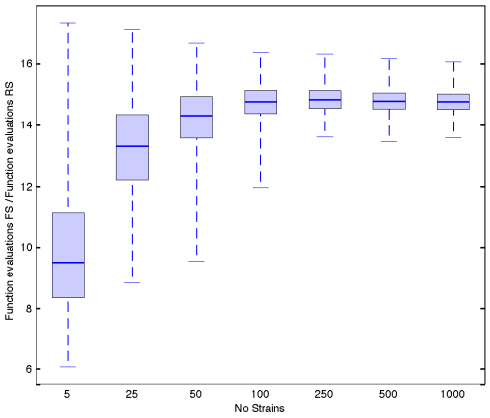

(b) Function Evaluations

Figure 4.4: **Performance analysis w.r.t. number of strains.** Box plot of the quotient between the performance of the FS and the RS considering different numbers of strains. For each strain, the system is evaluated 1000 times with parameters taken randomly according to Table 4.1. (a) shows the performance w.r.t. runtime while (b) w.r.t. the number of times that the ODE function was evaluated.

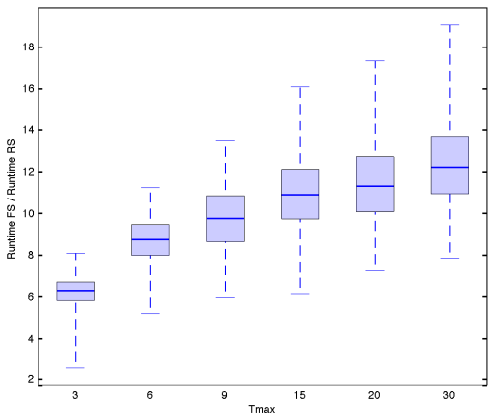

(a) Runtime

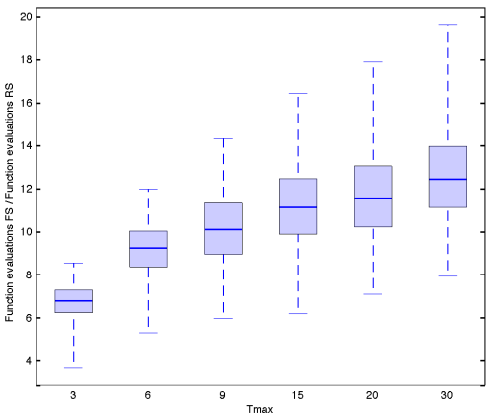

(b) Function Evaluations

Figure 4.5: **Performance analysis w.r.t. different time intervals.** Box plot of the quotient between the performance of the FS and the RS considering different time intervals. For each time interval, the system is evaluated 1000 times with parameters taken randomly according to Table 4.1 and 10 strains. (a) shows the performance w.r.t. runtime, while (b) w.r.t. the number of times that the ODE function was evaluated.

4.6 Conclusion

The existence of an asymptotic reduced dynamics for the model as proved in Section 4.3 allows a number of applications. One of them is the possibility of solving a simpler system for numerical simulations and predictions. Indeed, the full system leads to very stiff differential equations for realistic biological parameters because some components of the solution decay much more rapidly than others. By working with the reduced system we are avoiding this potential problem. Another application is the possibility of using it to calibrate the model in a more robust form. As mentioned in Subsection 4.5, we have that the time spent for the numerical solution of the system using our results are at least 5 times less than those spent to solve the original system. In some cases (higher number of strains) it came to be 17 times lower. The numerical solution of the system using the approach of our results still showed a better performance by analyzing the required number of function evaluations and the number of successful steps. This is very useful especially when it is necessary to solve the system many times, which is common in methods of parameter estimation. Yet another application is the possibility of inferring R_0 from the behavior and stability of the reduced dynamics in a simpler form. In fact, when we look at our results considering the original parameters without strains or treatment we obtain that $V(t) \sim \frac{k}{u}Y(t)$. Since the mean lifetime of free virus $1/u$ is a known parameter [SR88, Qui96, M$^+$00, SH03], this allows us to estimate k based on the values of infected cells Y and viral load V. Despite the clinical tests for HIV-1 used in large-scale provide the total CD4$^+$T count (infected and uninfected), a clinical test capable of estimating the infected CD4$^+$T cell count is already used in some research centers [S$^+$95].

It is also worth noting that the reduced system has the form of a food chain system [HS98], where the uninfected CD4$^+$T cells act as the environmental resources, the infected CD4$^+$T cells as prey and the CD8$^+$T cells as predators. Thus, a promising direction for future work is to study known results of food chain systems that can be applied to the reduced system, and verify the possibility of extending them to the original system.

Observe that, in the simplified case of only one strain, the system of ordinary differential equations discussed is similar (but not the same) to the model discussed in [Sou11]. System (4.6) has one more equation (z - equation) and the second equation has one more nonlinear term, correlating the infected cells (y) and the immune system (z). Furthermore, even in the case $z(t) \equiv 0$, the two systems do not match. Indeed, the equations involving the multiscale term do not have the same format. Thus, the results of the present chapter are related to those of [Sou11] but do not come as a consequence thereof.

One natural follow up of the present work would be to consider more general systems than those described by System (4.1) and analyze then at the light of [Szm91,Fen79]. We are currently pursuing such avenue.

CHAPTER 5

Parameter Estimation of HIV-1 Models

Knowledge of the values of the model parameters is of great relevance in the study of the in vivo HIV-1 infection. As we saw in Chapter 2, the long term dynamics of System (1.3) can be entirely described in terms of such parameters. From a biological view point, they exert significant influence on the infection chronicity. This is turn is related to the challenge that the immune response and the antiretroviral therapy has to overcome to defeat HIV-1.

In order to estimate the parameters involved in the dynamics of the HIV-1 infection several studies have been performed [PH$^+$95, PH$^+$96, PH$^+$00, PH$^+$07, DBRP10, RP$^+$10, BMSN97, Xia03, WZMP08, Llo01, Imm13]. However, some important parameters are not well-established, such as the HIV-1 basic reproductive ratio in the presence of the immune response and the HIV-1 infection rate.

In this chapter, we introduce a novel method to estimate these parameters by comparing clinical data in the chronic stage with predicted equilibrium points of System (1.1). The latter is considered to appropriately describe the dynamics of HIV-1 in the acute infection phase. The approach relies heavily on the asymptotic results of Chapter 2, and without such results the problem is much harder. To show the efficiency of our approach, we analyzed the errors obtained from synthetic data generated by the mathematical model and added multiplicative noise. In applying this method to actual data, we estimate the basic reproductive ratio in the presence of the immune response and the infection rate of 31 patients. Furthermore, we estimate a lower bound of the basic reproductive ratio in the absence of the immune response of these patients.

In Section 5.1, we present estimation methods, explaining the motivation and details involved. We also discuss the applicability of the method with respect to the prior knowledge of the other parameters involved. In Section 5.2, we complement this with an analyses of the method's robustness. For that, we evaluated the accuracy and precision of the relative error committed considering synthetic data. We also present an algebraic expression for the relative error of the methods. Finally, in Section 5.3, we performed the parameter estimates using clinical data.

5.1 Parameter Estimation Methods

A central point in the parameter estimation from clinical data is to check the feasibility of obtaining such data. Even more, when the parameters to be estimated are patient dependent, which is the case, for example, of the so called set point [SdMB$^+$13]. Concerning the HIV-1 infection data acquisition during the acute stage, there are two major problems. The first one is that not all HIV-1 laboratory tests are able to detect early infection. Moreover, patients rarely undergo HIV-1 laboratory tests in the first weeks of the infection because they do not suspect that they carry the virus [F$^+$03]. On the other hand, individuals with chronic infection constitute the majority (more than 95%) of all the diagnosed cases [SdMB$^+$13]. For this reason, we chose to consider clinical data from the chronic stage to formulate the parameter estimation methods.

With respect to the clinical data in the chronic stage, several studies have demonstrated that the concentrations of CD4$^+$T cells and the viral load balance remain relatively constant [SH03, SdMB$^+$13, GC04]. Sometimes, even CD8$^+$T cells are considered approximately constant [GC04]. Then, we can use the clinical data of the patient obtained during the chronic stage to get an approximation of these equilibrium concentrations for the patient.

On the other hand, System (1.1) is considered to appropriately describe the HIV-1 infection in the acute phase, since the viral genetic variability occurs mainly in the chronic phase and, in the beginning of the infection, the patient usually is not under treatment. Since, under certain assumptions, this model has only one equilibrium point which is globally asymptotically stable (Theorem 2.2), it is reasonable to assume that the equilibrium point of this system corresponds to the chronic stage. As the description of the equilibrium point depends on the system parameters (see Theorem 2.1), by comparing it with clinical data allow us to find expressions to estimate some parameters. This is the main idea of the method that we are proposing.

The parameters of interest are the HIV-1 basic reproductive ratio in the presence of the immune response, R_I, the infection rate, β, and the HIV-1 basic reproductive ratio in the absence of the immune response, R_0.

The basic reproductive ratio is a crucial quantity to determine the behavior of the HIV-1 dynamics [NB96, NM00, Kor04, Pas05, SZ11]. This quantity is interpreted as the number of newly infected cells that arise from one infected cell when almost all cells are uninfected. The infection rate describes the efficacy that virions infect uninfected cells, including the rate at which viral particles find uninfected cells, the rate of virus entry, and the probability of successful infection.

These parameters are of great relevance in the study of the HIV-1 dynamics, influencing not only the behavior of the viral load, but also the concentrations of the cells involved in the dynamics. They will impact the HIV-1 set point, which is a relatively stable level of the viral load [SdMB$^+$13, RP$^+$10]. The set point is a strong predictor for the HIV-1 chronicity [SdMB$^+$13, SH03], being related to the challenge that the immune response and the ART has to overcome to defeat HIV-1. Therefore, finding a way to determine these parameters for each patient is relevant not only in the determination of the acute infection course, but also in the understanding of

other infection stages. Furthermore, these parameters may help even in the choice of the ART appropriate to prevent AIDS.

Known Parameters

Some parameters and initial conditions involved in the HIV-1 dynamics are required to perform the estimates proposed along this chapter. Among them are the parameters d and u, and the initial condition X_0, whose values are already known. Indeed, it is reasonable to assume that, at the time preceding the infection, the CD4$^+$T cells concentration is the normal concentration of CD4$^+$T cells for healthy individuals. As this concentration is about one thousand cells per cubic millimeter [B$^+$92, NM00, LF85, M$^+$90], we have that $X_0 = 10^3$ cells/mm^3. Note that the normal concentration of CD4$^+$T cells for healthy individuals corresponds to the equilibrium point of the CD4$^+$T cells dynamics without infection. According to System (1.1), the CD4$^+$T cells dynamics without infection is given by

$$\dot{X} = \lambda - dX,$$

whose only equilibrium point is λ/d. Thus, the initial CD4$^+$T cell concentration is heavily related to the parameters λ and d, i.e. $X_0 = \lambda/d$.

As described in Chapter1, $1/d$ is the mean lifetime of uninfected CD4$^+$T cells. Since the half-life of susceptible cells is approximately 87 days [H$^+$99], we have that $d = \ln(2)/87$ days^{-1}. The mean lifetime of free virus is also known, about 6 hours [SR88, Qui96, M$^+$00, SH03, PH$^+$97], whence $u = \ln(2)/0.25$ days^{-1}.

Regarding to estimating R_0, also is necessary the prior knowledge of k/a. This quotient describes the total number of virions produced from any one infected cell [NM00], so-called burst size (B_s). Although many authors have performed estimates for B_s, its value is still controversial. Some authors estimate B_s between 10^3 and 4×10^3 viral particles [DP04, HN$^+$99, RWSH07],. This is much lower than that estimated by Chen et al., which is more than 10^4 viral particles. However all the aforementioned authors agree that the B_s is larger than 10^3viral particles. This minimum value for the burst size will be denoted by B_s^{min}.

Table 5.1 summarizes the values of the above parameters.

Parameter	Value
X_0	10^3 cells/mm^3
d	$\ln(2)/87$ days^{-1}
u	$\ln(2)/0.25$ days^{-1}
B_s^{min}	10^3 viral particles

Table 5.1: **Known Parameters.** Summary of parameter values that are required to perform the estimates proposed along this chapter.

Description of the Method

Let $\hat{X}_{eq}$, $\hat{V}_{eq}$, and $\hat{Z}_{eq}$ be the approximations of the CD4$^+$T cell count, the viral load, and the CD8$^+$T cell count in the chronic stage, respectively. These approximations can be obtained by the median of the clinical tests performed in the chronic phase.

On the other hand, let X_{eq}, Y_{eq}, V_{eq}, and Z_{eq} be the components of the endemic equilibrium point of System (1.1) that has an active immune response, i.e.

$$(X_{eq}, Y_{eq}, V_{eq}, Z_{eq}) = \left(\frac{X_0}{R_I}, \frac{du}{\beta k}(R_I - 1), \frac{d}{\beta}(R_I - 1), \frac{a}{p}\left(\frac{R_0}{R_I} - 1\right)\right). \tag{5.1}$$

Note that these expressions can be obtained from Theorems 2.1 and 2.2 in the case that $R_0 > R_I$. Indeed, as Equation (1.1) considers only one strain, the antigenic maximal set will be $\mathcal{J} = \{1\}$. Such set is trivially purely antigenic. Thus, the globally asymptotic stable equilibrium is the point $W_{0\{1\}}$ given by Equation (5.1), where we use that $X_0 = \lambda/d$.

Therefore, comparing the clinical data in the chronic stage with the equilibrium point means comparing $\hat{X}_{eq}$ with X_{eq}, $\hat{V}_{eq}$ with V_{eq}, and $\hat{Z}_{eq}$ with Z_{eq}. These allow us to obtain expressions to the estimate R_I, β, and R_0, as will be explicit below.

R_I Estimation

From the CD4$^+$T cell component of Equation (5.1), we have

$$\hat{R}_I = \frac{X_0}{\hat{X}_{eq}}. \tag{5.2}$$

Note that this R_I estimate only requires the prior knowledge of the parameter X_0, which is known.

β Estimation

From the CD4$^+$T cell and viral load components of Equation (5.1), we have

$$\hat{\beta} = \frac{d}{\hat{V}_{eq}}\left(\frac{X_0}{\hat{X}_{eq}} - 1\right). \tag{5.3}$$

If we consider the infection rate β as a parameter which is independent of the host, i.e. it is the same for all individuals, we can propose an alternative method for the β estimate

$$\hat{\beta} = \arg\min_{\beta>0}\left[\sum_{i=1}^{n}\left(\beta - \frac{d}{\hat{V}_{eq}^i}\left(\frac{X_0}{d\hat{X}_{eq}^i} - 1\right)\right)^2\right] \tag{5.4}$$

where n is the number of patients and the index i corresponds to the i-th patient.

A priori, the second way to estimate β is more appropriate, since it minimizes the errors from noise measurements. However, this method is strongly based on the assumption that the rate of the infection must be approximately the same for all individuals, which is not necessarily true. In fact, comparing the results obtained by the two methods from the clinical data, we have a strong indication that this assumption is not valid. As detailed in Section 5.3, the size of the interquartile range obtained by estimating β by Equation (5.3) is 3.52×10^{-5}, while the median estimate is 1.96×10^{-5}. The large interquartile range is an indication that the infection rate is patient dependent. Furthermore, the value obtained for the estimate using Equation (5.4) (4.56×10^{-5}) was greater than the 3rd quartile obtained by using Equation (5.3) (4.19×10^{-5}), which is also an indication that this assumption is not valid. Therefore, we consider more appropriate to estimate β individually by Equation (5.3). As the R_I estimation, the β estimation only requires prior knowledge of parameters already known, X_0 and d.

R_0 Estimation

From the CD8$^+$T cell component of Equation (5.1) and the estimate for the basic reproductive ratio in the presence of the immune response, $\hat{R}_I$, we can estimate R_0 by

$$\hat{R}_0 = \left(\frac{p\hat{Z}_{eq}}{a} + 1 \right) \hat{R}_I. \tag{5.5}$$

An alternative way can be obtained using the estimate for the infection rate $\hat{\beta}$

$$\hat{R}_0 = \frac{\hat{\beta} X_0}{u} B_s. \tag{5.6}$$

It is noteworthy that some authors already have proposed ways to estimate R_0. Lloyd et al. [Llo01] proposes to estimating R_0 with the same main idea of our work, i.e. they compare clinical data with equilibrium points of a mathematical model. In fact, they propose comparing the number of CD4$^+$T cells at the endemic equilibrium with clinical data of post-acute infection. As they consider the basic dynamics model, a model that does not include the influence of CD8$^+$T cells, CD4$^+$T cells component of the endemic equilibrium depends only on R_0 and X_0, enabling the estimation. The use of a model that ignores the immune response is based on the fact that the immune system is slow to respond against the initial infection. However, the effective response of immune system occurs during the acute infection [SdMB$^+$13], significantly affecting the dynamics post acute-infection. As the equilibrium points are different for the models with and without immune response, this simplification can lead to significant errors. Indeed, in the presence of a strong immune response the concentration of CD4$^+$T cells provided by the basic dynamics is $\lambda/(dR_0)$, instead of $\lambda/(dR_I)$. Thus, the relative error for this R_0 estimation (ignoring noise measurements) will be $(R_0 - R_I)/R_0$ and, if $R_I \ll R_0$, the error will be quite large. However, if we use the dynamics described by Equation (1.1), this idea is perfectly applicable to estimate R_I, as we proposed above.

Another method for estimating R_0 is the one proposed by Ribeiro et al. [RP$^+$10], which is an improvement of the proposal made by Nowak and May [NM00]. The main idea is to assume that, in the early infection, the viral load has an exponential growth rate, i.e. is $V(t) = V_0 e^{r_0 t}$, where r should be estimated from viral load of clinical data. Further assuming that, in the early infection, $X = X_0$ and using a model without the immune response, they obtain that

$$R_0 \approx \left(1 + \frac{r}{a}\right)\left(1 + \frac{r}{u}\right).$$

As they use only data of early infection and, in this period, the immune response is not significant, the use of a model which does not include CD8$^+$T cells is not a limitation. However, a significant problem to apply this method is that, to perform the r_0 estimation, clinical data is required for the period for which the viral load grows exponentially (the period in which X is approximately constant). But the peak viremia occurs approximately 3 to 4 weeks after the viral infection [SdMB$^+$13] and most patients do not seek medical attention during the first weeks after infection [F$^+$03]. As mentioned before, the majority (more than 95%) of diagnosed cases [SdMB$^+$13] occurs in the chronic infection. Thus, this method is not applicable to the majority of individuals with HIV-1.

Note that the R_0 estimation methods that we propose not suffer from these limitations, since Model (1.1) covers the influence of CD8$^+$T cells and the clinical data that we use refer to the chronic infection period.

However the estimation of R_0 by Equation (5.5) requires the prior knowledge of the parameter p, for which we not found the estimate. Another aspect of this estimate that must be analyzed, is the veracity of the assumption that CD8$^+$T cells are in balance in the acute phase.

Meanwhile, the estimate by Equation (5.6) requires the prior knowledge of X_0, u and the burst size B_s. As previously mentioned, the values of X_0 and u are not an issue.

The major problem concerns the lack of consensus on estimates of the burst size, as detailed previously. Thus, while we do not get a more refined estimate for the burst size, this form of estimating R_0, although efficiency (as shown forward), cannot be applied to real data. However, the minimal value of the burst size, B_s^{min}, is well established. This allows us to estimate a lower bound for R_0

$$\hat{R}_0^{min} = \frac{\hat{\beta} X_0}{u} B_s^{min}. \tag{5.7}$$

5.2 Robustness of the Method

In order to evaluate the robustness of the proposed parameter estimation method, it is necessary to evaluate the impact caused by the errors of the equilibrium point estimation and the noise in the measurements. As these parameters and the equilibrium points are in ratio scale, i.e. a scale which has a true meaningful zero, we can evaluate these influences using the relative error

$$\delta_A = \frac{\hat{A}}{A} - 1,$$

where A is the true value and $\hat{A}$ the estimated value.

Synthetic data

To calculate the relative errors, we consider synthetic data based on the numerical solution of System (1.1) and added to noise. In fact, in order to generate the numerical solutions faster and avoid numeric instability due to difference in scale of the parameters involved, we use the approximation of System (1.1) provided by the multiscale analysis made in Chapter 4.

For each simulation, the parameters R_I, β, and R_0 were chosen randomly in the intervals [1.1, 10], [10^{-6}, 10^{-3}] and]max$(8, R_I)$, 20], respectively. The choice of such intervals was performed taking into account the hypotheses of Theorem 2.2 to ensure that the equilibrium point given by Equation (5.1) is stable ($R_I < R_0$ and $R_0 > 1$). The other parameters were $a = \ln(2)/3$, $d = \ln(2)/87$, $b = \ln(2)/77$, $u = \ln(2)/(6/24)$, $X_0 = 10^3$, $Y_0 = 10^{-12}$, $V_0 = 10^{-6}$, $Z_0 = 10^{-6}$, $p = 1$. The parameters k and c were obtained against the parameters already determined.

In each simulation, fifteen time instants were chosen for which the numerical solutions were calculated. These times represent the date of clinical test of the simulated patient. The choice of such times was performed as follows

1st time: was taken randomly between 6 and 12 months after the beginning of the infection,
2nd to 15th time: were taken randomly from a normal distribution with mean in 6 month after the last time and standard deviation of 20 days.

These times were generated in this way taking into account that the periodicity of the viral load and the CD4$^+$T cell count tests recommended for patients in the chronic stage is 6 months [dep13], and that the chronic stage goes from about 6 months to 8 years after the infection [MK06, GC04].

After generating the numerical solutions, we added a multiplicative noise, in order to simulate the measurement error. Specifically, we multiply each component of the numerical solutions obtained by $e^{\alpha N}$ where N is a standard normal distribution and α the noise parameter. The analyses were performed considering the following values for α: 0, 0.05, 0.1, 0.15, 0.2, 0.25 and 0.3.

Estimate of the Equilibrium Values

Firstly, we analyze the relative error committed by estimating the components of the equilibrium point. Figure 5.1 suggests that the accuracy of the X_{eq} estimate is quite satisfactory. Note that the median of its relative errors (δ_X) did not exceed 0.1 even for $\alpha = 0.3$. With respect to the δ_V and δ_Z estimates, the median of its relative errors are slightly higher than the median of the δ_X. But still, they seem sufficiently satisfactory, since they do not exceed 0.3.

The estimates of X_{eq} and V_{eq} also showed a good precision, since their interquartile ranges are small (Figure 5.2(a) and (b)). However, the precision of Z estimate is not so good, as we can see by its interquartile ranges (Figure 5.2(c)).

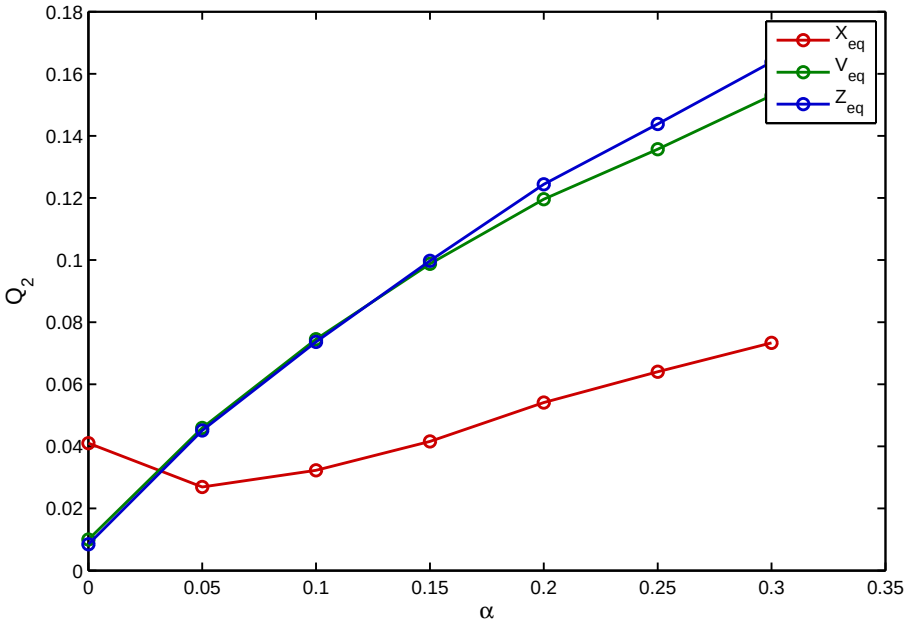

Figure 5.1: **Median of $|\delta_X|$, $|\delta_V|$, and $|\delta_Z|$.** The relative errors were obtained based on 10000 simulations for each α considered.

Estimate of the R_I

The robustness of the estimate of R_I is as good as that of X_{eq}. This can be observed in Figures 5.2(a) and 5.3.

This relationship becomes clear by looking at the relative error of the R_I estimates written as a function of the relative error of the X_{eq} estimation

$$\delta_{R_I} = -\left(1 + \frac{1}{\delta_X}\right)^{-1}.$$

As the robustness of the X_{eq} estimation is quite satisfactory so will be the robustness of the R_I.

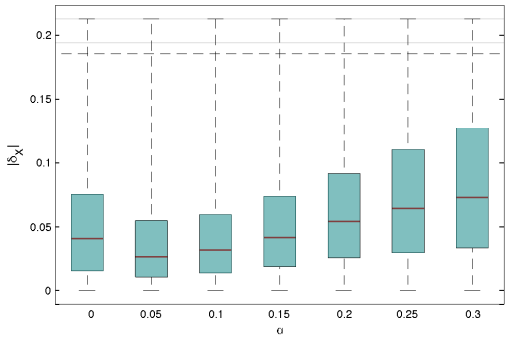

(a) Relative error of X_{eq}

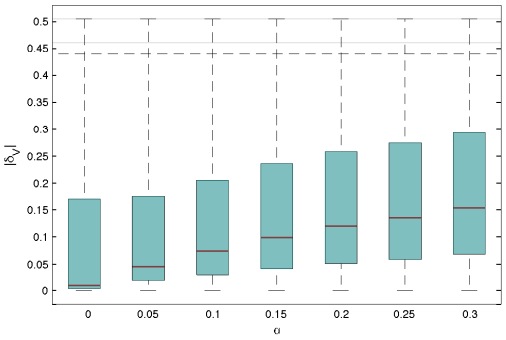

(b) Relative error of V_{eq}

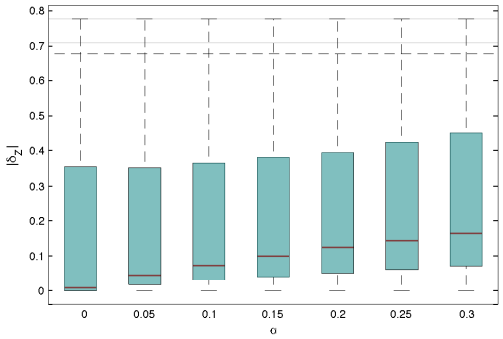

(c) Relative error of Z_{eq}

Figure 5.2: **Box plot of $|\delta_X|$, $|\delta_V|$, and $|\delta_Z|$.** The relative errors were obtained based on 10000 simulations for each α considered.

The β Estimation

The relative error obtained in the β estimation by Equation (5.3) is

$$\delta_\beta = (1+\delta_V)^{-1}(1+\delta_X)^{-1}\frac{R_I-(1+\delta_X)^{-1}}{R_I-1}-1.$$

Note that, the only problem will be in the case where R_I is very close to 1. Then, even for δ_X and δ_V very small, δ_β may be very large. However, the results obtained from the synthetic data, with $R_I \geqslant 1.1$, were quite satisfactory, as shown in Figure 5.4.

The R_0 Estimation

The relative error of the estimate given by Equation (5.5) is

$$\delta_{R_0} = \delta_Z(1+\delta_{R_I})\left(1-\frac{R_I}{R_0}\right)+\delta_{R_I}.$$

As $R_I < R_0$, $R_0 > 0$, and $R_I > 0$, we have that $1 - R_I/R_0 \in (0, 1)$. Thus, the relative error of such R_0 estimate depends on the relative errors of the estimates of Z_{eq} and R_I. As we saw

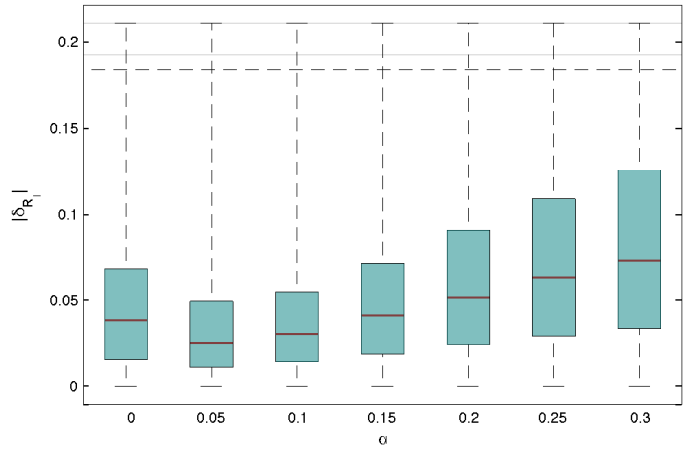

Figure 5.3: **Box plot of $|\delta_{R_I}|$.** The relative errors were obtained based on 10000 simulations for each α considered.

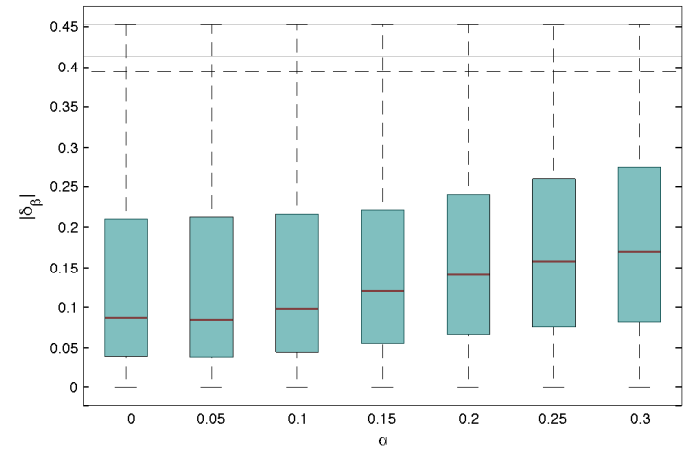

Figure 5.4: **Box plot of $|\delta_\beta|$.** The relative errors were obtained based on 10000 simulations for each α considered.

earlier, the estimate of Z_{eq} does not have a good precision (Fig.5.2(c)), impacting negatively in the robustness of this R_0 estimation.

Concerning the estimate provided by Equation (5.6), we obtain the following expression for its relative error

$$\delta_{R_0} = \frac{\hat{\beta} X_0 B_s/u}{\beta X_0 B_s/u} - 1 = \frac{\hat{\beta}}{\beta} - 1 = \delta_\beta.$$

So, the R_0 estimate will be as good as the β one and, as we saw earlier, it is quite satisfactory.

5.3 Parameter Estimation with Clinical Data

We obtained HIV-1 viral load and the CD4$^+$T Lymphocyte count data from 31 individuals HIV-1 positive. The data comes from SISCEL[1] and correspond to patients in the chronic phase of the HIV-1 infection without antiretroviral therapy. For each patients are available at least five viral load tests and five CD4$^+$T tests, corresponding to the chronic stage.

For all patients, we calculated R_I given by Equation (5.2) and the median found was 1.95. The first and the third quartiles found were 1.72 and 2.27, respectively. The values obtained for each patient, in ascending order, can be seen in Figure 5.5.

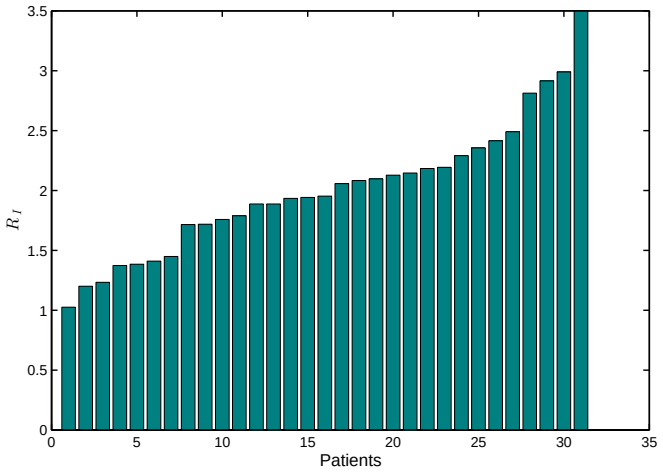

Figure 5.5: **Estimate of R_I for clinical data.** Estimated basic reproductive ratio in the presence of the immune response for each patient, given by Equation (5.2). The patients are organized in ascending order of $\hat{R}_I$.

With respect to the infection rate parameter estimated by Equation (5.3), we obtained a median of 1.96×10^{-5}mm^{3}virions^{-1} day^{-1}. The first and the third quartiles found were 0.67×10^{-5} and 4.19×10^{-5}mm^{3}virions^{-1} day^{-1}, respectively. Figure 5.6 shows the estimated beta for each patient.

As mentioned earlier, the estimate by Equation (5.4) does not seem appropriate. Applying this method for the clinical data, we obtained a β of 4.56×10^{-5}mm^{3}virions^{-1} day^{-1}. Note that this value is greater than the third quartile (Q3) of the β estimate by Equation (5.3), i.e. 4.19×10^{-5}mm^{3}virions^{-1} day^{-1}. This is a strong indication that the infection rate is patient dependent. Furthermore, the interquartile range obtained by the first method estimation was of 3.52×10^{-5}mm^{3}virions^{-1}, which is quite large if we consider the magnitude of β. Therefore, we consider that the estimate given by Equation (5.4) is not appropriate.

Finally, Equation (5.7) allowed us to estimate, for each patient, a lower bound for the basic reproductive ratio in the absence of the immune response, for which we obtained a median of 7.07 with an interquartile range of 2.41 to 15.2, as shown in Figure 5.7

[1]Sistema de Controle de Exames Laboratoriais da Rede Nacional de Contagem de Linfócitos CD4$^+$T /CD8$^+$T e Carga Viral, i.e. Control System for Laboratory Tests of the Brazilian Network for Lymphocyte Count (CD4$^+$T /CD8$^+$T) and viral load.

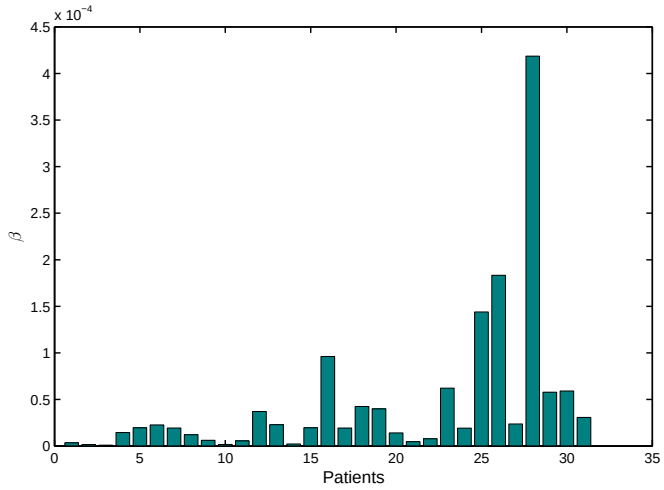

Figure 5.6: **Estimate of β for clinical data.** Estimated infection rate for each patient, given by Equation (5.3). The patients are organized in the same order that in Figure 5.5.

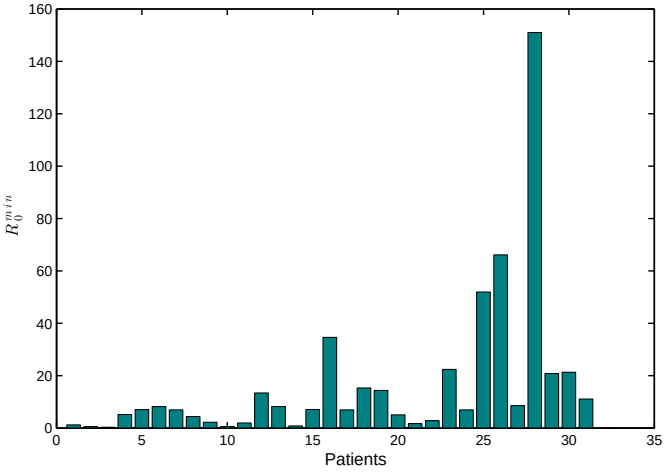

Figure 5.7: **Estimate of R_0^{min} for clinical data.** Estimation of a lower bound for the basic reproductive ratio in the absence of the immune response, for each patient, given by Equation (5.7). The patients are organized in the same order that in Figure 5.5.

5.4 Conclusion

The parameter estimation is a very significant aspect of the study of biological models, allowing a better understanding of complex biological systems. However, obtaining a good estimate is not always an easy process. One of the challenges concerns the collection of data, which are often scarce or unavailable. In the case of the HIV-1 infection, we saw that patients rarely perform clinical tests in the acute phase. This makes impracticable for most patients the parameter estimation that requires data from acute phase. Even when data are available for the period in question, they are enough to get a proper estimate. Several studies have been performed in order to find the minimal number of measurement of the variables for a complete determination of all parameters [XM03, JX05]. In this respect, our proposals are quite significative. Indeed, in our methods the clinical data comes from the chronic phase, avoiding the data shortage problem. Furthermore, as we use algebraic expressions (equilibrium points) to obtain the estimates, we get a well-posed estimation. Another problem in comparing the data with the solution curves of the mathematical model is the influence that the initial conditions will have on the estimates. As the equilibrium points of System (1.1) do not depend on the initial conditions, we do not have this problem.

Another challenge in parameter estimation is to achieve a robust method, since normally the data has measurement noise. Using noise corrupted data, we show in Section 5.2 that our method is robust. The proposed estimates for the $CD4^+T$ cells equilibrium and viral load equilibrium were satisfactory. However, the estimate for the $CD8^+T$ cells equilibrium did not show good precision. One reason maybe due to the assumption that the $CD8^+T$ cell count balance in the chronic phase is not the correct one. Additionally, we have another problem to estimate the equilibrium value of $CD8^+T$ cells. Not all laboratories perform tests of the $CD8^+T$ cell count, greatly reducing the amount of data.

Anyway, we avoided this issue by proposing an alternative estimate for R_0 that does not depend on the concentration of $CD8^+T$ cells.

We emphasize that the estimate of the basic reproductive ratios and the infection rate for each patient is of great importance to determine the severity of the disease in this patient. Consequently, this can help to determine the appropriate treatment for each patient.

Part II
Dynamics of Residential Burglaries

CHAPTER 6

Dynamics of Residential Burglaries

In recent decades, crime has become a major problem in most urban areas around the world. Getting a better understanding of these events is very important in the study of criminology with major implications for the development of strategies for effective crime prevention.

Along history various schools of thought have proposed different ways of considering crime [Gor10]. However, the study of criminal behavior using mathematical tools is a fairly new idea [RB10]. Mathematical modeling can be a powerful tool in the fight against crime. It may be used to guide decision-making, develop policies, or to evaluate specific strategies aimed at reducing crime. A number of mathematical models have been proposed in order to describe criminology using different mathematical approaches such as agent-based models [FFM$^+$12, Eps02, HB$^+$11, Gro07, MHS10, B$^+$11, Win03], game theory [SBD10, MKSD12], epidemic or predator–prey models making use of ordinary differential equations [SNHGP11, Var66, CSB12, NHP08, B$^+$11], and reaction–diffusion models using partial differential equations [BRR13, BN10, RB10, PJ11, SBBT10] - we refer to Sooknanan [SBC13] and Gordon [Gor10] for a review on mathematical modeling of criminality.

Although crimes occurrences are present almost everywhere, crimes do not appear to be uniformly distributed. Research concerned with burglary indicates that it is clustered not only at places but also in time [PJ11]. These aggregates of criminal occurrences are commonly referred to as *hotspots*.

In this context, mathematical tools have been applied to better understand the mechanisms governing these hotspots. Motivated by empirical observations of spatio-temporal clusters of crime, Short et al. [SDP$^+$08] present a quantitative mathematical model for residential burglary. They consider a two-dimensional lattice model, where each site is characterized by a dynamic attractiveness variable, and where each criminal is represented as a random walker. The burglar dynamics are coupled to the level of attractiveness of target sites. The degree of attractiveness of each site is a quantity that depends of previous burglary events at the same location and

memory effects from burglaries at neighboring sites, incorporating the repeat (or near-repeat) effect and the so-called *broken windows* theory. The repeat (or near-repeat) effect, refers to the hypothesis that residential burglars prefer to return to a previously burglarized house, or the ones adjacent to it. The broken windows theory, regards to the idea that past crimes create an image of a crime-tolerant neighborhood, stimulating new occurrences of crimes. Based on this discrete model, Short et al. [SDP$^+$08] also exhibit a reaction-diffusion model, whose local existence and uniqueness of solutions is proved by Rodriguez and Bertozzi [RB10]. This continuous model is related to several other well-studied models, such as the Keller-Segel model for aggregation based on chemotaxis. In this context, the robbers play role of bacteria, and the attractiveness of each location the role of the chemical.

In [SBBT10], Short et al. present a bifurcation analysis of the bifurcations of this reaction-diffusion model in order to detect crime hotspots. With this analysis, they obtained that crime hotspots form when enhanced risk of repeated crimes diffuses locally, but not so far as to bind distant crime together.

In [SDBT09], Short et al. conduct a study of the hotspots under a somewhat different perspective. Instead of studying a model that encompass the repeat effect and the broken windows theory, they analyze the evidence of these effects in the burglary data collected from Long Beach, CA. For that, they perform different counting methods and determine the probability distribution functions for the time intervals between repeated offenses. Then, they compare these distributions with the theoretical distributions in which the repeat effects are due solely to persistent risk heterogeneity. They found that risk heterogeneity alone cannot explain the observed distributions, while a form of event dependence can.

Similar to Short et al. [SDBT09], our goal in this chapter is to ascertain the validity of some assumptions regarding the burglaries hotspots. Specifically, we want to study these theories based on real data of residential burglaries from a medium size Brazilian urban center (see Section 6.3 for the details of the data).

Many theories have been presented to explain burglaries hotspots. Besides the repeat (or near-repeat) effect and the broken windows theory, many other aspects may be able to influence the burglaries hotspots. Among them we can mention, the structure of the urban environment, time of the year, social level of the neighborhood, seasonal conditions, features of each residence, presence of policing, economic conditions, periods for which the residences are usually unoccupied, etc. We can separate these hypotheses according to three main aspects: temporal, spatial, and spatio-temporal. By temporal aspects, we refer to factors such as week day, time of year, or seasonal conditions. By spatial aspects, we mean factors that depend only on the spatial component (at least in the short term), such as the structure of the urban environment or the features of each residence. Finally, by spatio-temporal aspects, we mean factors that will vary both in space and time. For example, the raise in the number of burglaries in a certain region caused by previous events. That is, we are considering the possibility of an influence in the current burglaries due to past burglaries (event dependence).

We analyze the real data of residential burglaries taking into account the influence of these

main aspects. Specifically, we performed tests in order to investigate the presence of temporal, spatial, and spatio-temporal agglomerations (clusters) that could be statistically significant. These analysis are shown in Sections 6.4, 6.5, and 6.6, respectively. The main tool used in the spatial and spatio-temporal analysis was the measure of homogeneity given by the Ripley's K function. A brief review of this function is given in Section 6.1. In Section 6.2 we present some examples to illustrate the analyses methods.

6.1 Preliminaries: Ripley's K Function

Consider a set of spatial points within a finite spatial region. We shall denote this region by a *study region*. In order to analyze the spatial arrangements of these points, a fundamental problem is inferring whether a given arrangement is merely random or the result of some process. A natural starting point is investigate if the points satisfy the Complete Spatial Randomness (CSR) hypothesis, that is, if the points are equally likely to occur anywhere and do not interact with each other. More precisely, CSR asserts that the number of points in any subregion of the study region follows a homogeneous spatial Poisson process. The random countable subset Π is called a homogeneous spatial Poisson process with intensity λ (number of points per unit of area) if, for all Borel set V, the random variables $N(V) := |\Pi \cap V|$ satisfy:

- If V_1, V_2, ..., V_m are disjoint Borel sets, then $N(V_1)$, $N(V_1)$, ..., $N(V_n)$ are independent random variables,
- $N(V)$ has the Poisson distribution with parameter $\lambda|V|$:

$$P(k, V) = \frac{(|V|\lambda)^k e^{-|V|\lambda}}{k!}.$$

$P(k, V)$ is the probability of finding exactly k points within an area V and with intensity λ.

In this context, a very useful tool is *Ripley's K function*, also known as the *K function* and the *reduced second moment function*. The K function gives a measure of the spatial homogeneity with a distinguishing feature from others methods in this toolset, it summarizes spatial dependence (clustering or dispersion) over a range of distances [Dix02]. The K function is defined by

$$K(r) = \lambda^{-1}\mathbf{E}[N_r],$$

where λ is the intensity of points and N_r is the number of points within a distance r of a randomly chosen event.

For a homogeneous Poisson process in $\mathbb{R}^2$ this expected value can be analytically evaluated: $K(r) = \pi r^2$. For a set of points within a defined study region A, the K function (technically its sample-based estimate) is defined as

$$K(r) = \frac{1}{\hat{\lambda}} \sum_i \sum_{j \neq i} \frac{I(d_{ij} \leqslant r)}{N}, \tag{6.1}$$

where $\hat{\lambda} = N/|A|$ is the estimated intensity, N is the number of points in the region A, $|A|$ is the area of A, d_{ij} are the distances between the i-th and j-th points, and $I(x)$ is the indicator function with the value 1 if x is true and 0 otherwise.

To gain an intuitive understanding of this estimate, consider a fixed r and consider the expression $\sum_i \sum_{j \neq i} I(d_{ij} \leqslant r)$. For each point i, we are counting the number of points inside the circle centered at the point i with radius r (not counting the center point). This is depicted by Figure 6.1(a). After doing this for each point, we divide by the total number of points, N, obtaining an average. In the case of CSR, this will be the number of points in any circular region of radius r, i.e., the intensity multiplied by the area of the circle of radius r. The K function estimate will be this average divided by estimated intensity, $\hat{\lambda}$.

However, Equation (6.1) does not consider the boundary of A for the expected value estimation. This leads to edge effects, that arise because the points outside the boundary of the study region are not counted, even if they are within distance r of a point in the study region. Consequently, the outcome may be biased, especially at large values of r. Taking this into account, Ripley [Rip76] proposed the following sample-based estimate for the K function

$$\hat{K}(r) = \frac{1}{\hat{\lambda}} \sum_i \sum_{j \neq i} \frac{I(d_{ij} \leqslant r)}{N w_{ij}}, \tag{6.2}$$

where w_{ij} is the weight function that provides the edge correction. The value of w_{ij} is the proportion of the circumference centered at the point i with a radius d_{ij} that falls in the study region (Figure 6.1(b)). If this circumference is completely inside A (case of Figure 6.1(a)), w_{ij} has the value of 1.

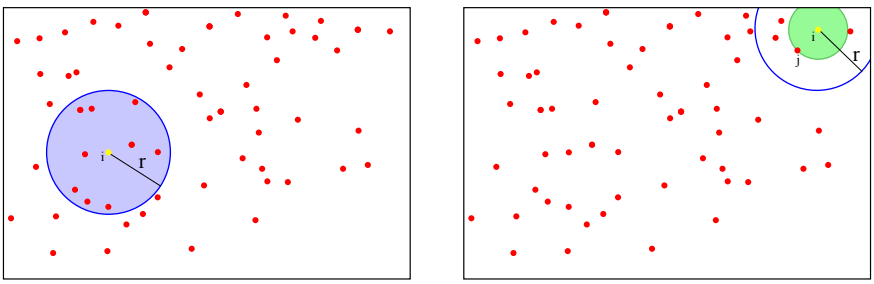

(a) (b)

Figure 6.1: **Estimated Ripley's K function.** (a) depicts the point counting of the estimated K function given by Equation (6.1). (b) depicts the edge correction. In the case that part of the circle (green) falls outside the domain, the weight function is the proportion of the circumference that falls in the study region.

In order to analyze the spatial homogeneity, the K function for observed data is usually compared to the K function for CSR. That is, if $K(r) > \pi r^2$ (or $G(r) > 1$), the observed points are more clustered than a homogeneous spatial Poisson process at the distance r. If $K(r) < \pi r^2$ (or $G(r) < 1$), the observed points are more dispersed than a homogeneous spatial Poisson process at the distance r.

In fact, to obtain a statistically significant result, we should compare the estimates of the K function for the observed points with the envelope of this functions for the CSR. The envelope is obtained by simulations of realizations of CSR. When the observed K value is larger than the envelope value, spatial clustering for that distance is statistically significant. When the observed K value is smaller than the envelope value, spatial dispersion for that distance is statistically significant (Figure 6.2).

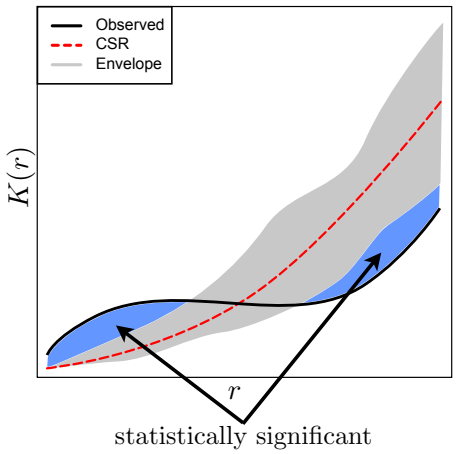

Figure 6.2: **Interpreting Ripley's K function.** When the observed K value is larger than the envelope value, spatial clustering for that distance is statistically significant. When the observed K value is smaller than the envelope value, spatial dispersion for that distance is statistically significant.

CSR and Ripley's K function are usually defined for two-dimensional spatial data. But they can be generalized for a spatial data in other dimensions. Note that, for a spatio-temporal domain, the CSR and Ripley's K function, can theoretically be treated as a pure spatial process by treating "time" as just another component of a vector space. But, in most applications, it is convenient to treat the space and time separately, in order to emphasize the characteristics of each variable. Although *CSR* is an acronym for the complete *spatial* randomness, we use the same acronym for the spatio-temporal case.

Regarding to K-Ripley function in the spatio-temporal case, the main idea is that counting the number of points is performed in cylinders instead of the circles. See Figure 6.3.

In this case the outcome is depicted as follows: when $K(u, v)$ is greater than the envelope for this point, (u, v) is marked by dark gray. This indicates statistically significant clustering. When $K(u, v)$ is smaller than the envelope for this point, (u, v) is marked by light pink. This indicates statistically significant clustering. See Figure 6.4.

For more details of the K function, we refer to [Rip76, Rip77, Cra12, GD09, Dix02, Rip79, GRD13].

Implementation of K function. All estimates of the K function used to generate the results from this chapter were performed using *The R Project for Statistical Computing*. Specifically, we use the functions *Kest*, and *envelope* of the *spatstat* package, and the *STIKhat* function of the *stpp* package.

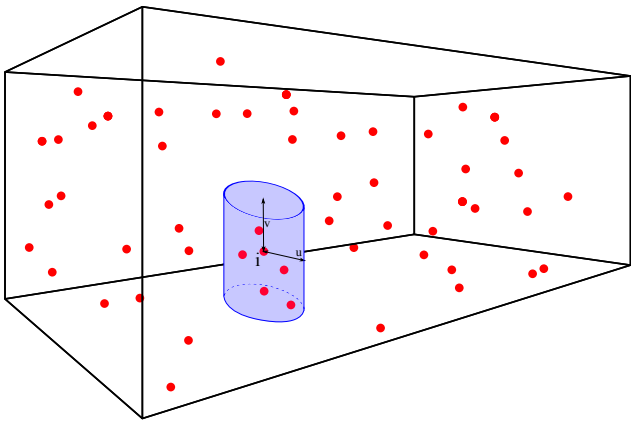

Figure 6.3: **Spatio-Temporal Ripley's K function.** Depicts the point counting of the estimated K function in a spatio-temporal domain. The spatial variable is represented by u as the time variable, by v.

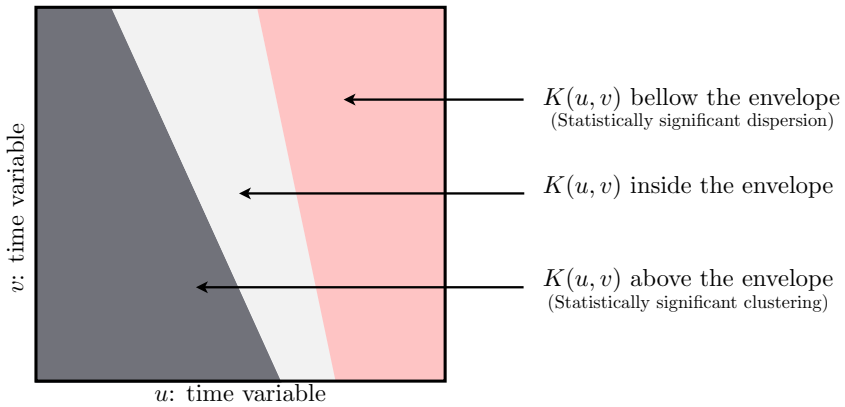

Figure 6.4: **Interpreting Ripley's K function (spatio-temporal).** The regions of the K function domain will be marked in accordance with the function value in relation to the envelope. If the K(u,v) is outside the envelope, this point will be represented by dark gray or light pink (above and below, respectively.

6.2 Examples

To illustrate the analyses methods used throughout this chapter, we present in this section the outcomes of such analyses for synthetic data. These synthetic data will not be necessarily generated following a specific distribution. Then, is not possible to evaluate analytically the K function, either in the spatial domain or in spatio-temporal domain. Therefore, we use the approximations of K functions described in the previous section. That is, we use the same procedure as we will apply to real data.

Data Set Description

In order to visualize the contribution of each type of analysis, we generate synthetic data with different types of agglomerations, regarding to temporal, spatial, and spatio-temporal aspect. Table 6.1 summarizes these choices. Each set of synthetic data contains 100 events whose spatial domain is the unit square of $\mathbb{R}^2$. The description of each set considered are described below.

Data Set	Temporal Clusters	Spatial Clusters	Spatio-Temporal Clusters
1	No	No	No
2	Yes	No	Yes
3	No	Yes	Yes
4	Yes	Yes	Yes
5	No	No	Yes

Table 6.1: **Data sets of synthetic data.** Types of clusters present in each synthetic data set.

Data Set 1: The spatial coordinates of the events were generated following a homogeneous Poisson distribution. The number of burglaries in each day was taking as a constant equal to 1. The choice of which location corresponds to which day was random. Figure 6.5 shows this set of synthetic data.

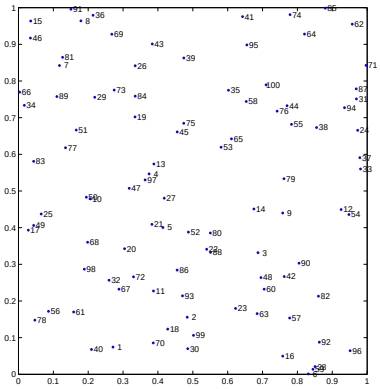

Figure 6.5: **Synthetic data set 1.** For each point of the data set, the spatial coordinates are depicted by the dots, while the temporal coordinate is depicted by the superscript number. Data set 1 was generated without temporal, spatial, and spatio-temporal cluster.

Data Set 2: The spatial coordinates of the events were generated following a homogeneous Poisson distribution in the unit square of $\mathbb{R}^2$. We consider that these events occurred over 15 days, and the number of thefts each day is given by the vector $[1, 4, 9, 16, 25, 16, 9, 4, 1, 2, 3, 4, 3, 2, 1]$, where the i-th coordinate is the number of events of the day i. The choice of which location corresponds to which day was random. Figure 6.6 shows this set of synthetic data.

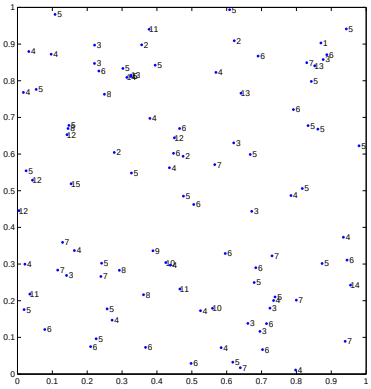

Figure 6.6: **Synthetic data set 2.** For each point of the data set, the spatial coordinates are depicted by the dots, while the temporal coordinate is depicted by the superscript number. Data set 2 was generated without temporal clusters, but with spatial clusters.

Data Set 3: The spatial coordinates of the events were generated in the unit square of $\mathbb{R}^2$ following a normal distribution with mean $[0.5, 0.5]$ and standard deviation $[0.15, 0.15]$. The number of burglaries in each day was taking as a constant equal to 1. The choice of which location corresponds to which day was random. Figure 6.7 shows this set of synthetic data.

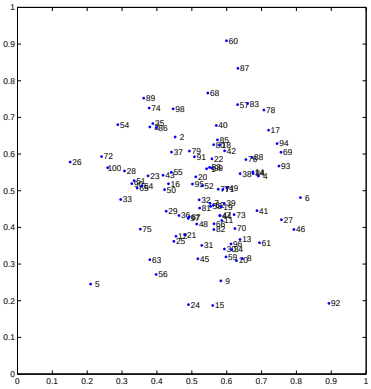

Figure 6.7: **Synthetic data set 3.** For each point of the data set, the spatial coordinates are depicted by the dots, while the temporal coordinate is depicted by the superscript number. Data set 3 was generated without spatial clusters, but with temporal clusters.

Data Set 4: The spatial coordinates of the events were generated in the unit square of $\mathbb{R}^2$ following a normal distribution with mean $[0.5, 0.5]$ and standard deviation $[0.15, 0.15]$. We consider that these events occurred over 15 days, and the number of thefts each day is given by the vector $[1, 4, 9, 16, 25, 16, 9, 4, 1, 2, 3, 4, 3, 2, 1]$, where the i-th coordinate is the number of events of the day i. For the first day, the location of the event was chosen to be the closest to the origin. For other days, the events location was chosen to be the closest to location of the event of the previous day. Figure 6.8 shows this set of synthetic data.

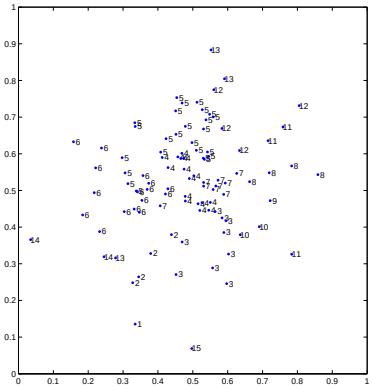

Figure 6.8: **Synthetic data set 4.** For each point of the data set, the spatial coordinates are depicted by the dots, while the temporal coordinate is depicted by the superscript number. Data set 4 was generated with spatial, temporal, and spatio-temporal clusters.

Data Set 5: The spatial coordinates of the events were generated following a homogeneous Poisson distribution in the unit square of $\mathbb{R}^2$. The number of burglaries in each day was taking as a constant equal to 1. For the first day, the location of the event was chosen to be the closest to the origin. For other days, the events location was chosen to be the closest to location of the event of the previous day. Figure 6.9 shows this set of synthetic data.

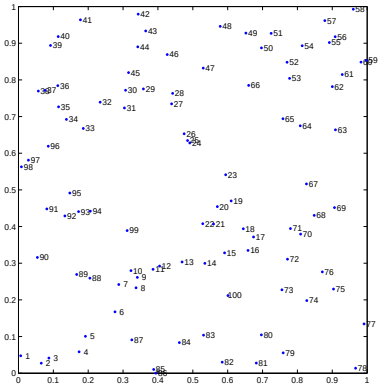

Figure 6.9: **Synthetic data set 5.** For each point of the data set, the spatial coordinates are depicted by the dots, while the temporal coordinate is depicted by the superscript number. Data set 5 was generated without spatial and temporal clusters, but with spatio-temporal clusters.

Outcome Analysis

As mentioned before, the analysis with respect to spatial and spatio-temporal clusters will be performed using the K-function, described in Section 6.1. The temporal analysis will be performed looking for the function that provides the number of daily events, along the time domain. In fact, as in K-function analysis, we will compare this function for the observed data with the envelope of this function for data randomly generated (homogeneous Poisson distribution). The days which the number of daily events is outside the envelope indicate a temporal clustering statistically significant.

Here we present the outcomes of the analysis for the synthetic data. Note that, all analysis showed the expected outcomes, taking into account the manner that the sets were generated.

Data Set 1: Figure 6.10(a) shows that the temporal analysis for Data Set 1 does not present temporal clustering, since the number of daily events is inside the envelope for all days. The K function analysis indicates that this data set does not display statistically significant spatial or spatio-temporal agglomerations. See Figures 6.10(b) and (c).

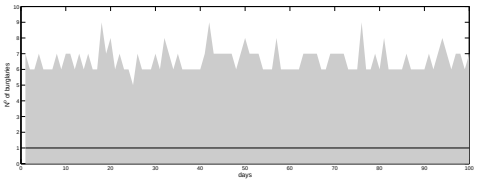

(a) Temporal Analysis

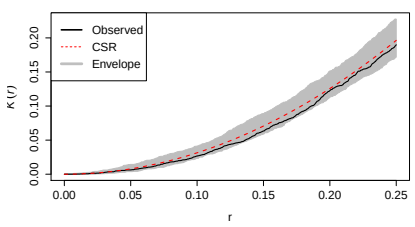

(b) Spatial Analysis

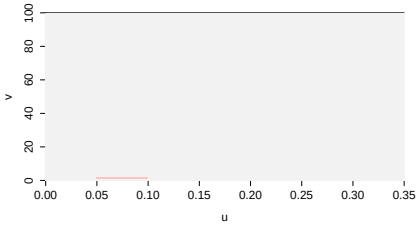

(c) Spatio-Temporal Analysis

Figure 6.10: **Analysis of data set 1.** According to the analysis, the data set 1 has not temporal, spatial, neither spatio-temporal clustering.

Data Set 2: According to the analysis, this data set has not spatial clustering, but it has temporal clustering (Figure 6.11). Furthermore, the spatio-temporal analysis indicates agglomeration for very small times (1 day) and large distances, and dispersion for large times.

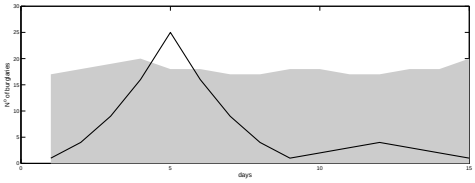

(a) Temporal Analysis

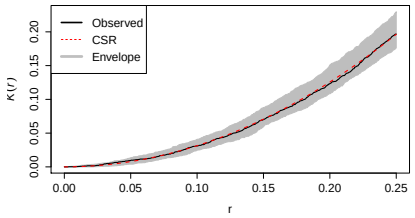

(b) Spatial Analysis

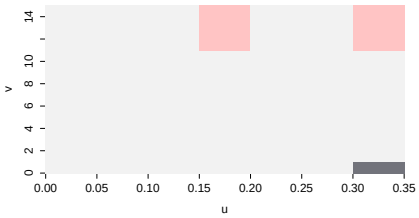

(c) Spatio-Temporal Analysis

Figure 6.11: **Analysis of data set 2.** According to the analysis, the data set 2 not present spatial clustering, but presents temporal and spatio-temporal clustering.

Data Set 3: According to the analysis, this data set has no temporal clustering, but will present spatial clustering. (Figure 6.12). Furthermore, the spatio-temporal analysis indicates agglomeration.

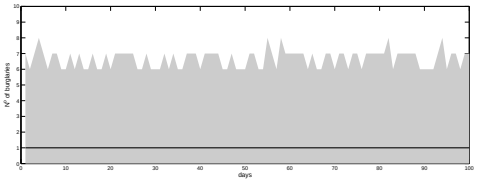

(a) Temporal Analysis

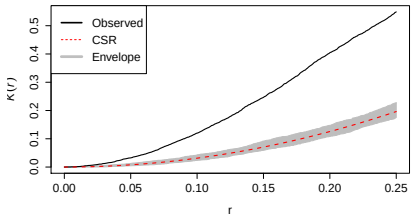

(b) Spatial Analysis

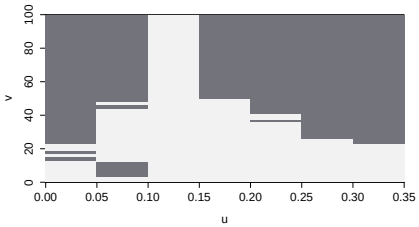

(c) Spatio-Temporal Analysis

Figure 6.12: **Analysis of data set 3.** According to the analysis, the data set 3 not present spatial clustering, but presents temporal and spatio-temporal clustering.

Data Set 4: The analysis indicates that this data set has spatial, temporal, and spatio-temporal clusters (Figure 6.13).

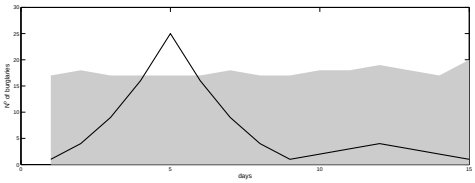

(a) Temporal Analysis

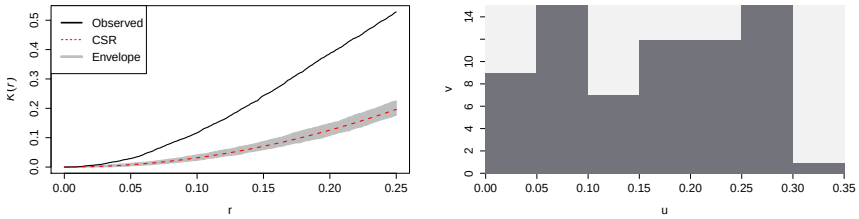

(b) Spatial Analysis (c) Spatio-Temporal Analysis

Figure 6.13: **Analysis of data set 4.** According to the analysis, the data set 4 not present spatial clustering, but presents temporal and spatio-temporal clustering.

Data Set 5: According to the analysis, this data set has not temporal clustering (Figure 6.14(a)), neither spatial clustering (Figure 6.14(b)). However, it has spatio-temporal agglomeration for small times and for all distances (region in dark gray in Figure). It also has dispersion for large times and almost all distances (region in light pink in Figure).

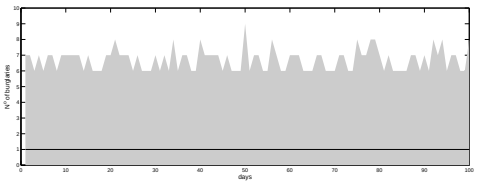

(a) Temporal Analysis

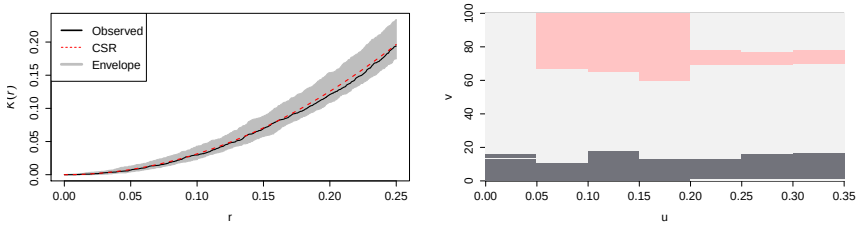

(b) Spatial Analysis (c) Spatio-Temporal Analysis

Figure 6.14: **Analysis of data set 5.** According to the analysis, the data set 5 not present temporal or spatial clustering, but presents spatio-temporal clustering.

6.3 Real Data Description

The data analyzed in this chapter refers to residential burglaries occurred in city of Cascavel, a municipality in the west of Paraná state, Brazil (Figure 6.15(a)). Cascavel is the 5th most populous city in Paraná with an urban population of 270,049 inhabitants according to an estimate from IBGE[1] in 2010. With an urban area of 55.8km^2, its urban population density, in 2010, was 4839.59 hab/km^2.

The data comes from the Police Department of Paraná state, therefore, they refer only to burglaries that were reported to the police. The data set contains information of date, time, and address, of residential burglaries occurred from 2010 to 2012. Before starting the analysis, we removed the repeated events (same day, time and place), events outside the urban region of Cascavel, and events with incomplete or incorrect address, resulting in 5,483 events. Then, we performed the geocoding, i.e. converting addresses into geographic coordinates (latitude and longitude). Figure 6.15(b) shows the location of these events on the map of Cascavel city.

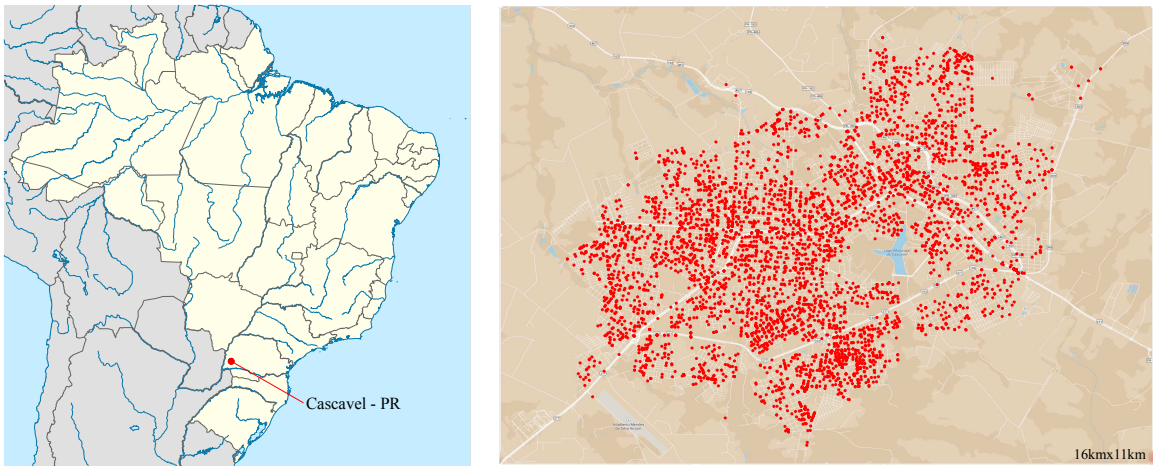

(a) (b)

Figure 6.15: **Residential burglaries in Cascavel.** (a) shows the location of Cascavel city in Brazil map. (b) shows the locations (red dot) of each residential burglary reported to the police from 2010 to 2012.

[1]Brazilian Institute of Geography and Statistics.

6.4 Temporal Clusters

In this section we will analyze the data from Cascavel's residential burglaries with respect to temporal agglomerations. The main idea is to ascertain whether there are periods of time for which the number of burglaries is significantly larger than in other periods.

First, we analyze the difference between the years for the total number of burglaries. Counting the number of residential burglaries along each year, we have that in 2010 it is significantly higher than the other years. In fact, in 2010 were recorded 46.5% more residential burglaries than in 2011, and 33% more than in 2012. However, considering only the data until 300th day of each year, these percentages fall to 4.6% and 4.1%, respectively. This indicates that the difference in the number of burglaries in 2010 relative to the other years is due, essentially, to the spike of burglaries on the months of November and December. This will become clearer in the following analysis.

Calculating the quartiles of the number of burglaries per day stratified by month, we obtain that November and December have an interquartile range significantly higher than other months, although their medians are similar (Figure 6.16(a)). However, note that this peak of burglary is not a characteristic of November and December in general, but only for 2010. Indeed, if we consider only the years 2011 and 2012, this high difference disappears (Figure 6.16(b)).

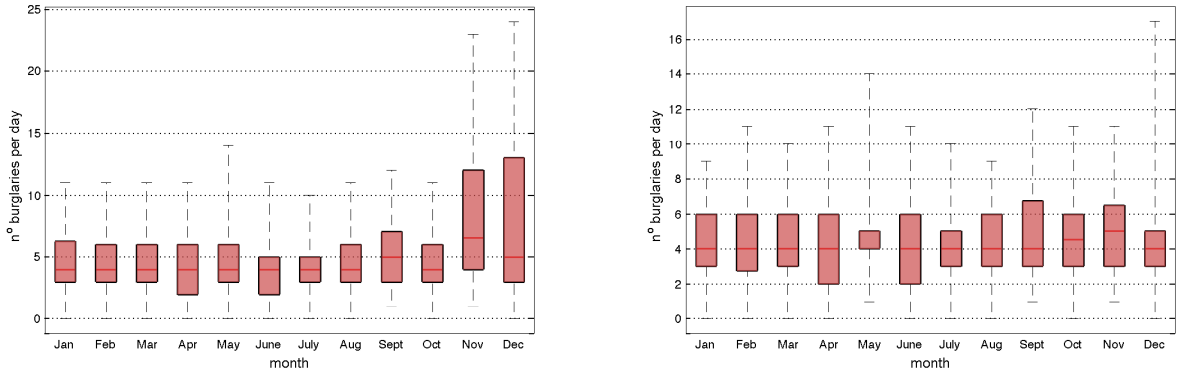

(a) 2010 to 2012

(b) 2011 and 2012

Figure 6.16: **Daily burglaries stratified by month.** Both figures show the number of burglaries per day in Cascavel stratified by month. In (a) the quartiles were obtained considering data from the years 2010 to 2012, while in (b) only the data from the years 2011 and 2012.

We also analyzed the data with respect to the number of burglaries per day taking into account the week day, the period of the month and day off. In the case of the day off we perform two comparisons. Firstly, we compare the number of burglaries per day on holiday with the others days. In fact we consider as holidays not only the day itself, but also the days of recesses caused by it. After that, we compare the number of burglaries per day on the weekends with the weekdays. The medians obtained in all cases are approximately the same and the interquartile range are small (Figure 6.17). Thus, these characteristics do not seem to cause a significant influence on the number of burglaries per day.

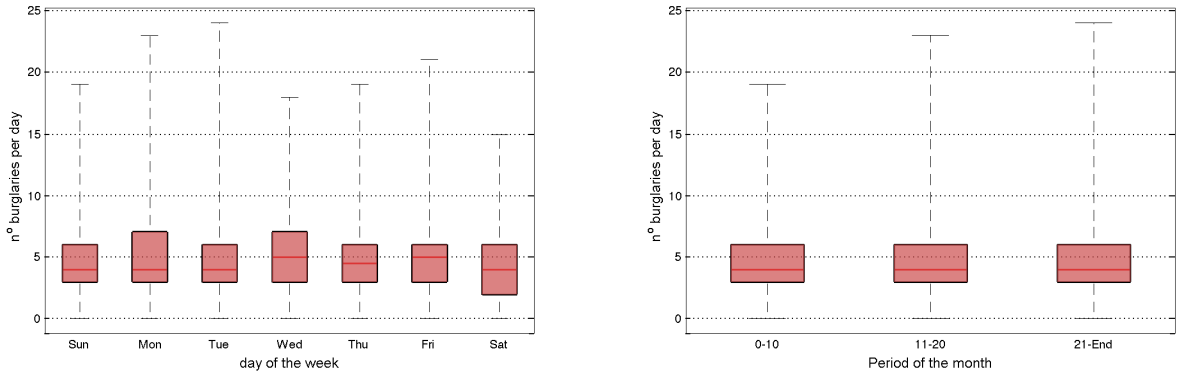

(a) Day of the week

(b) Period of the month

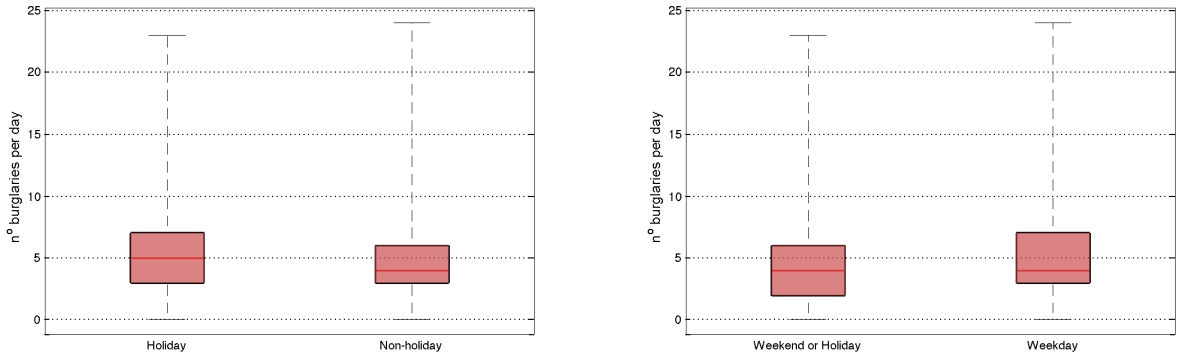

(c) Holiday vs non-holiday

(d) Weekend vs weekday

Figure 6.17: **Daily burglaries stratified.** Number of burglaries per day in Cascavel stratified by day of the week, in (a), period of the month, in (b), holiday or not holiday, in (c), and weekday or weekend, in (d).

In order to analyze if the number of burglaries per day is merely random, we compare the Cascavel data with several sets of random data. Specifically, each synthetic data set was generated by randomly choosing 5483 days between 1 and 1986. Note that 1986 days correspond to the three years for which we have the burglary data, and 5483 is the number of events (residential burglaries) over this period. After randomly choosing the days, we carried out the burglary count per day. Finally, we compare the number of daily burglary of Cascavel with the envelope computed with 10,000 synthetic data sets (Figure 6.18).

Note that, only the period between days 304 and 363 have a statistically significant increase in the number of burglaries compared with random data. This is the same period for which we have already detected a spike in burglaries (November and December 2010). According to our analysis, this spike seems to be an outlier, and not a pattern of the dynamic.

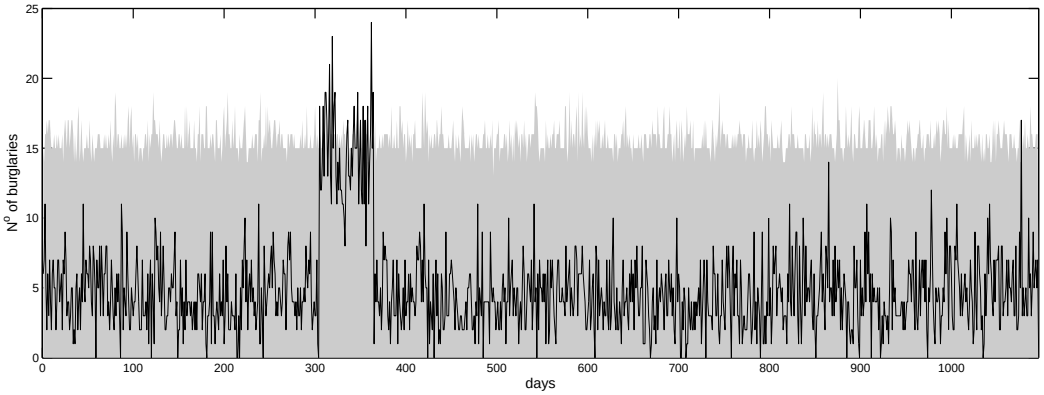

Figure 6.18: **Number of daily burglary.** Number of residential burglary per day along the years 2010, 2011, and 2012.

6.5 Spatial Clusters

In this section our focus will be on the analysis of the burglary data with respect to spatial agglomerations. Here, we shall call by point the location of each burglary (ignoring the day of the burglary).

First, we calculate the spatial intensity of burglaries, i.e. the number of burglaries per km^2 along the three years. This was calculated in a two-dimensional lattice with constant spacing of 500m. As shown in Figure 6.19, the spatial intensity varies significantly along the grid.

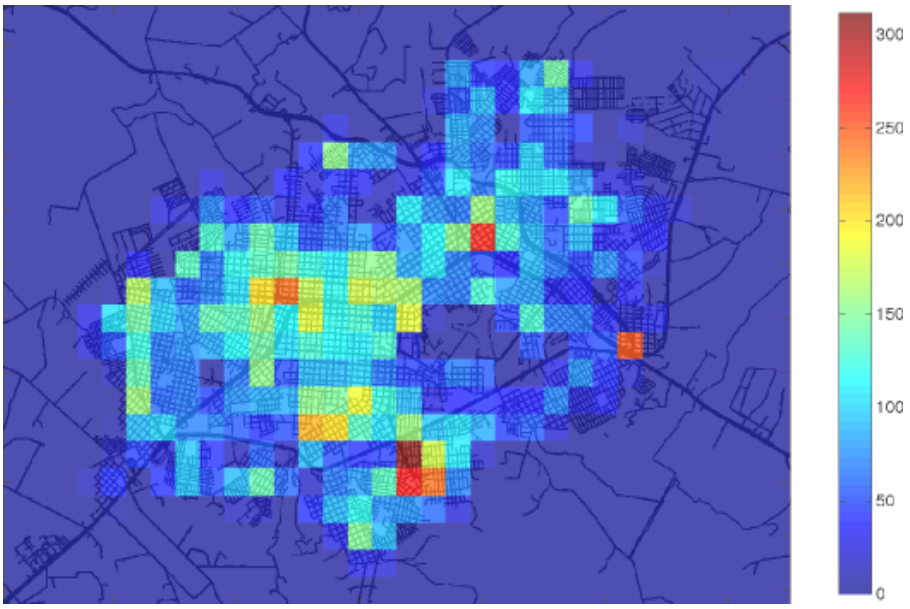

Figure 6.19: **Spatial intensity of burglaries in Cascavel.** Number of residential burglaries per km^2 in Cascavel over the years 2010, 2011 and 2013. The grid consists of squares of side 500m. The streets of Cascavel can be viewed in the watermark.

However, this intensity map does not allow us to analyze the data with respect to CSR. For this purpose we will use the K function.

To perform the K function analysis, we must first define the study region A. The choice of this region will impact significantly the outcome of the analysis, since the inclusion of uninhabited or non-residential areas will bias the outcome. It is noteworthy that our interest is to analyze spatial agglomerations of the data in residential regions, otherwise we mainly analyze the clustering of residential areas, not the clustering of residential burglaries. Indeed, consider three distinct borders to delimit the study region A, as shown in Figure 6.20(a). The first boundary is a rectangle containing all points (in red). The second frontier is the convex hull of the points (in yellow). The third was manually selected, avoiding the countryside and the city lake, and trying to contain almost all points. In fact, this region will contain 96% of the data. We will call this border by polygonal hull. Calculating the K function considering each one of these borders, we obtain different outcomes (Figure 6.20(b)). The function K indicates a more expressive agglomeration when considering the rectangular border instead of the convex hull. This in turn, also presents greater agglomeration than given by the polygonal hull border.

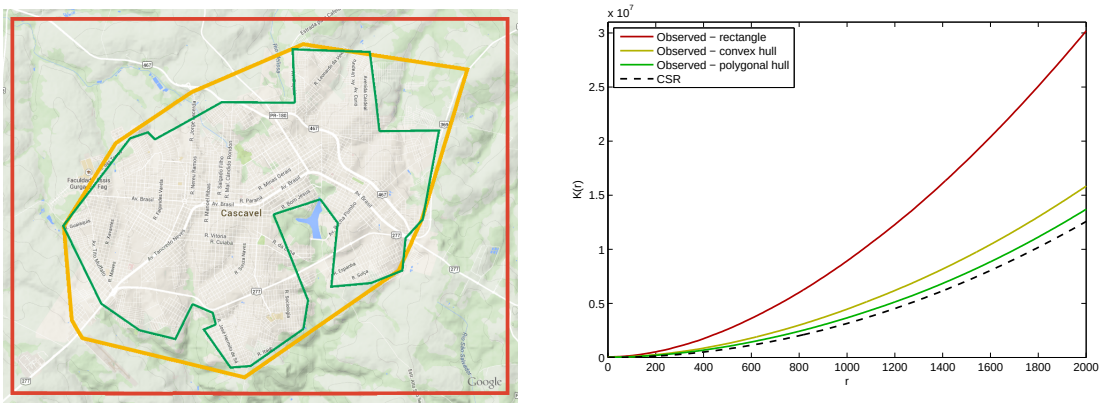

(a) (b)

Figure 6.20: **Influence of the region A.** Three possible choices for the borders of the data are displayed in (a). In red, a rectangle containing all points. In yellow, the convex hull of the points. In green, the polygonal hull, a border manually selected containing 96% of the points. The K function estimated considering each region and the K function for CSR are presented in (b), with r ranging from 0 to 2000 meters.

Note that, even in the case of a polygonal hull border, the K function indicates statistically significant spatial clustering for all r (Figure 6.21).

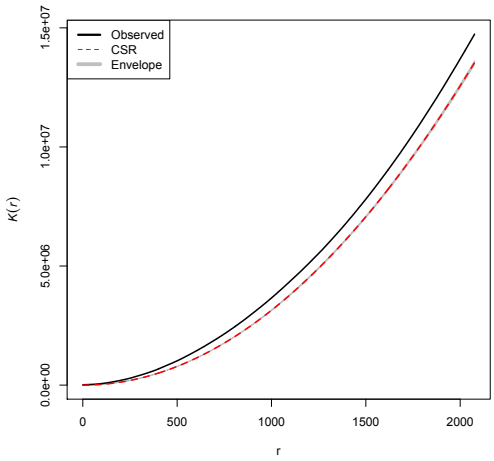

Figure 6.21: **K function - polygonal hull border.** The black line is the estimated K function for the observed data in the region delimited by the polygonal hull border. The figure also shows the K function for CSR, in red dotted line, and the envelope of the K function, in gray, computed with 500 simulations. The radius r ranging from 0 to 2000 meters.

Although most of the countryside and the city lake area are not included in this region, there are still many uninhabited or non-residential areas that may bias the result. For example, parks, industries, colleges, schools, commercial areas, and vacant land. To avoid these possible distortions, we opted to select 20 predominantly residential subregions of the city. These regions (Figure 6.22) were manually chosen avoiding the inclusion of any nonresidential or unoccupied area.

For each subregion we performed the K Riplye's analysis. No subregion showed a spatial

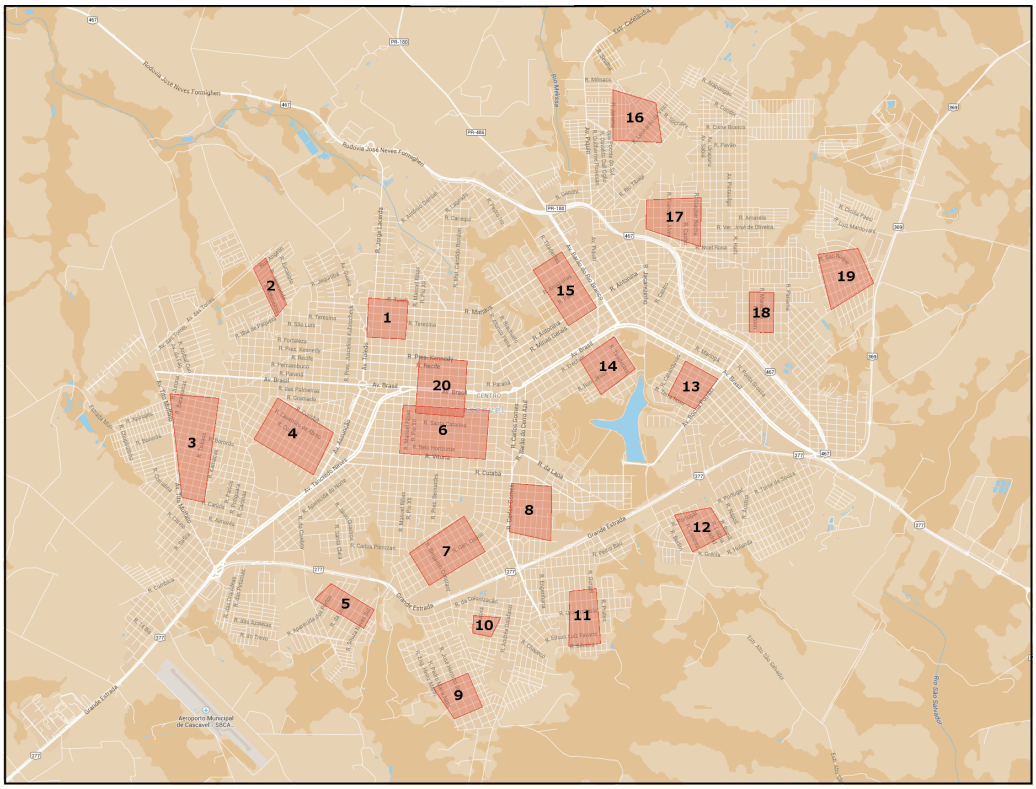

Figure 6.22: **Selected subregions of Cascavel.** These 20 regions of the Cascavel city were chosen avoiding include any nonresidential or unoccupied area, such as parks, industries, colleges, schools, commercial areas, and vacant land.

dispersion that is statistically significant. Regarding spatial clustering, only regions 3, 6, 7, 11, 17, and 20 presented some indication of statistically significant agglomeration (Figure 6.23). That is, only these subregions showed an interval for which the respective K function is greater than the envelope of the K function for CSR. The r values in these intervals are small, not exceeding 50 meters. In addition, the estimated K functions in these intervals are only slightly higher than the envelope.

In order to get an idea of how significant is this difference in terms of agglomeration, Figure 6.24 shows the K function analysis for two sets of data generated synthetically from a normal distribution. Both sets were generated considering a region with area of 1km^2 and 100 points. These values are approximately the same of the subregion 6.

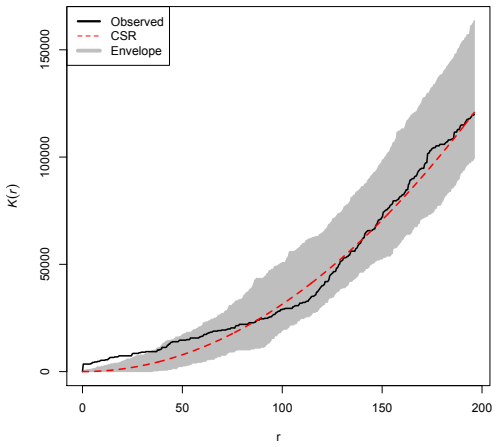

(a) Subregion 3

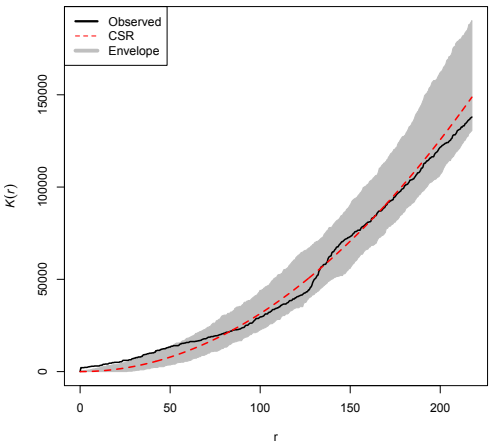

(b) Subregion 6

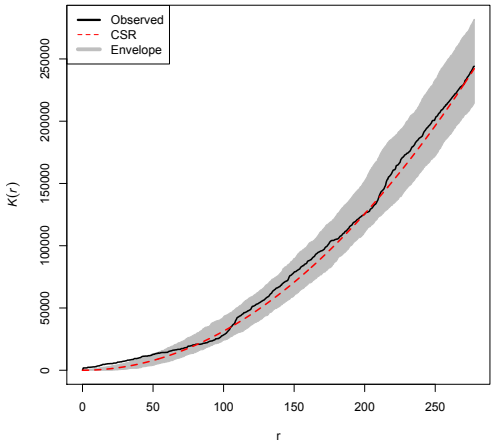

(c) Subregion 7

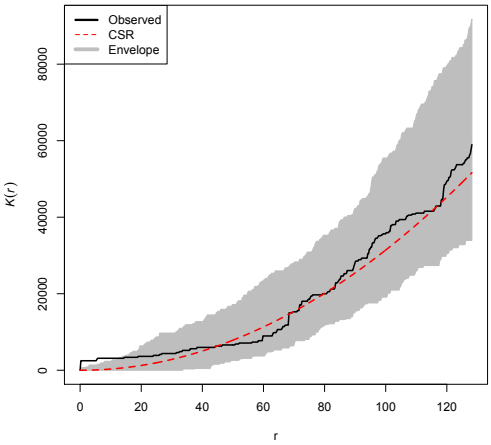

(d) Subregion 11

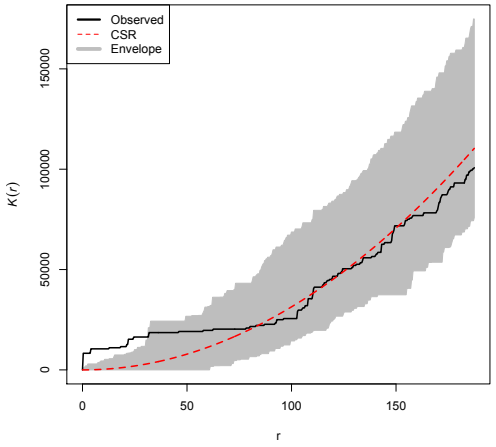

(e) Subregion 17

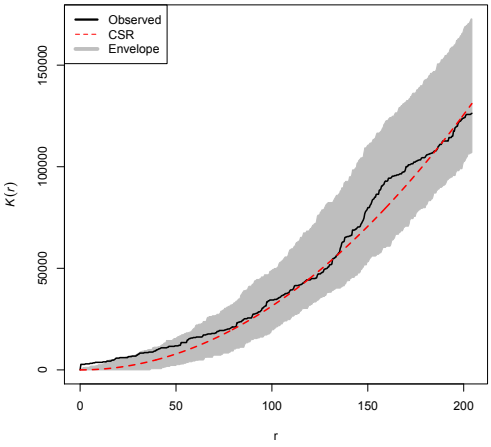

(f) Subregion 20

Figure 6.23: **Estimated K function - subregions.** The black line shows the estimated K function for the observed data in the respective subregion. The figures also show the K function for CSR, in red dotted line, and the envelope of the K function (in gray) computed with 10,000 simulations. The radius r is expressed in meters.

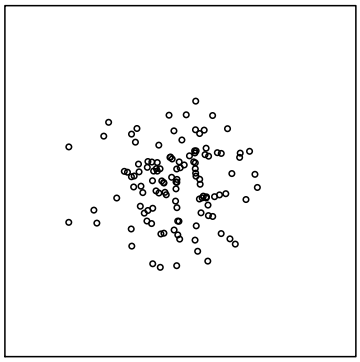

(a) Synthetic data 1

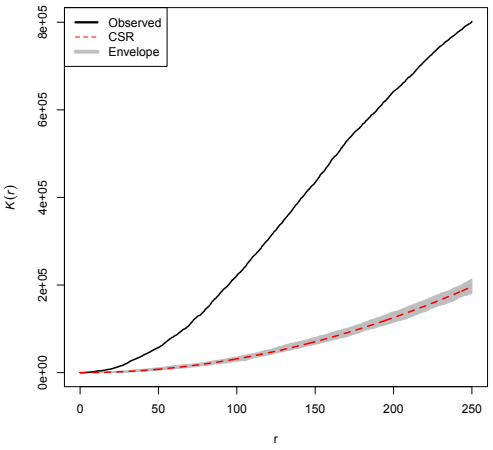

(b) K function for synthetic data 1

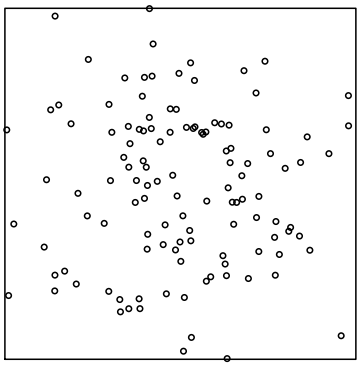

(c) Synthetic data 2

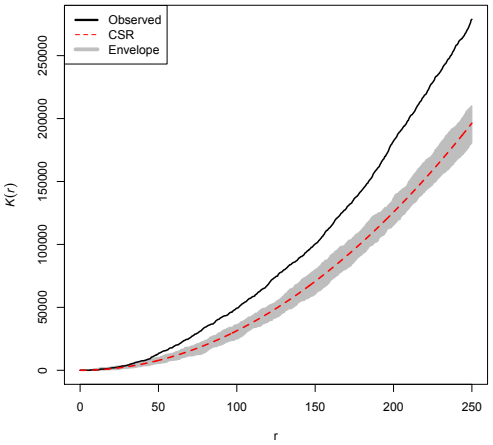

(d) K function for synthetic data 2

Figure 6.24: **K function for synthetic data.** On the left, two set of data generated synthetically from normal distribution, in a region with area of 1km^2 and 100 points each. On the right, the respective estimates of the K functions, in black. The graphs also show the K function for CSR, in red dotted line, and the envelope of the K function (in gray) computed with 10,000 simulations. The radius r is expressed in meters.

Although these subregions have not presented expressive indications of agglomeration, this does not imply regularity in all these subregions together. Indeed, looking at the average intensity of burglaries in each region (Figure 6.25) we note that there is a fairly significant change. For example, the region 10 has about 183 burglaries per km^2 against only 35 of the region 12 (along the three years).

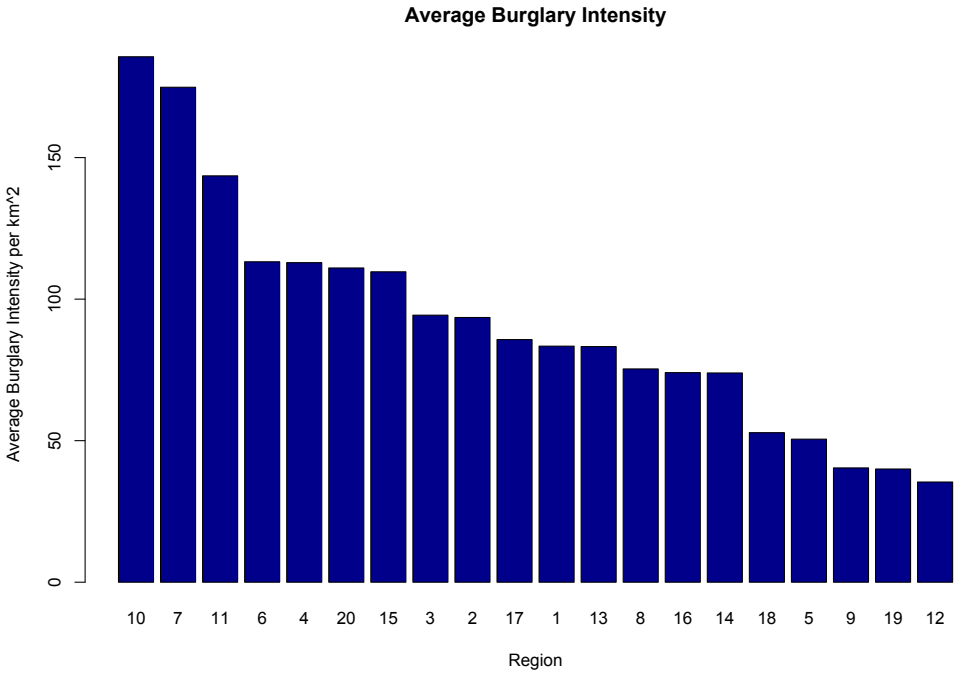

Figure 6.25: **Intensity of burglaries in the subregions.** Number of residential burglaries per km^2 in each subregion of Cascavel, along the years 2010, 2011 and 2012.

These results indicate a multiscale behavior. At small scales it is reasonable to look at the dynamics of residential burglaries as random events (CSR). While at larger scales these events display agglomeration.

6.6 Spatio-Temporal Clusters

In this section we will analyze residential burglaries with respect to spatio-temporal agglomerations. Our goal is to study the data regarding the event's dependence. That is, we want to know if there is any indication that the occurrence of an event influences the occurrence of future events.

For that, we analyze the dispersion of the points with the spatio-temporal K Ripley's function. Note that, in this section, point means a localization (spatial coordinates) and a day (temporal coordinate).

As we saw in Section 6.5, considering a large spatial region can cause a significant bias in the outcome of K function due to inclusion of uninhabited or non-residential areas. So we decided to perform the K-Ripley analysis on the sub-regions depicted in Figure 6.22, which have been chosen to avoid any nonresidential or unoccupied area, such as parks, industries, colleges, schools, commercial areas, and vacant land.

Moreover, these were the sub-regions for which we performed the spatial clustering analysis. By this way we can make comparisons between the outcomes of both analyses.

Only five sub-regions showed some spatio-temporal agglomeration (or dispersal) statistically significant. Namely, sub-regions 4, 7, 15, 19, and 20 (Figure 6.26). Sub-regions 4 and 7 showed agglomerations for small distances (up to 30m) and long period of time (practically for all times tested - 2 months). This indicates more a spatial agglomeration than a spatio-temporal one. Subregions 15 and 19 also showed agglomerations for small distances (up to 10m) and for 17 to 27 days and 39 to 60 days, respectively. Additionally, sub-regions 7 and 15 showed dispersion for a large distances (300m-320m and 240m-290m, respectively) and for a very short time (1 day). Note that these results are not expressive. On the other hand, sub-region 20 presented a more interesting result, with substantial spatio-temporal cluster for large distances (upper 200m) and time upper to 35 days. It is noteworthy that this subregion had already submitted agglomeration in the spatial analysis.

As in the spatial case, we will present an example in order to get an idea of how significant is this difference in terms of agglomeration. Consider synthetic data following a diffusion equation with diffusion coefficient of 5000 m^2/day, where the data were generated along 300 days with 5 burglaries per day. K-function analysis shows that for this data, there is a very significant spatio-temporal agglomeration (Figure 6.27).

Note that, the spatio-temporal clusters present in the synthetic data is much more significant than in the case of the Cascavel data. In addition, if we redo the analysis considering only the data from 2011 and 2012, no sub-region shows spatio-temporal clusters statistically significant.

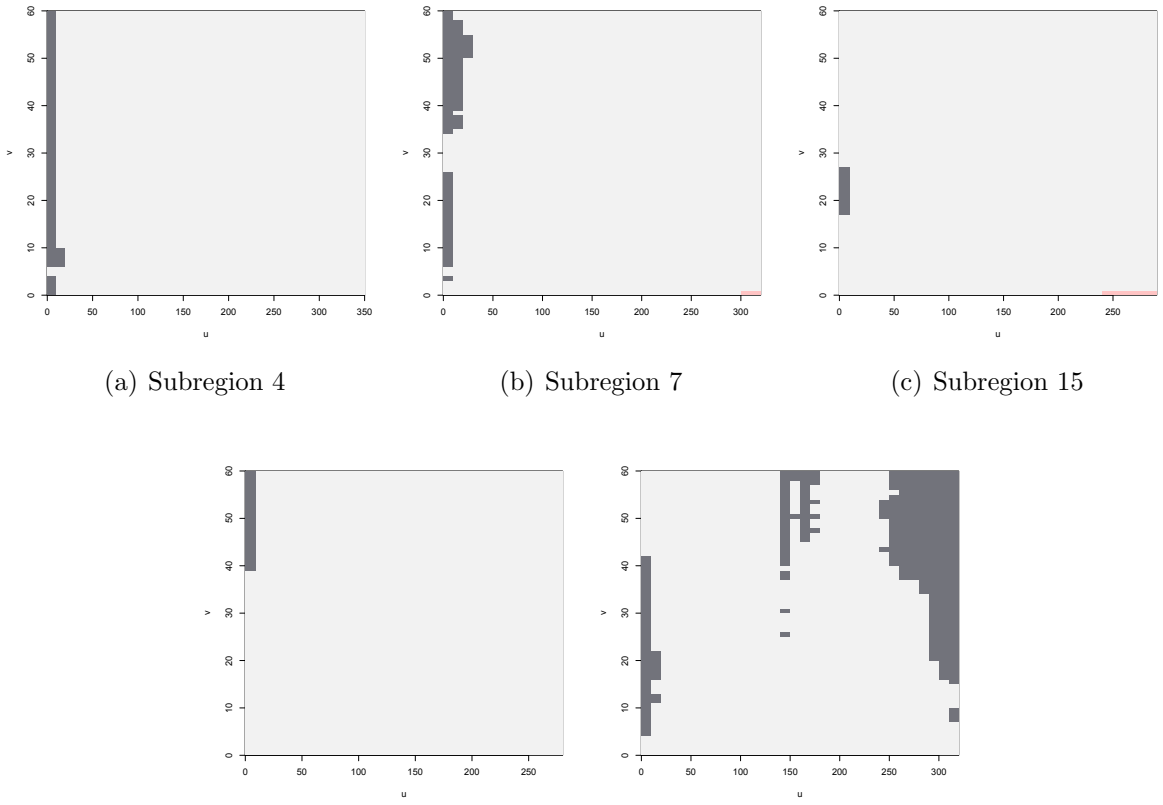

(a) Subregion 4 (b) Subregion 7 (c) Subregion 15

(d) Subregion 19 (e) Subregion 20

Figure 6.26: **Estimated spatio-temporal K function - subregions.** Outcome of the spatio-temporal K function estimates considering the sub-regions of Cascavel. Considering data from 2010 to 2012, the results for the sub-regions 4, 7, 15, 19, and 20 are shown in (a), (b), (c), (d), and (e), respectively. The colors of the points (u,v) indicate the position of the K function w.r.t. the envelope of the K function for CSR, computed with 10,000 simulations. The regions of the graph in light gray indicate the values of (u,v) for that K(u,v) is inside the envelope. The dark gray regions indicate that K(u,v) is above the envelope, and the light pink regions that K(u,v) is bellow the envelope. The variable of distance, u, is expressed in meters and the variable of time, v, in days.

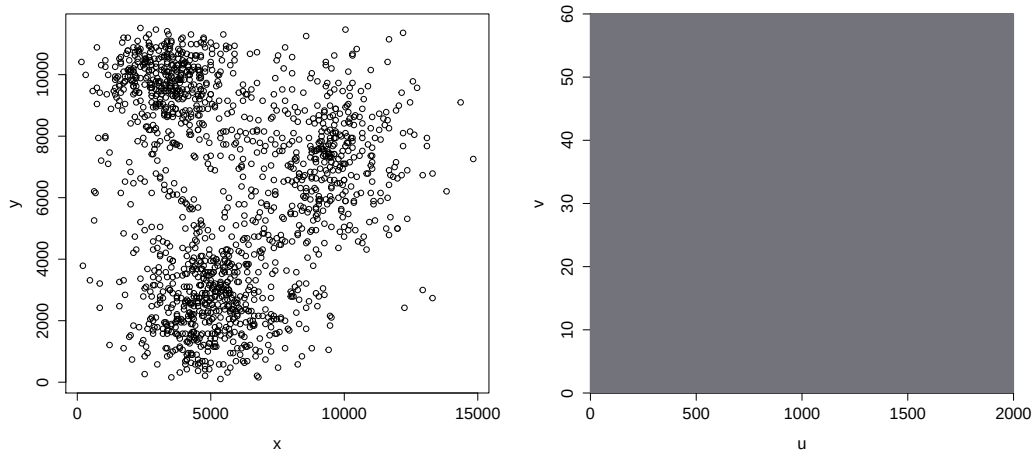

(a) Synthetic data

(b) K function for synthetic data

Figure 6.27: **K function for synthetic data.** On the left, a set of data generated synthetically from a diffusion equation with diffusion coefficient of 5000 m^2/day, where the data were generated along 300 days with 5 burglaries per day. On the right, the K-function outcome, indicating spatio-temporal agglomeration for all distances and times analyzed. The variable of distance, u, is expressed in meters and the variable of time, v, in days.

6.7 Discussion

According to the analysis performed, it is reasonable to model the residential burglaries in Cascavel as a inhomogeneous spatial Poisson process. However, many residential areas are not included in the analyzed subregions. Thus, it would be interesting to apply the analysis to the K-Ripley function considering the study region as all residential areas.

However, it is not easy to determine such regions in the map. A possibility is to select regions close to streets, avoiding uninhabited areas. Nonetheless, it is still including non residential areas.

Another possibility is to use a concave hull of the burglary locations. That is, a region of the plane containing all given points, and that its border is a simple polygon. Note that, removing a few points, the region on the plane delimited by the polygonal hull described in Section 6.5 (green line in Figure 6.20), is an example of convex hull. But, unlike the convex hull, there is not a unique concave hull for a given set of points. Thus, determining which concave hull is appropriate for the problem at hand is an interesting topic for a future work.

From a statistical view point, a possible work direction is to compare the data with a Cox process, which is a generalization of a Poisson process where the intensity is itself a stochastic process.

Another aspect to be considered is the possibility of geographic characteristics interfering in the connection between neighboring residences. That is, despite the distance between the two residences be small, there is a geographical obstacle (like a river) that prevents the easy locomotion from one to another. In this context, graph theory can be a very useful tool. For example, the graph nodes may represent the residences, while the graph edges link the neighboring houses that can be geographically connected.

6.8 Conclusion

The temporal analysis presented in Section 6.4, shows that the number of residential burglaries per day, between the years 2010 and 2012, had a large increase in November and December 2010. This peak period for burglaries cannot be explained by simply randomness, as shown in Figure 6.18. As this peak is the only one along the three years, it seems to be an isolated event, and not a pattern for residential burglaries. A possible explanation for this peak period for burglaries can be the temporary reduction of policing. In November 2010, there was a police force reallocation due to creation of the 5th Regional Military Police Command [Bra10].

Regarding to the spatial analysis, in Section 6.5, we have that the number of residential burglaries per km^2 along the three years, i.e. the intensity of burglaries, is not the same in all residential areas of Cascavel. This can be seen in Figure 6.19, which shows the intensity of residential burglaries throughout the region, including uninhabited areas . This can be also seen in Figure 6.25, that shows a bar graph with the spatial intensity of residential burglaries calculated for 20 subregions of Cascavel. However, this macro-scale behavior does not appear to be present on a smaller scale, since the K function analyze of 20 subregions of Cascavel shown to be approximately random (Figure 6.23). One hypothesis that fits this observation is that the burglars have a higher preference (attractiveness) for certain areas of the city, due to geographical or social features. However, inside these regions the choice of the target is almost random.

This peak period for burglaries also caused a bias in the first tests with respect to the spatio-temporal clusters. Indeed, considering the data along the three years, the spatio-temporal K analysis indicates a slight agglomeration in 4 of the 20 subregions analyzed. Among these four, two have also an indication of dispersion. See Figure 6.26.

However, considering only the data along 2011 and 2012, such clusters disappear. Thus, it is reasonable to consider that, in small scale, the burglaries are not event dependent.

Despite the burglaries in the subregions studied looks like a homogeneous spatial Poisson process, the intensity of burglaries is not the same in all the subregions. Therefore, it seems reasonable to model the residential burglaries as a inhomogeneous spatial Poisson process (the intensity is not constant). One way would be to model the intensity of burglaries as a spatial function constant for parts. Despite such a simplistic model, it may be useful to monitor the intensity of burglaries and test hypotheses about policing. Figure 6.28 shows a simulation performed considering the data from 2011. The real data was used to estimate the intensity in each square of a grid of lattice of 1 km. After that, points were taken according to the intensity estimated.

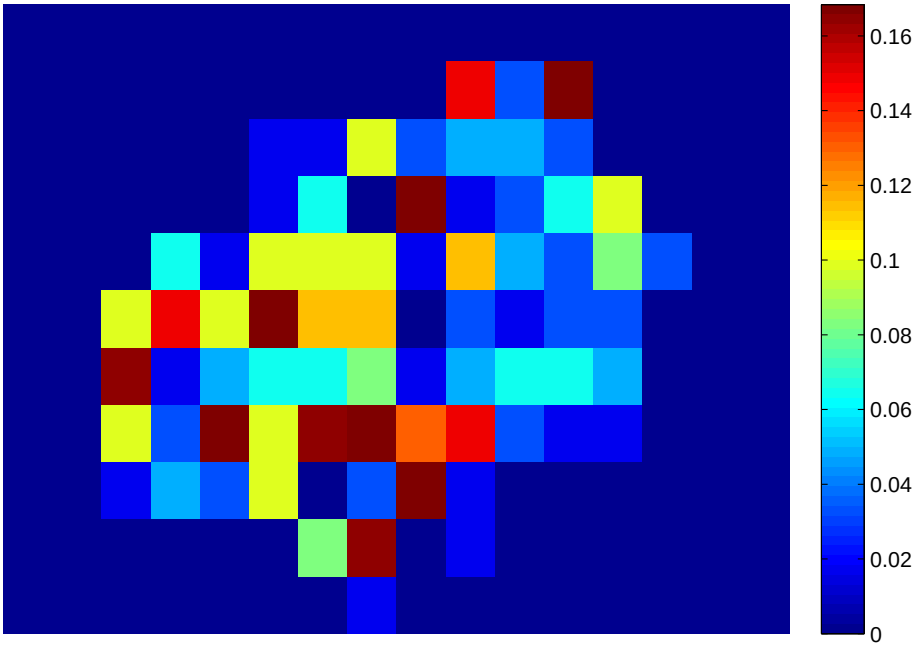

Figure 6.28: **Simulation of Residential burglaries in Cascavel.**

Bibliography

[B+92] Margarita Bofill et al. Laboratory control values for CD4 and CD8 T lymphocytes. implications for HIV-1 diagnosis. *Clinical & Experimental Immunology*, 88(2):243–252, 1992.

[B+11] Tibor Bosse et al. Agent-based vs. population-based simulation of displacement of crime: A comparative study. *Web Intelligence and Agent Systems*, 9(2):147–160, 2011.

[BMSN97] Sebastian Bonhoeffer, Robert M May, George M Shaw, and Martin A Nowak. Virus dynamics and drug therapy. *Proceedings of the National Academy of Sciences*, 94(13):6971–6976, 1997.

[BN10] Henri Berestycki and Jean-Pierre Nadal. Self-organised critical hot spots of criminal activity. *European Journal of Applied Mathematics*, 21(4-5):371–399, 2010.

[Bob10] Nara Bobko. Estabilidade de Lyapunov e propriedades globais para modelos de dinâmica viral. Master's thesis, Federal University of Paraná, 2010.

[BPL13] Jacek Banasiak, Eddy Kimba Phongi, and Miroslaw Lachowicz. A singularly pertubed SIS model with age structure. *Mathematical Biosciences and Engineering*, 10(3):499–521, 2013.

[Bra10] Brasil. Decreto estadual 8.743, de 12 de novembro de 2010. Creates the 5th regional military police command, based in cascavel, 2010.

[BRR13] Henri Berestycki, Nancy Rodriguez, and Lenya Ryzhik. Traveling wave solutions in a reaction-diffusion model for criminal activity. *Multiscale Modeling & Simulation*, 11(4):1097–1126, 2013.

[BZ15] Nara Bobko and Jorge P Zubelli. A singularly pertubed HIV model with treatment and antigenic variation. *Mathematical Biosciences and Engineering*, 12(1):1–21, 2015.

[C+08] Myron S Cohen et al. The spread, treatment, and prevention of HIV-1: evolution of a global pandemic. *The Journal of clinical investigation*, 118(4):1244–1254, 2008.

[Coo86] Leon N Cooper. Theory of an immune system retrovirus. *Proceedings of the National Academy of Sciences*, 83(23):9159–9163, 1986.

[Cra12] Michael J Crawley. *The R book*. John Wiley & Sons, 2012.

[CSB12] Donna Marie Giselle Comissiong, Joanna Sooknanan, and Balswaroop Bhatt. Criminals treated as predators to be harvested: A two prey one predator model with group defense, prey migration and switching. *Journal of Mathematics Research*, 4(4):p92, 2012.

[DBRP10] Rob J De Boer, Ruy M Ribeiro, and Alan S Perelson. Current estimates for HIV-1 production imply rapid viral clearance in lymphoid tissues. *PLoS computational biology*, 6(9):e1000906, 2010.

[dep13] *Protocolo clínico e diretrizes terapêuticas para o manejo da infecção pelo HIV em adultos*. Departamento de DST, Aids e Hepatites Virais - Ministério da Saúde, 2013.

[Dix02] Philip M Dixon. Ripley's k function. *Encyclopedia of environmetrics*, 2002.

[DP04] Narendra M Dixit and Alan S Perelson. Complex patterns of viral load decay under antiretroviral therapy: influence of pharmacokinetics and intracellular delay. *Journal of Theoretical Biology*, 226(1):95–109, 2004.

[DRK09] Daniel C Douek, Mario Roederer, and Richard A Koup. Emerging concepts in the immunopathogenesis of Aids. *Annual review of medicine*, 60:471, 2009.

[Eps02] Joshua M Epstein. Modeling civil violence: An agent-based computational approach. *Proceedings of the National Academy of Sciences of the United States of America*, 99(Suppl 3):7243–7250, 2002.

[F+03] Eberhard W Fiebiga et al. Dinâmica da viremia do HIV e da soroconversão de anticorpos em doadores de plasma: implicações para diagnóstico e estadiamento da infecção primária pelo HIV. *Aids*, 17:1871–1879, 2003.

[Fen79] Neil Fenichel. Geometric singular perturbation theory for ordinary differential equations. *Journal of Differential Equations*, 31(1):53–98, 1979.

[FFM+12] Maria Fonoberova, Vladimir A Fonoberov, Igor Mezic, Jadranka Mezic, and P Jeffrey Brantingham. Nonlinear dynamics of crime and violence in urban settings. *Journal of Artificial Societies and Social Simulation*, 15(1):2, 2012.

[FM94] Simon DW Frost and Angela R McLean. Germinal centre destruction as a major pathway of HIV pathogenesis. *Journal of Acquired Immune Deficiency Syndromes*, 7(3):236–244, 1994.

[GC04] Naveed Gulzar and Karen FT Copeland. CD8+ T-cells: function and response to HIV infection. *Current HIV research*, 2(1):23–37, 2004.

[GD09] Edith Gabriel and Peter J Diggle. Second-order analysis of inhomogeneous spatio-temporal point process data. *Statistica Neerlandica*, 63(1):43–51, 2009.

[GKCM13] James B Gilmore, Anthony D Kelleher, David A Cooper, and John M Murray. Explaining the determinants of first phase HIV decay dynamics through the effects of stage-dependent drug action. *PLoS computational biology*, 9(3):e1002971, 2013.

[Gor10] Mirta B Gordon. A random walk in the literature on criminality: A partial and critical view on some statistical analyses and modelling approaches. *European Journal of Applied Mathematics*, 21(4-5):283–306, 2010.

[GRD13] Edith Gabriel, Barry Rowlingson, and Peter J Diggle. stpp: an r package for plotting, simulating and analyzing spatio-temporal point patterns. *Journal of Statistical Software*, 53(2):1–29, 2013.

[Gro07] Elizabeth R Groff. Simulation for theory testing and experimentation: An example using routine activity theory and street robbery. *Journal of Quantitative Criminology*, 23(2):75–103, 2007.

[H+99] Marc Hellerstein et al. Directly measured kinetics of circulating T lymphocytes in normal and HIV-1-infected humans. *Nature medicine*, 5(1):83–89, 1999.

[HB+11] Rachel A Hegemann, Andrea Bertozzi, et al. Geographical influences of an emerging network of gang rivalries. *Physica A: Statistical Mechanics and its Applications*, 390(21):3894–3914, 2011.

[HN+99] Richard D Hockett, Martin A Nowak, et al. Constant mean viral copy number per infected cell in tissues regardless of high, low, or undetectable plasma HIV RNA. *The Journal of experimental medicine*, 189(10):1545–1554, 1999.

[HS98] Josef Hofbauer and Karl Sigmund. *Evolutionary games and population dynamics*. Cambridge University Press, 1998.

[Imm13] Taina Tuulia Immonen. *Computational Models of Ex Vivo HIV-1 Dynamics and Fitness Across Scales*. PhD thesis, Case Western Reserve University, 2013.

[JX05] Annah M Jeffrey and Xiaohua Xia. Identifiability of HIV/Aids models. *Deterministic and stochastic models of Aids epidemics and HIV infections with intervention*, page 255, 2005.

[KC96] Jirayr Kevorkian and Julian D Cole. *Multiple scale and singular perturbation methods*, volume 114. Springer New York, 1996.

[Kir96] Denise Kirschner. Using mathematics to understand HIV immune dynamics. *AMS notices*, 43(2), 1996.

[Kor04] Andrei Korobeinikov. Global properties of basic virus dynamics models. *Bulletin of Mathematical Biology*, 66(4):879–883, 2004.

[KW97] Denise Kirschner and Glenn F Webb. A mathematical model of combined drug therapy of HIV infection. *Computational and Mathematical Methods in Medicine*, 1(1):25–34, 1997.

[LF85] H Clifford Lane and Anthony S Fauci. Immunologic abnormalities in the acquired immunodeficiency syndrome. *Annual review of immunology*, 3(1):477–500, 1985.

[Llo01] Alun L Lloyd. The dependence of viral parameter estimates on the assumed viral life cycle: limitations of studies of viral load data. *Proceedings of the Royal Society of London. Series B: Biological Sciences*, 268(1469):847–854, 2001.

[M+90] Joseph L Malone et al. Sources of variability in repeated T-helper lymphocyte counts from human immunodeficiency virus type 1-infected patients: total lymphocyte count fluctuations and diurnal cycle are important. *Journal of Acquired Immune Deficiency Syndromes*, 3(2):144–151, 1990.

[M+00] Joseph M McCune et al. Factors influencing T-cell turnover in HIV-1–seropositive patients. *Journal of Clinical Investigation*, 105(5):R1, 2000.

[MHS10] Nick Malleson, Alison Heppenstall, and Linda See. Crime reduction through simulation: An agent-based model of burglary. *Computers, environment and urban systems*, 34(3):236–250, 2010.

[MK06] Mee Ling Munier and Anthony Kelleher. Acutely dysregulated, chronically disabled by the enemy within: T-cell responses to HIV-1 infection. *Immunology and cell biology*, 85(1):6–15, 2006.

[MKSD12] Michael McBride, Ryan Kendall, Martin B Short, and Maria R D'orsogna. Crime, punishment, and evolution in an adversarial game. *UCI Department of Economics Working Paper*, pages 12–13, 2012.

[NB96] Martin A Nowak and Charles RM Bangham. Population dynamics of immune responses to persistent viruses. *Science*, 272(5258):74–79, 1996.

[NHP08] Juan C Nuño, Miguel A Herrero, and Mario Primicerio. A triangle model of criminality. *Physica A: Statistical Mechanics and its Applications*, 387(12):2926–2936, 2008.

[NM00] Martin Nowak and Robert M May. *Virus dynamics: mathematical principles of immunology and virology*. Oxford University Press, 2000.

[NP02] Patrick W Nelson and Alan S Perelson. Mathematical analysis of delay differential equation models of HIV-1 infection. *Mathematical Biosciences*, 179(1):73–94, 2002.

[OB78] Steven A Orszag and Carl M Bender. *Advanced mathematical methods for scientists and engineers*. Mac Graw Hill, 1978.

[oH12] Joint United Nations Programme on HIV/Aids. Global report: UNAIDS report on the global Aids epidemic 2012. 2012.

[P+97] Gilles Pialoux et al. Central nervous system as a sanctuary for hiv-1 infection despite treatment with zidovudine, lamivudine and indinavir. *Aids*, 11(10):1302–1303, 1997.

[Pas05] Dayse H Pastore. *A dinamica do HIV no sistema imunológico na presença de mutação*. PhD thesis, IMPA, 2005.

[PH+95] Alan S Perelson, David D Ho, et al. Rapid turnover of plasma virions and CD4 lymphocytes in HIV-1 infection. *Nature*, 373(6510):123–126, 1995.

[PH+96] Alan S Perelson, David D Ho, et al. HIV-1 dynamics in vivo: virion clearance rate, infected cell life-span, and viral generation time. *Science*, 271(5255):1582–1586, 1996.

[PH+97] Alan S Perelson, David D Ho, et al. Decay characteristics of HIV-1-infected compartments during combination therapy. 1997.

[PH+00] Alan S Perelson, David D Ho, et al. Modeling plasma virus concentration during primary HIV infection. *Journal of Theoretical Biology*, 203(3):285–301, 2000.

[PH+07] Alan S Perelson, David D Ho, et al. Determination of virus burst size in vivo using a single-cycle SIV in rhesus macaques. *Proceedings of the National Academy of Sciences*, 104(48):19079–19084, 2007.

[PJ11] Ashley B Pitcher and Shane D Johnson. Exploring theories of victimization using a mathematical model of burglary. *Journal of Research in Crime and Delinquency*, 48(1):83–109, 2011.

[PKDB93] Alan S Perelson, Denise E Kirschner, and Rob De Boer. Dynamics of HIV infection of CD4+ T cells. *Mathematical biosciences*, 114(1):81–125, 1993.

[PN99] Alan S Perelson and Patrick W Nelson. Mathematical analysis of HIV-1 dynamics in vivo. *SIAM review*, 41(1):3–44, 1999.

[PR08] Alan S Perelson and Ruy M Ribeiro. Estimating drug efficacy and viral dynamic parameters: HIV and HCV. *Statistics in medicine*, 27(23):4647–4657, 2008.

[Qui96] Thomas C. Quinn. HIV viral load. *The Hopkins HIV Report*, 8(3), 1996.

[RB10] Nancy Rodriguez and Andrea Bertozzi. Local existence and uniqueness of solutions to a pde model for criminal behavior. *Mathematical Models and Methods in Applied Sciences*, 20(supp01):1425–1457, 2010.

[RHS95] David L Robertson, Beatrice H Hahn, and Paul M Sharp. Recombination in Aids viruses. *Journal of molecular evolution*, 40(3):249–259, 1995.

[Rip76] Brian D Ripley. The second-order analysis of stationary point processes. *Journal of applied probability*, pages 255–266, 1976.

[Rip77] Brian D Ripley. Modelling spatial patterns. *Journal of the Royal Statistical Society. Series B (Methodological)*, pages 172–212, 1977.

[Rip79] Brian D Ripley. Tests ofrandomness' for spatial point patterns. *Journal of the Royal Statistical Society. Series B (Methodological)*, pages 368–374, 1979.

[RP+10] Ruy M Ribeiro, Alan S Perelson, et al. Estimation of the initial viral growth rate and basic reproductive number during acute HIV-1 infection. *Journal of virology*, 84(12):6096–6102, 2010.

[RPCH04] Andrew Rambaut, David Posada, Keith A Crandall, and Edward C Holmes. The causes and consequences of HIV evolution. *Nature Reviews Genetics*, 5(1):52–61, 2004.

[RWSH07] Cavan Reilly, Steve Wietgrefe, Gerald Sedgewick, and Ashley Haase. Determination of simian immunodeficiency virus production by infected activated and resting cells. *Aids*, 21(2):163–168, 2007.

[S+95] Merle A Sande et al. *The medical management of Aids.* Number Ed. 4. WB Saunders, 1995.

[SBBT10] Martin Bowen Short, Paul Jeffrey Brantingham, Andrea Louise Bertozzi, and George Tita. Dissipation and displacement of hotspots in reaction-diffusion models of crime. *Proceedings of the National Academy of Sciences*, 107(9):3961–3965, 2010.

[SBC13] Joanna Sooknanan, Balswaroop Bhatt, and Donna MG Comissiong. Another way of thinking: A review of mathematical models of crime. *Mathematics TODAY*, page 131, 2013.

[SBD10] Martin Bowen Short, Paul Jeffrey Brantingham, and Maria Rita D'Orsogna. Cooperation and punishment in an adversarial game: How defectors pave the way to a peaceful society. *Physical Review E*, 82(6):066114, 2010.

[SDBT09] Martin Bowen Short, Maria Rita D'Orsogna, Paul Jeffrey Brantingham, and George Tita. Measuring and modeling repeat and near-repeat burglary effects. *Journal of Quantitative Criminology*, 25(3):325–339, 2009.

[SDL03] Hal L Smith and Patrick De Leenheer. Virus dynamics: a global analysis. *SIAM Journal on Applied Mathematics*, 63(4):1313–1327, 2003.

[SdMB+13] Elaine Sanae Sumikawa, Leonardo Rapone da Motta, Maria Luiza Bazzo, Miriam Franchini, and Orlando da Costa Ferreira Junior. *Manual Técnico para o diagnóstico da infecção pelo HIV*. Ministério da Saúde, 2013.

[SDP+08] Martin B Short, Maria R D'ORSOGNA, Virginia B Pasour, George E Tita, Paul J Brantingham, Andrea L Bertozzi, and Lincoln B Chayes. A statistical model of criminal behavior. *Mathematical Models and Methods in Applied Sciences*, 18(supp01):1249–1267, 2008.

[SH03] Viviana Simon and David D Ho. HIV-1 dynamics in vivo: implications for therapy. *Nature Reviews Microbiology*, 1(3):181–190, 2003.

[SH11] Paul M Sharp and Beatrice H Hahn. Origins of HIV and the Aids pandemic. *Cold Spring Harbor perspectives in medicine*, 1(1):a006841, 2011.

[Sie12] Nourridine Siewe. *The Tikhonov Theorem In Multiscale Modelling: An Application To The SIRS Epidemic Model*. PhD thesis, AIMS, 2012.

[SNHGP11] Juan Carlos Sanz Nuño, Miguel Ángel Herrero García, and Mario Primicerio. A mathematical model of a criminal-prone society. *Discrete And Continuous Dynamical Systems*, 4(1):193–207, 2011.

[Sou11] Max O Souza. Multiscale analysis for a vector-borne epidemic model. *Journal of mathematical biology*, pages 1–25, 2011.

[SR88] Mohan Somasundaran and HL Robinson. Unexpectedly high levels of HIV-1 RNA and protein synthesis in a cytocidal infection. *Science*, 242(4885):1554–1557, 1988.

[SZ11] Max O Souza and Jorge P Zubelli. Global stability for a class of virus models with cytotoxic T lymphocyte immune response and antigenic variation. *Bull. Math. Biol.*, 73(3):609–625, 2011.

[Szm91] Peter Szmolyan. Transversal heteroclinic and homoclinic orbits in singular perturbation problems. *Journal of differential equations*, 92(2):252–281, 1991.

[TVS84] Andrey N Tikhonov, Adelaida B Vasileva, and Aleksei Georgievich Sveshnikov. *Differential Equations*. Springer-Verlag Berlin, 1984.

[Var66] Louis G Vargo. A note on crime control. *The Bulletin of mathematical biophysics*, 28(3):375–378, 1966.

[VB90] Adelaida B Vasileva and Valentin F Butuzov. *Asimptoticheskie Metody v Teorii Singulyarnykh Vozmushchenij*. Moskva: Vysshaya Shkola, 1990.

[VRM+10] Naveen K Vaidya, Libin Rong, Vincent C Marconi, Daniel R Kuritzkes, Steven G Deeks, and Alan S Perelson. Treatment-mediated alterations in HIV fitness preserve CD4+ T cell counts but have minimal effects on viral load. *PLoS computational biology*, 6(11):e1001012, 2010.

[W+99] Hulin Wu et al. Characterization of viral dynamics in human immunodeficiency virus type 1-infected patients treated with combination antiretroviral therapy: relationships to host factors, cellular restoration, and virologic end points. *Journal of Infectious Diseases*, 179(4):799–807, 1999.

[Was02] Wolfgang Wasow. *Asymptotic expansions for ordinary differential equations*. Dover Publications, 2002.

[WDP98] Lawrence M Wein, Rebecca M D'Amato, and Alan S Perelson. Mathematical analysis of antiretroviral therapy aimed at HIV-1 eradication or maintenance of low viral loads. *Journal of theoretical biology*, 192(1):81–98, 1998.

[Win03] Pinata Winoto. A simulation of the market for offenses in multiagent systems: is zero crime rates attainable? In *Multi-Agent-Based Simulation II*, pages 181–193. Springer, 2003.

[WS07] Xia Wang and Xinyu Song. Global properties of a model of immune effector responses to viral infections. *Advances in Complex Systems*, 10(04):495–503, 2007.

[WZMP08] Hulin Wu, Haihong Zhu, Hongyu Miao, and Alan S Perelson. Parameter identifiability and estimation of HIV/Aids dynamic models. *Bulletin of mathematical biology*, 70(3):785–799, 2008.

[Xia03] Xiaohua Xia. Estimation of HIV/Aids parameters. *Automatica*, 39(11):1983–1988, 2003.

[Xia07] Xiaohua Xia. Modelling of HIV infection: Vaccine readiness, drug effectiveness and therapeutical failures. *Journal of Process Control*, 17(3):253–260, 2007.

[XM03] Xiaohua Xia and Claude H Moog. Identifiability of nonlinear systems with application to HIV/Aids models. *Automatic Control, IEEE Transactions on*, 48(2):330–336, 2003.